UNIVERSIDADE FEDERAL DE MINAS GERAIS
Instituto de Ciências Biológicas
Programa de Pós-Graduação em Zoologia

Larissa Costa Coimbra Santos Dumbá

DENTAL ECOMORPHOLOGY, PHYLOGENY AND BIOGEOGRAPHY OF TAPIRIDAE (MAMMALIA, PERISSODACTYLA)

Belo Horizonte
2023

Larissa Costa Coimbra Santos Dumbá

DENTAL ECOMORPHOLOGY, PHYLOGENY AND BIOGEOGRAPHY OF TAPIRIDAE (MAMMALIA, PERISSODACTYLA)

Versão final

Tese apresentada ao Programa de Pós-Graduação em Zoologia da Universidade Federal de Minas Gerais, como requisito parcial à obtenção do título de Doutora em Zoologia.

Orientador: Mario Alberto Cozzuol
Co-orientador: Raoul Van Damme

Belo Horizonte
2023

043 Dumbá, Larissa Costa Coimbra Santos.
Dental ecomorphology, phylogeny and biogeography of Tapiridae (Mammalia, Perissodactyla) [manuscrito] / Larissa Costa Coimbra Santos Dumbá. – 2023.
144 f. : il. ; 29,5 cm.

Orientador: Mario Alberto Cozzuol. Co-orientador: Raoul Van Damme.
Tese (doutorado) – Universidade Federal de Minas Gerais, Instituto de Ciências Biológicas. Programa de Pós-Graduação em Zoologia.

1. Zoologia. 2. Perissodáctilos. 3. Filogenia. 4. Evolução Biológica. 5. Biogeografia. 6. Dispersão de Sementes. I. Cozzuol, Mario Alberto. II. Damme, Raoul Van. III. Universidade Federal de Minas Gerais. Instituto de Ciências Biológicas. IV. Título.

CDU: 591

Ficha catalografica elaborada pela bibliotecária Fabiane C. M. Reis – CRB: 6/2680

UNIVERSIDADE FEDERAL DE MINAS GERAIS

INSTITUTO DO CIÊNCIAS BIOLÓGICAS

PÓS-GRADUAÇÃO EM ZOOLOGIA

ATA DE DEFESA DE TESE

LARISSA COSTA COIMBRA SANTOS DUMBÁ

Ao vigésimo quarto dia do mês de fevereiro do ano de dois mil e vinte e três, às quatorze horas, realizou- se, por webconferência, a defesa de Doutorado da Pós-Graduação em Zoologia, de autoria da Doutoranda **Larissa Costa Coimbra Santos Dumbá** intitulada: "Dental ecomorphology, phylogeny and biogeography ɗ Tapiridae (Mammalia, Perissodactyla)". Abrindo a sessão, o Presidente da Banca, Prof. Dr. Mario Alberto Cozzuol, após dar a conhecer aos presentes o teor das Normas Regulamentares do Trabalho Final, passou a palavra para a candidata para apresentação de seu trabalho. Esteve presente a Banca Examinadora composta pelos membros: Annie Schmaltz Hsiou, Adalberto José dos Santos, Elizete Celestino Holanda, Larissa Rosa de Oliveira, e demais convidados. Seguiu-se a arguição pelos examinadores, com a respectiva defesa da candidata. Após a argüição, apenas os Srs. Examinadores permaneceram na sala para avaliação e deliberação acerca do resultado final, a saber: o trabalho foi APROVADO SEM ALTERAÇÕES

Belo Horizonte,

24 de fevereiro de 2023

Assinatura dos membros da banca examinadora

Documento assinado eletronicamente por **Adalberto Jose dos Santos**, **Professor do Magistério Superior**, em 27/02/2023, às 13:58, conforme horário oficial de Brasília, com fundamento no art. 5º do Decreto nº 10.543, de 13 de novembro de 2020.

Documento assinado eletronicamente por **Mario Alberto Cozzuol**, **Membro**, em 27/02/2023, às 15:43, conforme horário oficial de Brasília, com fundamento no art. 5º do Decreto nº 10.543, de 13 de novembro de 2020.

Documento assinado eletronicamente por **Annie Schmaltz Hsiou**, **Usuária Externa**, em 28/02/2023, às 16:43, conforme horário oficial de Brasília, com fundamento no art. 5º do Decreto nº 10.543, de 13 de novembro de 2020.

Documento assinado eletronicamente por **Elizete Celestino Holanda**, **Usuário Externo**, em 28/02/2023, às 19:48, conforme horário oficial de Brasília, com fundamento no art. 5º do Decreto nº 10.543, de 13 de novembro de 2020.

Documento assinado eletronicamente por **Larissa Rosa de Oliveira**, **Usuária Externa**, em 01/06/2023, às 14:19, conforme horário oficial de Brasília, com fundamento no art. 5º do Decreto nº 10.543, de 13 de novembro de 2020.

A autenticidade deste documento pode ser conferida no site https://sei.ufmg.br/sei/controlador_externo.php?acao=documento_conferir&id_orgao_acesso_externo=0, informando o código verificador **2102853** e o código CRC **60C61742**.

Referência: Processo nº 23072.229818/2021-05

SEI nº 2102853

ACKNOWLEDGMENTS

I thank Mario Alberto Cozzuol, who guided me not only on these PhD but since my Masters. Thank you for giving me the space I needed to work but also for being there when I needed. Thank you for your patience, your availability and for the funny videos shared and all the politics talks during coffee time in the laboratory. Thank you for supporting my professional dreams (wherever they are) and for cheering for me. You are a great part of my professional career and I could not have wished for a better person to guide me.

I'm also thankful for my collaborators in Brazil: Flávio Rodrigues dos Santos and Daniel Casali. Their experience contributed a lot to this thesis, and I will always be thankful for their support.

I thank the Coordenação de Aperfeiçoamento de Pessoal de Nível Superior (CAPES), Deutscher Akademischer Austauschdienst (DAAD) and Royal Belgian Zoological Society (RBZS) grant for the financial support of my studies in Brazil and in Europe.

A special "thank you" to Universiteit Antwerpen staff, where I learned so much.

I am grateful to the curators of the collections in Europe which granted me access and/or sent me photographs and related data of the specimens I studied.

To the evaluation committee members, for kindly accepting the invitation: Dr. Adalberto Santos, Dra. Annie Hsiou, Dra. Elizete Holanda and Dra. Larissa Oliveira.

I also thank my colleagues and professors of the Zoology Graduate Program who contributed to my professional growth. My special thanks to Snaydia Resende and Ana Luísa Damaceno, my graduate friends, for all the talks and friendship through rough times.

To my psychologist Kerollyn Lopes, without whom I would never been able to deal with anxiety, helping me go through this PhD and the pandemic time more smoothly.

To my dearest friends outside the university: Andressa Roquini, Denise Arantes, Tatiane Siqueira, Bárbara Milward, Janine Fonseca, Renata Sander, Izabela Machado, Lucas Pereira. You guys made these past 4 and a half years much lighter and funnier, and for that I will always be thankful!

To my brother Gilson Dumbá, thanks for all the laughs, game nights and support. I love you.

To my boyfriend Milton Drummond, you were one of the biggest responsible for me not giving up when my mother died. You have been my very best support, friend, boyfriend, partner. This PhD is yours too. I am proud of being here today with you standing by my side, love. Thank

you for understanding and being there for me in all of my most stressed phases, my long periods dealing with anxiety and everything else. I love you until the end.

To my mother Maria Arminda Costa who unfortunately did not live to see me being here today, but was and will always be my greatest encouragement and support. “Thank you” will never be enough to describe how grateful I am for everything that you thaught me, provided for me, and for all the love you gave me for the 28 years I had the pleasure to have you here as my mom. I dedicate my PhD to you.

“I will take these broken wings and you’ll watch me burn across the sky” (Speechless – Naomi Scott)

RESUMO

A família Tapiridae (Mammalia, Perissodactyla) tem sido amplamente estudada na literatura nas últimas décadas. No entanto, a taxonomia da família apresenta inúmeras sinonímias e várias espécies foram descritas com base em caracteres dentários e/ou fragmentos de crânio. Trabalhos anteriores mostraram que esse é um cenário problemático, pois dentes possuem pouca informação filogenética em *Tapirus*. Esta tese de Doutorado tem como objetivo propor o uso de caracteres dentários em inferências ecomorfológicas de dispersão de sementes para antas. Esta tese também tem como objetivo reavaliar a filogenia, os tempos de divergência e a evolução morfológica da família Tapiridae com alterações em matrizes morfológicas discretas anteriores, especialmente no que diz respeito a um menor uso de caracteres dentários. No capítulo 1, a ordenação e os resultados estatísticos sugerem que a morfologia dentária é conservada entre as espécies de *Tapirus* e que o tamanho é o principal fator que afeta a variação. Esta é uma evidência que sugere que a morfologia dentária apenas não é confiável para distinguir ou descrever espécies de anta. A área de superfície oclusal (ASO) dos dentes de *Tapirus* como um preditor do potencial de dispersão de sementes apontou que as antas sul-americanas são boas dispersoras. As antas norte-americanas apresentam ASO variáveis, as antas asiáticas têm baixa capacidade de dispersão e todas as antas europeias provavelmente foram dispersoras eficientes. No capítulo 2, realizamos análises filogenéticas incluindo uma matriz quantitativa de dados morfométricos 2D + matriz de dados qualitativos. Usamos um número maior de caracteres cranianos em relação aos caracteres dentários na matriz qualitativa, e nenhum caráter dentário foi usado na matriz quantitativa. A inclusão de dados morfométricos 2D em matrizes morfológicas discretas parece não ter impacto significativo nas topologias. O gênero *Tapirus* foi recuperado como monofilético em nossas três hipóteses filogenéticas. As antas norte-americanas são polifiléticas. As antas sul-americanas formam um clado. Tapiridae divergiu em algum ponto do Eoceno Médio ao Oligoceno Superior, na América do Norte. *Tapirus* também se originou na América do Norte com tempos de divergência que vão desde o último Oligoceno/Início do Mioceno até o final do Mioceno. Às três topologias, foram aplicados os modelos biogeográficos DEC e DIVA, disponíveis no pacote BioGeoBEARS do programa R. Tapiridae não-*Tapirus* dispersaram-se pelo menos duas vezes da América do Norte para a Eurásia, segundo análises biogeográficas. *Tapirus* dispersaram-se da América do Norte para a Eurásia múltiplas vezes e para a América do Sul em um único evento. A maioria das nossas inferências biogeográficas são consistentes com a presença de pontes terrestres transitórias ou permanentes. Esta tese representa a primeira hipótese filogenética para Tapiridae

incluindo espécies de *Tapirus* europeias, juntamente com a primeira análise biogeográfica formal para a família Tapiridae.

PALAVRAS-CHAVE: Tapiridae. *Tapirus*. Evolução morfológica. Morfologia dentária. Dispersão de sementes. Morfologia craniana. Morfometria Tradicional. Morfometria Geométrica. Parcimônia. Paleoecologia. Biogeografia.

ABSTRACT

Family Tapiridae (Mammalia, Perissodactyla) has been widely studied in the literature in the past decades. However, the taxonomy of the family showed numerous synonymies and several species were described based on dental and/or fragmented cranial remains. Previous works have shown how problematic it is, as teeth carry low phylogenetic information for *Tapirus*. This thesis aims to propose the usage for dental characters in ecomorphology inferences of seed dispersal for tapirs. This thesis also aimed to reassess the phylogeny, divergence times and morphological evolution of Tapiridae with changes to previous discrete morphological matrices, especially regarding a lesser usage of dental characters. In chapter 1, ordination and statistical results suggest that tooth shape is conservated between *Tapirus* species and that size is the main factor affecting variation. This evidence suggests that tooth shape alone is not reliable for distinguishing or describing tapir species. The occlusal surface area (OSA) of tapir cheek teeth as a predictor of seed dispersal potential pointed to South American tapirs being good seed dispersers. North American tapirs present variable OSAs, Asian tapirs have a low capacity for dispersion and all European tapirs were probably efficient seed dispersers. In chapter 2, we performed phylogenetic analyses including both discrete and quantitative 2D morphometric matrices. We used a larger number of cranial characters over teeth characters in the discrete matrix, and no dental characters were used in the quantitative matrix. The inclusion of 2D morphometric data in discrete morphological matrix seems not have significant impact on topologies. Genus *Tapirus* was recovered as monophyletic in our three phylogenetic hypotheses. North American tapirs are polyphyletic. South American tapirs form a clade. Tapiridae diverged at some point from the Middle Eocene to the Late Oligocene, in North America. *Tapirus* also originated in North America with divergence times ranging from the latest Oligocene/Early Miocene to the Late Miocene. DEC and DIVA biogeographic models available in the BioGeoBEARS package of R programming environment were applied to the three topologies. Tapirids dispersed at least two times from North America to Eurasia, as shown by biogeographic analysis. *Tapirus* dispersed from North America to Eurasia multiple times and to South America in a single event. Most of our biogeographic inferences are consistent with the presence of transient or permanent land bridges. This thesis represents the first phylogenetic hypothesis for tapirids including European *Tapirus*, along with the first formal biogeographic analysis for the family.

KEYWORDS: Tapiridae. *Tapirus*. Morphological evolution. Teeth shape. Seed dispersal. Traditional Morphometry. Geometric Morphometry. Parsimony. Paleoecology. Biogeography.

LISTA DE ILUSTRAÇÕES

LISTA DE TABELAS

SUMMARY

INTRODUCTION

The family Tapiridae Burnett, 1830 comprises perissodactyl herbivorous mammals that belong to the superfamily Tapiroidea Burnett, 1830 (Figure 1). Tapiridae belongs to the suborder Tapiromorpha (see Figure 1) Haeckel, 1866, along with Rhinocerontoidea Gray, 1821, and their extinct relatives.

The superfamily Tapiroidea also includes four other families: Deperetellidae Radinsky, 1965 and Lophialetidae Matthew & Granger, 1923, from the Lower Tertiary of Asia; Helaletidae Osborn, 1892 of questionable monophyly (Holbrook 1998, 2001) and Isectolophidae Peterson, 1919, (McKenna & Bell 1997), although Colbert (2005) considers the position of the latter as uncertain inside Tapiromorpha.

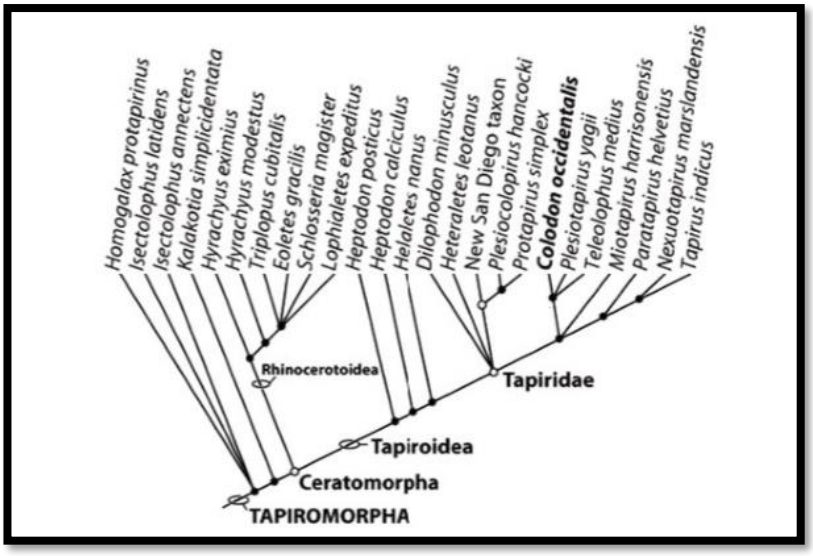

Figure 1. Tapiromorpha and Superfamily Tapiroidea according to Colbert et al. 2005.

Family Tapiridae includes ten genera: *Protapirus* Filhol, 1877 was described for the Late Oligocene/Lower Miocene of Europe and North America (Albright 1998); *Plesiotapirus* (Qiu, Yan & Sun 1991) from for the Middle/Late Miocene of Asia; *Eotapirus* Cerdeno & Ginsburg, 1988, and *Tapiriscus* Kretxoi, 1951, were described respectively for the Lower Miocene and Upper Miocene of Europe; *Miotapirus* Qiu, Yan & Sun, 1991, and *Tapivarus* Marsh, 1877, described for the Late Oligocene/Lower Miocene (Albright 1998) of North America; *Paratapirus* Depéret and Douxami, 1902, from the Early Miocene of Europe (Cerdeño and Gisburg 1988), *Colodon* Marsh, 1890, was described for the Middle Eocene/Late Oligocene of North America (Marsh 1980, Holbrook 1998) and has been previously discussed as a possible Tapiridae genus (Colbert 2005, Bai et al. 2020) as further discussions will be made regarding this group on Chapter 2; *Nexuotapirus* Albright 1998, from the Late Oligocene of

North America (Albright 1998); and genus *Tapirus* Brisson, 1762, the only Tapiridae with living representatives. Species described for Tapiridae are shown in Table 1.

Table 1. 62 Tapiridae species according to their genera, time and locality of divergence, as the references that follows.

Species	**Time and locality**	**Reference**
† *Tapirus telleri* Hofmann, 1893	Middle Miocene Europe/Asia	Deng and Chen 2008
† *Tapirus polkensis* Olsen, 1960	Middle Miocene, North America	Gibson 2011
† *Tapirus johnsoni* Schultz et al., 1975	Middle Miocene, North America	Holanda and Ferrero 2012
† *Tapirus webbi* Hulbert, 2005	Late Miocene, North America	Hulbert 2005
† *Tapirus simpsoni* Schultz et al., 1975	Late Miocene, North America	Hulbert 2005
† *Tapirus priscus* Kaup, 1833	Late Miocene, Europe	Guérin and Eisenmann 1994
†*Tapirus balkanicus* Spassov and Ginsburg,1999	Late Miocene, Europe	Spassov and Ginsburg, 1999
† *Tapirus antiquus* Kaup, 1833	Late Miocene, Europe	Spassov and Ginsburg, 1999
† *Tapirus hungaricus* Meyer, 1867	Late Miocene, Europe	Spassov and Ginsburg, 1999
† *Tapirus hezhengensis* Deng and Chen, 2008	Late Miocene, Asia	Deng and Chen 2008
† *Tapirus teilhardi* Zdansky, 1935	Late Miocene, Asia	Ji et al. 2015
† *Tapirus augustus* Matthew and Granger, 1923	Late Pleistocene, Asia	Tong et al. 2002
Tapirus indicus Desmarest, 1819	Middle/Late Miocene, Asia	Cozzuol et al. 2013, 2014
Tapirus bairdii Gill, 1865	Late Miocene/Pliocene, America	Cozzuol et al. 2013, 2014
† *Tapirus jeanpivetaui* Boeuf, 1991	Pliocene, Europe	Spassov and Ginsburg, 1999
† *Tapirus arvernensis* Croizet and Jobert, 1828	Pliocene, Europe	Rustioni 1992
† *Tapirus yunnanensis* Shi et al., 1981	Pliocene, Asia	Ji et al. 2015
† *Tapirus merriami* Frick, 1921	Pliocene, North America	Hulbert 2010
† *Tapirus haysii* Leidy, 1859	Pliocene, North America	Hulbert 2010
† *Tapirus sanyuanensis* Huang, 1991	Pleistocene, Asia	Tong 2005
† *Tapirus peii* Li, 1979	Pleistocene, Asia	Tong et al. 2002
† *Tapirus sinensis* Owen, 1870	Pleistocene, Asia	Tong et al. 2002
† *Tapirus veroensis* Sellards, 1918	Pleistocene, North America	Hulbert 2010
† *Tapirus lundeliusi* Hulbert, 2010	Pleistocene, North America	Hulbert 2010

† *Tapirus cristatellus* Winge, 1906	Pleistocene, South America	Holanda et al. 2007
† *Tapirus mesopotamicus* Ferrero and Noriega, 2007	Pleistocene, South America	Ferrero and Noriega 2007
† *Tapirus greslebini* Rusconi, 1934	Pleistocene, South America	Holanda et al. 2011
† *Tapirus oliverasi* Ubilla, 1983	Pleistocene, South America	Ubilla 1983
† *Tapirus rioplatensis* Cattoi, 1957	Pleistocene, South America	Ubilla 1983
† *Tapirus tarijiensis* Ameghino, 1902	Pleistocene, South America	Holanda et al. 2011
† *Tapirus rondonienses* Holanda et al., 2011	Pleistocene, South America	Holanda et al. 2011
† *Tapirus dupuyi* Cattoi, 1951	Pleistocene, South America	Cattoi 1951
† *Tapirus australis* Rusconi, 1928	Pleistocene, South America	Tonni 1992
Tapirus kabomani Cozzuol et al. 2013	Pleistocene, South America	Cozzuol et al. 2013, 2014
Tapirus pinchaque Roulin, 1829	Pleistocene, South America	Cozzuol et al. 2013, 2014
Tapirus terrestris Linnaeus, 1758	Pleistocene, South America	Cozzuol et al. 2013, 2014
† *Paratapirus helvetius* Meyer 1867	Oligocene/Miocene, Europe	Scherler 2011
† *Paratapirus intermedius* Filhol 1885	Oligocene/Miocene, Europe	Scherler 2011
†*Protapirus obliquidens*, Wortman and Earle 1893	Early Oligocene, North America	Albright 1998
† *Protapirus simplex* Wortman and Earle 1893	Early Oligocene, North America	Bayshashov and Billa 2011
† *Protapirus aginensis* Richard 1938	Early Oligocene, Europe	Albright 1998
† *Protapirus bavaricus* Oettingen-Spielberg 1952	Late Oligocene, Europe	Albright 1998
† *Protapirus priscus* Filhol 1874	Late Oligocene, Europe	Albright 1998
† *Protapirus douvillei* Filhol 1885	Early Miocene, Europe	Scherler et al. 2011;
† *Protapirus gromovae* Biryukov 1972	Early Miocene, Europe	Scherler et al. 2011;
† *Tapiravus rarus* Marsh 1877	Early/Middle Miocene, North America	Colbert and Schoch 1998

† *Tapiravus validus* Marsh 1871	Middle Miocene, North America	Albright 1998
†*Miotapirus harrisonensis* Schlaikjer 1937	Early Miocene, North America	Colbert and Schoch 1998
† *Nexuotapirus robustus* Albright, 1998	Late Oligocene, North America	Albright 1998
† *Nexuotapirus marslandensis* Albright, 1998	Late Oligocene, North America	Albright 1998
† *Eotapirus ruber* Cerdeno and Ginsburg 1988	Early Miocene, Europe	Cerdeno and Ginsburg, 1988
†*Eotapirus broennimanni* Schaub and	Early Miocene, Europe	Scherler et al. 2011
† *Plesiotapirus yagii* Qiu et al. 1991	Middle Miocene, Asia	Qiu et al. 1991
†*Tapiriscus pannonicus* Kretzoi 1951	Middle Miocene, Europe	Franzen 2013
†*Colodon cingulatus* Douglass 1902	Eocene/Oligocene, North America	Albright 1998
†*Colodon copei* Osborn and Wortman 1895	Eocene/Oligocene, North America	Osborn 1918
†*Colodon inceptus* Matthew and Granger 1925	Eocene, Asia	Matthew and Granger 1925
†*Colodon kayi* Hough 1955	Eocene, North America	Wilson and Schiebout 1984
†*Colodon occidentalis* Leidy 1868	Eocene/Oligocene, North America	Schoch 1989
†*Colodon orientalis* Borissyak 1918	Eocene/Oligocene, Asia	Bayshashov and Billia 2011
†*Colodon stovalli* Wilson and Schiebout 1984	Eocene, North America	Wilson and Schiebout 1984
†*Colodon woodi* Gazin 1956	Eocene, North America	Colbert and Schoch 1998

Five living species were described for *Tapirus* in South and Central America and southeastern Asia. Genus *Tapirus* was more diverse in the past (Janis 1984). Thirty fossil species have been described for it, occupying regions in Europe, Asia, North, Central and South America. Amongst other characteristics, the presence of a mobile proboscis is attributed to all *Tapirus* (Janis 1984).

Although many works have studied Tapiridae species in the past decades, it is still controversial to differentiate some extinct species of *Tapirus* from Tapiridae non-*Tapirus* ones

(Ferrero and Noriega 2012). An aspect that introduces confusion in this matter regards the usage of dental characters to describe extinct species. Despite the several characters that help identifying a living tapir, some dental features are frequently interpreted wrongly and/or are not sufficient when applied for the identification of extinct species. For instance, the bilophodonty degree in upper premolars and molars is characteristic to all *Tapirus* (1984), but many Asian and European extinct Tapiridae without a clear distinction of two lophs have been assigned to *Tapirus*. Many *Tapirus* species have also been previously described based on a few teeth or based on one tooth only. This is problematic if we consider that there are few morphological dental relevant differences between *Tapirus* species, the most significant being their size (Tong et al. 2002; Perini et al. 2011, Dumba et al, 2022).

Morphometric analysis have provided important contributions to better understanding the evolution of morphological patterns in the literature (Dumbá et al. 2019, 2022). In chapter 1, this thesis aims to analyze wide teeth traditional morphometric *Tapirus* data to test previous hypotheses that stated that the most significant differences between *Tapirus* species teeth are due to its size and not shape. Following morphometric results and statistical analyses, we studied patterns of seed dispersion evolution in *Tapirus* through the calculation of the occlusal surface area (OSA) available for chewing. We tested OSA as a predictor for seed dispersal capacity in tapirs, using data available in the literature for the dispersion status of *T. indicus*, *T. bairdii*, T. *pinchaque* and *T. terrestris*. Therefore, we identified a more reliable use for tapir teeth, the most common type of data in museum collections for this group. We also provided evidences that can help preserve current and future tropical forest ecosystems, by confirming previous hypotheses that presented tapirs as seed dispersers. Chapter 1 was published at the Biological Journal of the Linnean Society (Dumbá et al. 2022).

Regarding the phylogenetic aspects of Tapiridae, few attempts were made in order to establish phylogenetic hypotheses to this group, being the most recent the ones that included only South American, Asian and North American species (Hulbert 2010, Holanda and Ferrero 2012; Cozzuol et al. 2013, 2014). Until phylogenetic relations between European and other tapirids is further studied, time and place where the family diverged cannot be estimated with precision. This fact claims the attention to the necessity of building more complete hypotheses that also include European *Tapirus* in phylogenetics assessments of Tapiridae. Therefore, in chapter 2, the present work presents the widest taxa sampled phylogeny of Tapiridae so far, based on cranial and dental morphological qualitative and quantitative characters. Maximum parsimony and Bayesian inferences were performed, the latter approach with the Mkv model (Lewis 2001), widely used in the literature for morphological evolutionary studies (Casali et al.

2022). Divergence times estimations were also made through Bayesian analysis. Based on the phylogenetic results, a biogeographic analysis was made. Biogeographic models DIVA and DEC, available in the BioGeoBEARS package of R programming environment were applied to the topologies obtained. Chapter 2 included species from 6 out of 10 Tapiridae genera: *Tapirus*, *Paratapirus*, *Protapirus*, *Nexuotapirus*, *Colodon* and *Plesiotapirus* (see Table 1). *Tapiriscus*, *Eotapirus*, *Miotapirus* and *Tapivarus* were not included in phylogenetic and biogeographic inferences due to the lack of complete cranial materials, at least to our knowledge. Chapter 2 will be submitted soon to a scientific journal.

Regarding this Doctorate, many museum collections were visited abroad (which are detailed in Acknowledgments section of chapters 1 and 2). Morphometric data obtained were sent to curators of those museum collections, in order to contribute with the preservation of data.

Objectives

I) Test for significant morphological and size differences between cheek teeth of *Tapirus* species using Traditional Morphometric and statistical approaches;

II) Calculate cheek teeth OSA for living and extinct *Tapirus* and use it as a seed dispersal predictor for tapir species, based on seed dispersal information available in the literature;

III) Build morphological hypotheses for the phylogeny of Tapiridae based on qualitative and quantitative cranial, dental and postcranial characters, through Maximum Parsimony and Bayesian inferences;

IV) Propose divergence times estimates for Tapiridae, *Tapirus* and minor groups based on Bayesian analysis;

V) Analyze hypothesis of biogeographic events and ancestral geographic distributions that led to the current distributions of *Tapirus* through DEC and DIVA models.

Published on Biological Journal of the Linnean Society, 2022.

CHAPTER 1 - Dental occlusal surface and seed dispersal evolution in *Tapirus* (Mammalia: Perissodactyla)

LARISSA COSTA COIMBRA SANTOS DUMBÁ1,*, , FLÁVIO HENRIQUE GUIMARÃES RODRIGUES2, , JAMIE ALEXANDER MACLAREN3,4, and MARIO ALBERTO COZZUOL5,

1*Programa de Pós Graduação, Zoologia/Departamento de Zoologia, Instituto de Ciências Biológicas, Universidade Federal de Minas Gerais, Avenida Antônio Carlos 6627, Belo Horizonte, Minas Gerais, Brazil*

2*Departamento de Genética, Ecologia e Evolução, Instituto de Ciências Biológicas, Universidade Federal de Minas Gerais, Avenida Antônio Carlos 6627, Belo Horizonte, Minas Gerais, Brazil*

3*Evolution and Diversity Dynamics Laboratory, Department of Geology, Université de Liège, Quartier Agora, Allée du six Août 14, 4000 Liège, Belgium*

4*Functional Morphology Laboratory, Department of Biology, Universiteit Antwerpen, Universiteitsplein 1, 2610 Wilrijk, Antwerpen, Belgium*

5*Departamento de Zoologia, Instituto de Ciências Biológicas, Universidade Federal de Minas Gerais, Avenida Antônio Carlos 6627, Belo Horizonte, Minas Gerais, Brazil*

Received 8 October 2021; revised 3 February 2022; accepted for publication 3 February 2022

ABSTRACT

Most tapirs are good seed dispersers. An exception is the Malayan tapir, *Tapirus indicus*, a seed predator (mainly of large seeds). Little is known about the capacity for tapirs to disperse seeds throughout their evolutionary history. We used the occlusal surface area (OSA) of tapir cheek teeth as a predictor of seed dispersal potential in living and extinct tapir species. We used *T. indicus* as a reference for an extant tapir that mostly eats seeds. The OSA was calculated by multiplying the maximal width and length of molars and premolars. A threshold based on *T. indicus* OSA was projected onto a box plot analysis and used as a predictor for tapir seed dispersal potential. Ordination and statistical results suggest that tooth shape is uniform between *Tapirus* species and that size is the main factor affecting variation. Maxillary teeth show greater variation in shape than mandibular teeth between species. The results suggest that extant South American tapirs are good seed dispersers. North American tapirs present variable OSAs, and Asian tapirs have a low capacity for dispersion. All European tapirs were probably efficient seed dispersers. We present the first morphometric evidence for seed dispersal capacity in tapirs, with ramifications for tapir palaeoecology.

KEYWORDS: feeding adaptation – Mammalia – morphometrics – palaeoecology – teeth.

INTRODUCTION

Teeth are the most commonly preserved structures in vertebrate fossils (Famoso *et al.*, 2013). The morphology of these structures is key to understanding herbivorous mammal diets, such as those of perissodactyls (e.g. horses and tapirs). Herbivore teeth are effective food processors; their main function is to break down tough cell walls and release nutrients for enzymic digestion and absorption (Ungar, 2015). Successful mastication involves many complex processes, such as neural and sensory control and the combined actions of muscles, bones and teeth (Damuth & Janis, 2011; Ungar, 2015; Van Linden *et al.*, 2022); in addition, the study of tooth morphology in extant mammals allows inferences to be made about the feeding ecology of closely related extinct species (Ungar, 2015).

Among the extant Perissodactyla, the tapirs (Tapiridae) are widely regarded as having changed little in their dental shape and feeding ecology through time (DeSantis & MacFadden, 2007; Perini *et al.*, 2011). The crown group *Tapirus* includes the largest mammalian herbivores in South and Central American rainforests (Cozzuol *et al.*, 2013, 2014); all are brachydont (low-crowned; see Supporting Information, Figure S1) browsers (Bodmer, 1990), feeding mainly on a variety of herbs, leaves and fruits (Rodrigues *et al.*, 1993; Downer, 1996; Brooks *et al.*, 1997; Dumbá *et al.*, 2019). Sweet-tasting fruit seems to be the preferred forage for tapirs, both in captivity and in the wild (Janzen, 1982a; Bodmer, 1991; Downer, 1996). Tapirs are hindgut fermenters with an enlarged caecum; although large hindgut fermenters are known to feed mainly on low-quality forage (Demment & Van Soest, 1985; Bodmer, 1990), the selective browsing shown by tapirs suggests that they will select high-quality food (such as fruits) when available (Williams & Petrides, 1980; Bodmer, 1990). The majority of modern tapir species are involved in seed dispersal for a range of forest fruits (Olmos, 1997). Extant Neotropical tapirs (*Tapirus terrestris* Linnaeus, 1758, *Tapirus pinchaque* Roulin, 1829 and *Tapirus bairdii* Gill, 1865) are essential for rainforest fruiting trees and have been shown to be effective dispersers for seeds of varying size (Campos-Arceiz *et al.*, 2012). In contrast, the geographically (and somewhat morphologically) separate Malayan tapir, *Tapirus indicus* Desmarest, 1819, shows evidence of preferential predation of large seeds (> 20 mm; Campos-Arceiz *et al.*, 2012) rather than passing them whole through the digestive tract (Schwarm *et al.*, 2009). Nevertheless, *T. indicus* remains an important disperser for fruits with small seeds (< 20 mm; (Campos-Arceiz *et al.*, 2012). There would, therefore, appear to be a distinct difference in the treatment of large seeds during feeding by modern Neotropical and Asian tapir species.

Neotropical tapirs are considered effective dispersers of large-seeded plants, such as palms (Fragoso, 1997; Giombini *et al.*, 2009), but also act as predators of large seeds (Janzen,

1982a, b). Their position on the seed disperser–predator spectrum seems to depend on the plant species and its seed composition (Janzen, 1982a; Brooks *et al.*, 1997; Campos-Arceiz *et al.*, 2012), ultimately meaning that modern Neotropical tapirs disperse large seeds more frequently. It is not known whether the digestive tract of *T. indicus* is more hostile to large seeds, although there is recent evidence suggesting that *T. indicus* possesses higher bite forces than modern Neotropical tapirs (even when corrected for body size; Van Linden *et al.*, 2022). Whatever the causative agent, the result is that *T. indicus* is a notably poorer large seed disperser in comparison to other extant tapir species (Campos-Arceiz *et al.*, 2012). In fact, when compared with other ungulates, tapirs are known to be very inefficient seed predators (Bodmer, 1991) and have been diagnosed as long-distance dispersers (Olmos, 1997), potentially providing a maintenance or engineering service for their habitats. Despite many articles being dedicated to the study and understanding of modern tapir feeding ecology and tapir tooth evolution (e.g. Williams & Petrides, 1980; Janzen, 1981, 1982a; Williams, 1984; Brisola, 1989; Bodmer, 1991; Downer, 1996; Rodrigues *et al.*, 1993; Perini *et al.*, 2011), little is known about the capacity for tapirs to disperse and predate seeds through their evolution.

Intuitively, tapirs with smaller teeth have lower occlusal surface areas (OSAs) available for chewing and are therefore expected to have less effective mastication and better dispersal potential for all seed types. For tapirs with larger teeth (and often larger skulls and bite forces; see Van Linden *et al.*, 2022), it is logical that only seeds large and/or strong enough to withstand the power stroke of mastication will be dispersed. This a priori assumption leads us to infer that tooth size (and corresponding OSA for seed processing) should be a solid indicator for seed dispersion or seed predation by different tapir species. The OSA is related directly to the quantity of food that can be caught between the upper and lower tooth rows, and the usage of OSA as a predictor of chewing effectiveness assumes that an increase in OSA is directly correlated with the amount of food processed between upper and lower tooth rows during mastication (Pérez-Barbería & Gordon, 1998). We therefore hypothesize that tapir species with large teeth, such as *T. indicus*, will have greater OSA available for mastication and will present increased killing effectiveness and lower dispersion rates for large seeds. The opposite would be true for species with small teeth. Based on dispersal data available for extant *Tapirus* species (in the papers by Brooks *et al.*, 1997; Campos-Arceiz *et al.*, 2012), we calculated OSA per extant tapir species and related it to their corresponding dispersion potential to build an ecomorphological feeding bracket/threshold. Finally, based on this feeding bracket, we inferred the seed dispersion/predation potential for tapirs with no dispersion information currently available, including extinct tapirs from around the world and the recently described *Tapirus*

kabomani Cozzuol *et al*., 2013, and place our results into an ecological/palaeoecological context.

MATERIAL AND METHODS

Specimens

Images of skulls and complete (or near-complete) tooth rows of 24 *Tapirus* species were collected first hand and from published sources. Owing to the variable presence/absence of upper and lower tooth rows in fossilized tapirs, two separate datasets were used: lower dentition and upper dentition (Supporting Information, Tables S1 and S2). Fourteen species yielded data for both upper and lower dentition. The complete list of specimens, dental age per specimen, locality and references is given in the Supporting Information (Tables S3–S6). Only premolars and first and second molars (Figs 1, 2) were included, as specimens with m3/M3 erupted are scarce No sexual dimorphic variation is observed in the tapir cranium (Rojas *et al.*, 2021), hence sex was not accounted for in our analysis.

Morphometric measurements

Tooth shape was quantified using length and width measures of the upper and lower check teeth. Linear measurements were taken using scaled photographs and images from published articles. The tooth row was placed parallel to a scale bar such that all orientations of the photographs taken were the same for each specimen. Measurements were recorded in ImageJ (Schneider *et al.*, 2012). Lower dentition measurements followed the methods of Perini *et al.*, (2011) (Figure 1); measurements for upper teeth followed the methods of Hulbert (2005) (Figure 2). Adult specimens, identified by the full eruption of M2/m2 (Hulbert *et al.*, 2009; Cozzuol *et al.*, 2014; Moyano & Giannini, 2017), were preferred. Analysing only adult specimens removed the risk of ontogenetic allometry in occlusal surfaces. Premolars and molars were measured; incisors and canines of tapirs are not heavily involved in mastication (Winkler & Kaiser, 2015) and therefore do not present significant occlusal areas of interest in the present study.

Ordination analyses

Linear measurements were analysed initially using principal components analyses (PCA) to extract the main axes of sample variation. The PCAs were performed using Past v.4.03 (Hammer *et al.*, 2001), with iterative imputations to reduce the effect of missing values. Two separate datasets were used for upper (N = 80) and lower (N = 127) tooth shape and area analyses (Supporting Information, Table S1), maximizing species coverage. Species-averaged PCAs was performed to investigate dental shape across different time bins (Upper Miocene,

Pliocene and Pleistocene–Holocene) and allowing for equal numerical comparisons (mean values taken for species with multiple specimens).

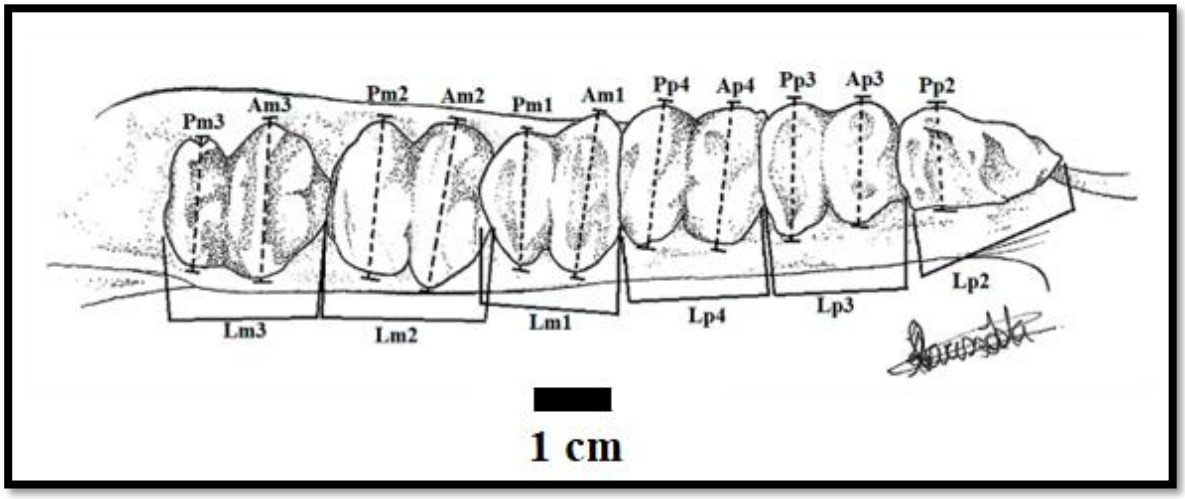

Figure 1. Representation of the occlusal view of a *Tapirus* left hemimandible, showing the 17 measurements taken for characterizing lower cheek teeth (following Perini *et al.*, 2011). Length measurements are taken from the tips of the bracket lines (maximal length of tooth). Abbreviations: Am1, width of the anterior portion of m1; Am2, width of the anterior portion of m2; Am3, width of the anterior portion of m3; Ap3, width of the anterior portion of pm3; Ap4, width of the anterior portion of pm4; Lm1, length of m1; Lm2, length of m2; Lm3, length of m3; Lp2, length of pm2; Lp3, length of pm3; Lp4, length of pm4; Pm1, width of the posterior portion of m1; Pm2, width of the posterior portion of m2; Pm3, width of the posterior portion of m3; Pp2, width of posterior portion of pm2; Pp3, width of posterior portion of pm3; Pp4, width of posterior portion of pm4. Illustration drawn by L.C.C.S.D.

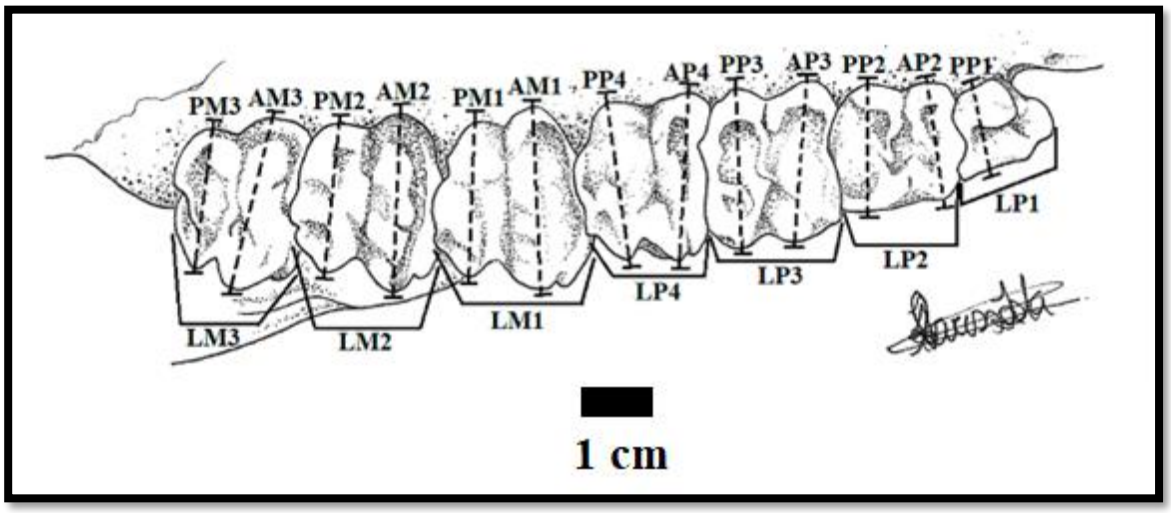

Figure 2. Representation of the occlusal view of *Tapirus* left maxillary premolars and molars, showing the 20 measurements taken for characterizing upper cheek teeth (following Hulbert, 2005). Length measurements are taken from the tips of the bracket lines (maximal length of tooth). Abbreviations: AM1, width of the anterior portion of M1; AM2, width of the anterior portion of M2; AM3, width of the anterior portion of M3; AP2, width of the anterior portion of PM2; AP3, width of the anterior portion of PM3; AP4, width of the anterior portion of PM4; LM1, length of M1; LM2, length of M2; LM3, length of M3; LP1, length of PM1; LP2, length of PM2; LP3, length of PM3; LP4, length of PM4; PM1, width of the posterior portion of M1; PM2, width of the posterior portion of M2; PM3, width of the posterior portion of M3; PP1, width of the posterior portion of PM1; PP2, width of the posterior portion of PM2; PP3, width of the posterior portion of PM3; PP4, width of the posterior portion of PM4. Illustration drawn by L.C.C.S.D.

Occlusal surface area

Cheek-tooth (molars and premolars) OSA has been measured in previous studies of ungulate feeding behaviour by multiplying, for each tooth, the maximum width by the length (Janis, 1988, 1995; Pérez-Barbería & Gordon, 1998); we follow this procedure in the present work. Cheek teeth in tapirs present a nearly quadrangular shape (Figs 1, 2), which allows an easy application of this technique. Skulls and complete (or nearly complete) tooth rows of 22 *Tapirus* species were analysed for upper dentition OSA (80 specimens), with 16 *Tapirus* species being analysed for lower dentition OSA (130 specimens) (Supporting Information, Table S2). After calculating the OSA for each tooth along the tooth row, we summed the values to obtain the final tooth row OSA per specimen in square millimetres (upper and lower separately). Final OSA values were visualized using univariate box plots, one for upper and one for lower tooth row OSAs. Box plot visualizations were performed in Past v.4.03, graphically depicting the OSA range per species. Species with only one specimen available were represented by a single line in the graph.

Seed dispersal capacity

To evaluate the capacity for seed dispersal in each tapir species, we extracted dispersion and predation data from published sources (Janzen, 1982a; Williams, 1984; Brisola, 1989; Bodmer, 1991; Downer, 1996; Rodrigues *et al.*, 1993; summarized by Olmos, 1997; Campos-Arceiz *et al.*, 2012). Successful 'seed predation' has been defined by the absence of defecated seeds, excretion of crushed seed cases and/or intestinal germination of the seeds (Janzen, 1982a; Williams, 1984), whereas successful 'seed dispersion' has been defined as at least some of the seeds being unbroken in the final stages of digestion in the gut, and subsequent excretion of a viable seed. Tapir seed dispersal comparisons for large- and small-seeded plant species have been documented in the past (Neotropical spp. reviewed by Olmos, 1997; Malayan assessed by Campos-Arceiz *et al.*, 2012). Using these published accounts of seed dispersal/predation by four extant tapir species (*T. bairdii*, *T. terrestris*, *T. pinchaque* and *T. indicus*), we present a qualitative and quantitative comparison between modern species (Figure 3). Seed size has not been quantified uniformly in these previous studies, with some authors categorizing seeds as 'small', 'medium' or 'large' and others using seed length as a continuous variable (L.C.C.S.D., pers. obs.). In the present study, we do not favour either approach; rather, we offer visual representations of collated seed dispersal data from numerous sources and provide both quantitative (where possible) and qualitative information based on seed size and tapir dispersal efficacy (Figure 3). For the purposes of this comparison, we consider seeds with < 25% survival

as being predated, > 50% survival as being dispersed and 26–49% survival as being poorly dispersed

(Figure 3). These collated data were then compared qualitatively with our OSA results for modern tapirs and placed into a palaeoecological context with regard to the dispersal potential for extinct tapir species.

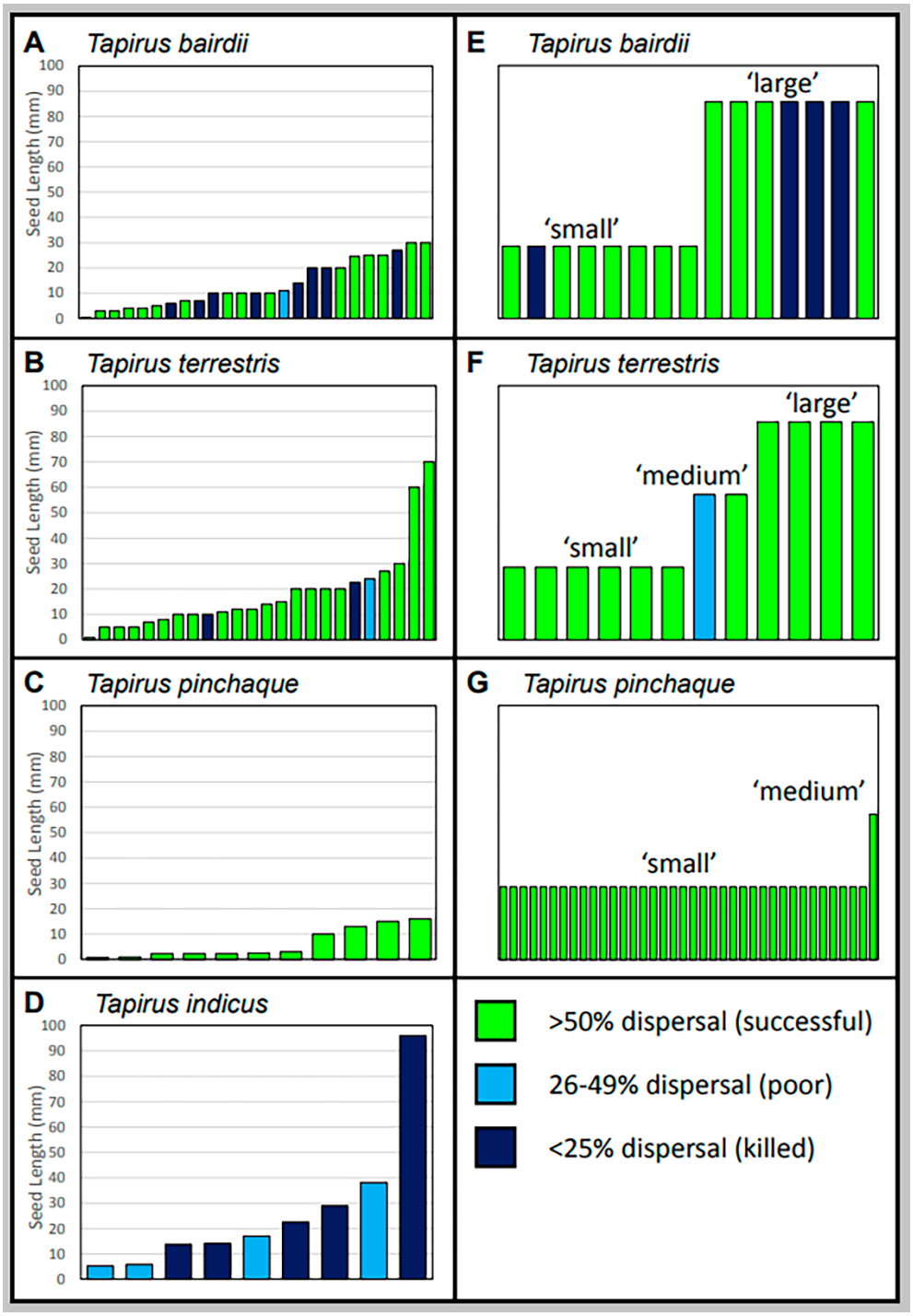

Figure 3. Quantitative and qualitative summation of available seed dispersal data for four extant tapirs (*Tapirus bairdii*, *Tapirus terrestris*, *Tapirus pinchaque* and *Tapirus indicus*). A–D, quantitative seed size and dispersal information was collated from published works detailing seed length (in millimetres)

and dispersal by tapirs. E–G, qualitative dispersal data were collated from published works that provided only categorical estimates of seed size (‘small’, ‘medium’ and ‘large’), with no continuous scale; no qualitative dispersal data are available at this time for *T. indicus*. Seed species are plotted along the *x*-axis; details of plant species, seed size, dispersal data and sources can be found in the Supporting Information, Tables S3 to S6.

Statistical analyses

To investigate interspecific differences in tooth shape from linear measurements of both upper and lower cheek teeth, principal component (PC) scores were assessed using a non-parametric permutational multivariate analysis of variance (PerMANOVA) capable of handling cases with only one sample. Pairwise comparisons were performed to detect whether significant differences were present between dental morphospace occupation by each species. The PerMANOVA results were corrected for multiple comparisons using a Holm–Bonferonni correction; the Holm–Bonferroni correction was chosen in this study to avoid false positives attributable to the high number of samples for some species vs. others (Holm, 1979). Also to avoid false positives, the value of α was set at 0.01 (99%). To establish whether tapir species could be identified from linear measurements of dentition, a linear discriminant analysis and classification table were used to test for accurate identification to species level. A high percentage classification would indicate greater potential for using dental measurements to identify tapirs at the species level. Classifications were jackknifed (leave-one-out cross-validation) to ensure that the inclusion of certain species or specimens did not skew the results. Species-averaged PC scores were also examined using a PerMANOVA to test for significant differences in morphospace occupation between geological epochs (Upper Miocene, 13.7–5.3 Mya; Pliocene, 5.3–2.6 Mya; Pleistocene, 2.6–0.01 Mya).

To test for significant differences between OSA ranges, two separate tests were performed. First, to investigate all species in the study, a non-parametric Kruskal–Wallis test was used to compare differences in median values across the univariate data; the non-parametric Kruskal–Wallis test was chosen because it can accommodate samples with only one sample. Dunn’s post hoc test for pairwise comparisons was performed, with Holm–Bonferroni corrections for multiple comparisons (Holm, 1979). Second, a subset of the data that consisted of species with at least two representatives was tested using a parametric one-way analysis of variance (ANOVA) to test for differences between sample means; this test was not possible mathematically for species with fewer than two specimens. A post hoc Tukey’s honest significant difference (HSD) test was implemented for pairwise comparisons, using Bonferroni-style adjustments for multiple comparisons derived from Holland & Copenhaver (1988).

Finally, mean average OSAs for species with upper and lower tooth rows available were compared using an ordinary least squares regression to determine whether upper and lower tooth row occlusal areas exhibit a strong correlation relationship, or whether species with, for example, large upper tooth rows do not have correspondingly large lower tooth rows. Given that all specimens used were adults, variation in the upper/lower tooth row OSAs of species with only a few available tooth rows were not considered to have affected the regression result.

All statistical analyses were performed in Past v.4.03, with an α value of 0.01 (99%) to avoid false positives in data with greatly different sample sizes; comparisons between species averaged data, where sample sizes were roughly equal, with less risk of false positives, were assessed with an α of 0.05 (95%). Statistical analyses results (tables S7 to S15) are available in the online version of this article at the publisher's web-site.

RESULTS

Shape analysis

Principal components analysis morphospaces based on linear measurements for both upper and lower tooth rows exhibit very high percentage variation along PC1 (Figure 4, upper teeth, 84.4%; Figure 5, lower teeth, 74.6%). Loadings for all PCs are available in the Supporting Information (Figs S2–S7). Loadings on PC1 for both upper and lower tooth rows (Supporting Information, Figs S2, S5) are all positively correlated, strongly implying that measurement magnitude (i.e. size) is the major factor contributing to variance along PC1; any morphospace overlap between species along PC1 is therefore interpreted as representing similarity in tooth size (and size-correlated variation in shape) between species. This pattern was not unexpected, because dental shape has been hypothesized to vary very little between tapirs (Guérin & Eisenmann, 1994; Perini *et al.*, 2011). It was important for the estimation of OSA as a dispersal proxy to establish that tooth shape was not radically different between tapir species; we therefore tested statistically all axes that were not correlated with size (PC2–PC17) to investigate significant differences in species occupation of morphospace.

The morphospace of upper teeth PC2 (7.9%) vs. PC3 (1.7%) (Figure 4B) demonstrates a large degree of species overlap; the most notable exception is *Tapirus indicus*, which occupies regions with low PC2 values. PerMANOVA incorporating PC2–PC17 (i.e. those not strongly correlated with size) suggests overall significant differences between teeth; pairwise comparisons for upper and lower teeth suggest several pairwise differences common for both tooth rows, predominantly between modern South American species (*T. terrestris* and *T. kabomani*) and other taxa with more than one sample (excel files, Tables S7 and S8), but also between *T. indicus* and other modern species. Linear discriminant analysis based on PC2 and

PC3 scores for the upper tooth row measurements suggests only 10.23% accurate species assignment, indicating very low discriminatory power for tapir upper teeth using linear measurements and excluding size (Table S9).

The morphospace of lower tooth row PC2 (8.63%) vs. PC3 (4.30%) (Figure 5B) again describes a large degree of overlap in tooth shape between species; discriminant analysis based on PC2 and PC3 (Figure 5B) suggests only 15.75% accurate species assignment, again indicating very low discriminatory power for tapir lower teeth using linear measurements exclusive of size information (Table S10). Classification tables for linear discriminant analysis can be found in the Supporting Information, Tables S3 and S4. Species averaged morphometric data were analysed using a PerMANOVA to investigate differences in the shape/size of teeth through three time bins (Upper Miocene, Pliocene and Pleistocene); all PC axes were used, including the 'size axis' PC1, in order to examine overall tapir dental patterns through time. No overall significant difference was identified for upper or lower teeth ($P > 0.05$); however, pairwise comparisons suggested that Pliocene and Pleistocene species included in this sample exhibit significant differences from one another in upper tooth size/shape (Table S11), with a near-significant value ($P = 0.052$) for lower teeth between the same time bins (Table S11).

Overall, our shape analyses indicate that tooth size is the major factor influencing the variation in species; we therefore conclude that tooth shape (independente of size) will have had minimal influence on differences in OSA available for chewing between species, because OSA is a size-dependent analysis.

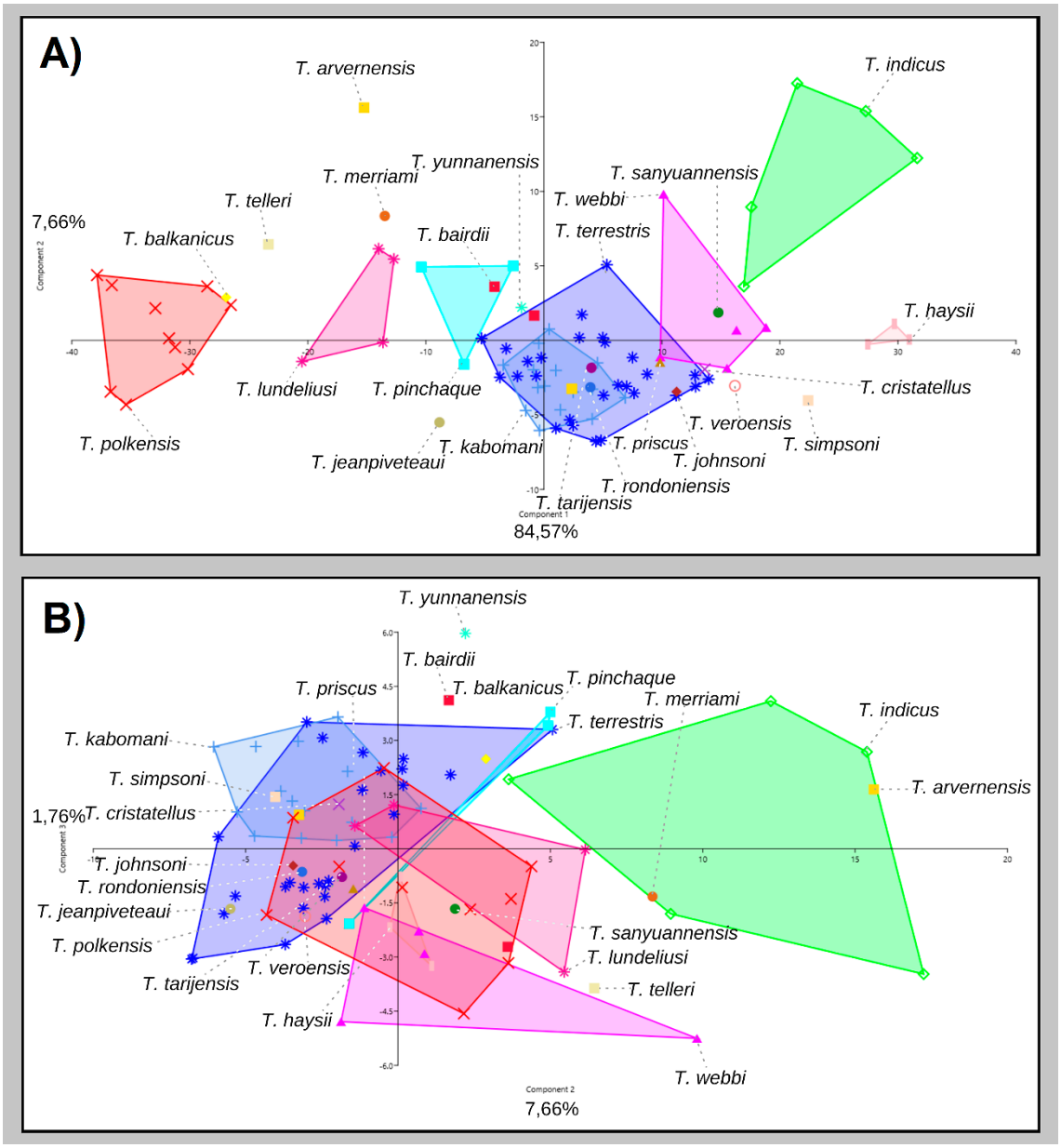

Figure 4. Principal components analysis (PCA) of complete upper dentition, using traditional morphometry (*N* = 88) and performed in Past v.4.03. A, principal component (PC)1 (84.57%) vs. PC2 (7.66%). B, PC2 (7.66%) vs. PC3 (1.76%). Extant species: *Tapirus terrestris* (dark blue stars), *Tapirus kabomani* (blue '+' symbols), *Tapirus pinchaque* (blue filled squares), *Tapirus bairdii* (red filled squares) and *Tapirus indicus* (green diamonds). Extinct species: *Tapirus cristatellus* (purple '×'), *Tapirus veroensis* (pink circles), *Tapirus sanyuanensis* (green dots), *Tapirus haysii* (pink bars), *Tapirus yunnanensis* (blue stars) *Tapirus webbi* (pink filled triangles), *Tapirus priscus* (dark yellow filled triangle), *Tapirus simpsoni* (peach filled square), *Tapirus lundeliusi* (pink stars), *Tapirus polkensis* (red triangles), *Tapirus arvernensis* (yellow filled triangle), *Tapirus merriami* (brown filled circle), *Tapirus telleri* (beige filled square), *Tapirus jeanpiveteaui* (beige filled circle), *Tapirus tarijensis* (purple filled circle), *Tapirus rondoniensis* (blue filled circle), *Tapirus balkanicus* (yellow filled circle) and *Tapirus johnsoni* (brown filled diamond).

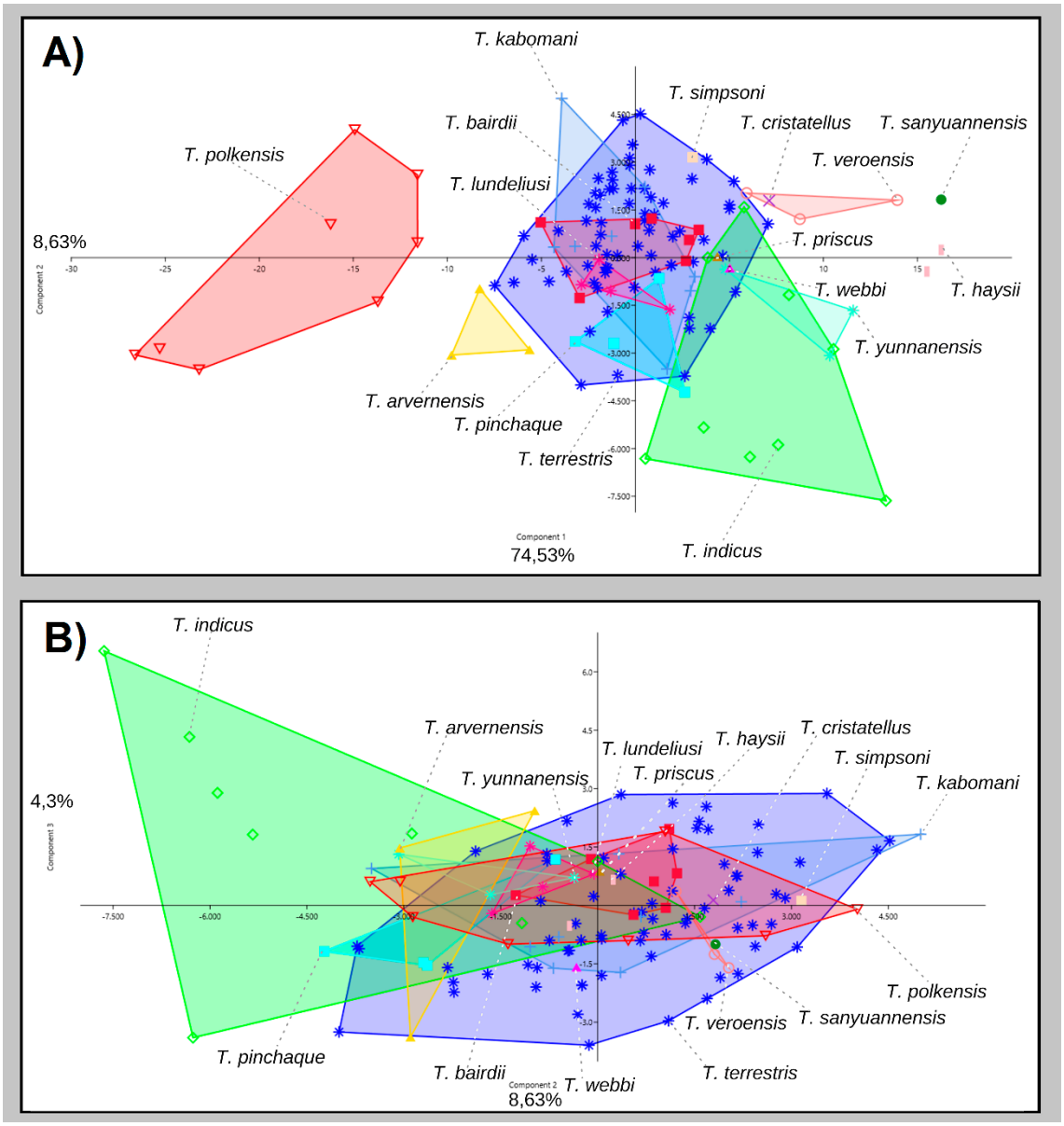

Figure 5. Principal components analysis (PCA) of complete lower dentition, using traditional morphometry (*N* = 127) and performed in Past v.4.03. A, principal component (PC)1 (74.53%) vs. PC2 (8.63%). B, PC2 (8.63%) vs. PC3 (4.30%). Extant species: *Tapirus terrestris* (dark blue stars), *Tapirus kabomani* (blue '+' symbols), *Tapirus pinchaque* (blue filled squares), *Tapirus bairdii* (red filled squares) and *Tapirus indicus* (green diamonds). Extinct species: *Tapirus cristatellus* (purple '×'), *Tapirus veroensis* (pink circles), *Tapirus sanyuanensis* (green dots), *Tapirus haysii* (pink bars), *Tapirus yunnanensis* (blue stars), *Tapirus webbi* (pink filled triangle), *Tapirus priscus* (dark yellow filled triangle), *Tapirus simpsoni* (peach filled square), *Tapirus lundeliusi* (pink stars), *Tapirus polkensis* (red inverted triangles) and *Tapirus arvernensis* (yellow filled triangle).

Box plot analysis of seed dispersal capacity

Box plots present the ranges of OSA values per species (single value for species with one representative) and are split by geographical region representing the known occurrence of each species (upper tooth row, Figure 6; lower tooth row, Figure 7).

Given that the modern Malayan tapir, *T. indicus*, is inferred as a predator of big seeds, we include a shaded region in Figures 6 and 7 representing the range of the lower 50% of *T. indicus* OSAs. Tapir OSAs shown below this threshold are inferred as generally good dispersers of multiple sizes of seed (such as the modern *T. terrestris*, *T. pinchaque* and *T. bairdii*; Figs 6, 7), whereas tapirs shown above the threshold are inferred as capable of predominantly killing larger seeds and dispersing very small seeds that might escape the power stroke during mastication. Species falling within the threshold may or may not be (or have been) good dispersers, because there is intraspecific variation within *T. indicus* itself (Campos-Arceiz *et al.*, 2012). By using dispersion data from living species and taking those species as a model for past tapir ecology (Figure 3), we infer whether fossil species were or were not good seed dispersers.

Upper tooth row OSA

Figure 6 shows upper tooth row OSA per *Tapirus* species examined in this study. Almost all tapirs in the study fall below the threshold defined by the OSA range of *T. indicus* (Figure 6); the only species that present upper OSAs exceeding the transitional region are the Late Miocene *Tapirus webbi*, the Pleistocene *Tapirus haysii* and *T. simpsoni* (species from North America). The absence of multiple Asiatic species in the upper OSA data precludes comprehensive conclusions on that geographical region, although estimates of body size for several Asiatic tapir species indicate comparable or greater sizes than *T. indicus* (MacLaren *et al.*, 2018), suggesting that comparable upper tooth row OSAs might be expected. Based on the upper OSA box plot, most tapirs in this sample (including all South American and European species) would be more effective seed dispersers than *T. indicus*. Non-parametric Kruskal–Wallis testing on the full sample of species with OSAs available (22 spp.) suggested significant differences across sample medians for the entire sample; pairwise comparisons using Dunn's post hoc are presented in Table S12. Pairwise differences were found to be significant between the modern *T. indicus* and most South American species (excluding *Tapirus mesopotamicus*, $P = 0.297$; *Tapirus tarijensis*, $P = 0.499$) and between *T. indicus* and all Eurasian species except for *T. priscus* ($P = 0.553$). The Miocene dwarf tapir *Tapirus polkensis* exhibited the most significant differences in median maxillary OSA values from the other taxa, most notably from the reputedly 'large tapirs' *T. haysii*, *T. webbi* and *T. indicus*. Parametric ANOVA testing on a

subsample of species with at least two specimens (ten spp.) suggested overall significant differences in the sample means; pairwise comparisons using Tukey's HSD post hoc test are presented in Table S13. Highly significant differences between subsample means were identified between most pairs. *Tapirus webbi* exhibits significantly different mean OSAs from all other species in the subsample, and both *T. indicus* and *T. polkensis* again exhibit significant differences from most other species. Notably, extant Neotropical tapirs (*T. terrestris*, *T. kabomani*, *T. pinchaque* and *T. bairdii*) exhibit no significant differences from one another in upper tooth row OSA.

It is possible that the upper tooth row size (and occlusal area) might be influenced by overall cranial morphology (Dumbá *et al.*, 2019; Van Linden *et al.*, 2022) or by factors not directly related to feeding (Zhou *et al.*, 2019). In contrast to the cranium (and associated upper tooth row), the mandible and lower tooth row are almost exclusively involved in feeding. Given that the lower teeth act on food items during food processing more directly than the upper teeth (F.H.G.R. pers. obs.), we believe that lower tooth row OSA might show a more targeted signal determining whether seeds will be crushed or dispersed.

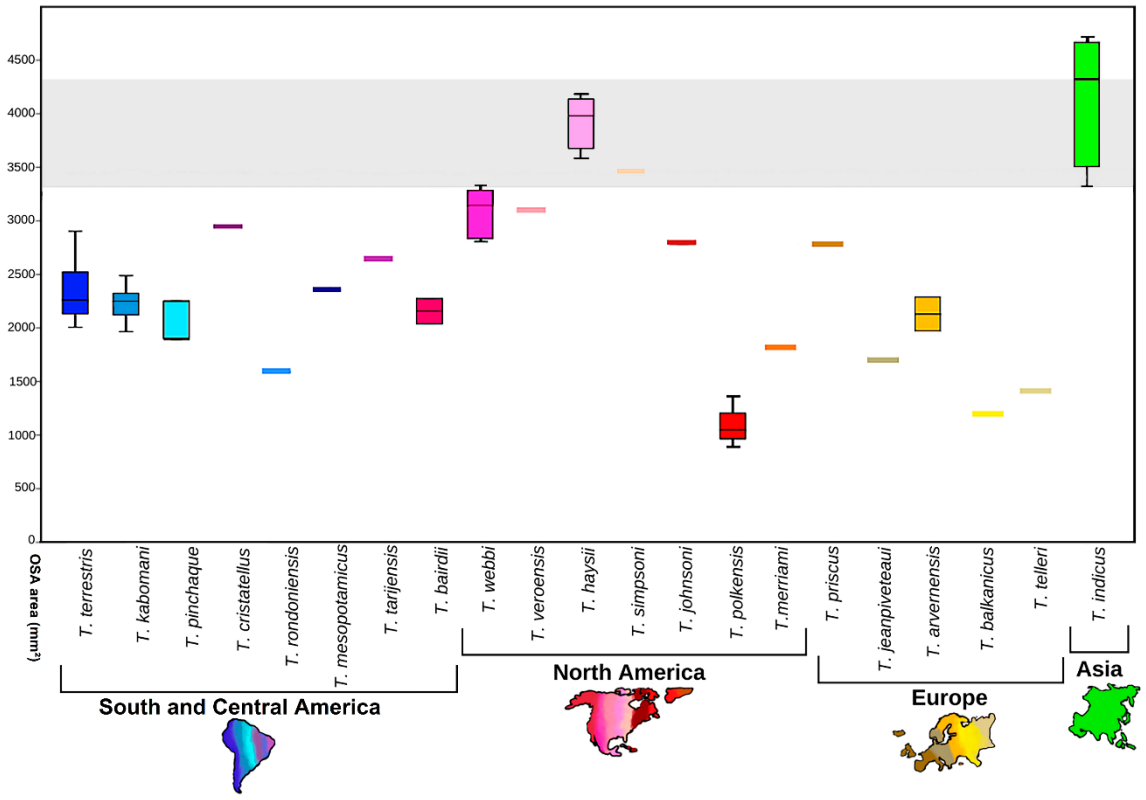

Figure 6. Box plot of occlusal surface area (OSA) for upper dentition. The *y*-axis represents OSA (in square millimetres). *Tapirus* species are listed according to their geographical locality. Species represented by a single coloured line were sampled by a single specimen. The predicted seed predation/dispersion threshold is represented by the grey horizontal region. Box plots were performed in Past v.4.03; all colours, continent shapes and the grey transition threshold were added in Adobe Photoshop and Adobe Sketch programs.

Lower tooth row OSA

Box plots of lower teeth OSA are presented in Figure 7. The means for all but one of the South American species fall below the transitional area (*Tapirus cristatellus*, *N* = 1), suggesting that South American tapirs have notably smaller lower tooth row OSAs and might therefore be better seed dispersers. This finding is strongly supported by both qualitative and quantitative seed dispersal results for modern South American species (Figure 3). The only Neotropical tapirs that fall above that strip in this analysis (*T. cristatellus*, < 5% of *T. terrestris*) were probably bad dispersers of large seeds. The modern Central American tapir *T. bairdii* is here inferred as an efficient disperser based on OSA, falling below the threshold; this is also supported by seed size and dispersal data (Figure 3; see Brookes *et al.*, 1997). Despite its large size (Quse & Fernandes-Santos, 2014), the lower tooth row specimens of *T. bairdii* (*N* = 8) in this study demonstrated comparable OSAs to the overall smaller *T. terrestris*, *T. kabomani* and *T. pinchaque* (Figure 7) and yield no significant differences in OSA from these species after Dunn's or Tukey's HSD pairwise testing tables S12 to S15. North American *Tapirus* exhibit a wide range of OSA conditions: *T. webbi*, *Tapirus veroensis* and *T. haysii* have large lower OSAs, particularly large in *T. haysii* (Figure 7). In contrast, the dwarf tapir *T. polkensis* has the lowest OSA of all species sampled.

European species (*N* = 2) demonstrate divergent scores, with *T. priscus* well within the range of *T. indicus* but the smaller *T. arvernensis* far below the threshold; this suggests that *T. arvernensis* was probably a better disperser of small and large seeds than *T. priscus*, with the latter potentially acting as a successful seed predator.

Regarding the Asiatic species, our lower tooth row OSA data show that all species were likely to be poor dispersers of large seeds, with all species falling within or above the threshold. Kruskal–Wallis tests on the full mandibular sample (16 spp.) suggested significant differences across sample medians; pairwise comparisons using Dunn's post hoc test are presented in table S14. Significant differences in median lower OSA values were found mostly between the dwarf *T. polkensis* and all other species apart from *T. arvernensis* and *Tapirus lundeliusi* (table S14). The modern *T. indicus* differs significantly from modern Neotropical species and smaller North American (*T. polkensis* and *T. lundeliusi*) and Eurasian species (*T. arvernensis*) represented by more than one specimen (table S15. The ANOVAs on a subsample of species with at least two lower tooth rows (13 spp.) suggested overall significant differences in the sample means; pairwise comparisons using Tukey's HSD post hoc test are presented in table S15. Highly significant differences are identified between several pairs. Modern Neotropical species

especially demonstrate multiple pairwise differences from extinct and modern species; however, modern Neotropical tapirs demonstrate no significant differences from one another (P = 1). *Tapirus indicus* exhibits significantly different mean OSAs from most species, with the exception of the Eurasian *T. priscus*, *Tapirus sanyuanensis* and *Tapirus yunannensis* and the larger species from the subgenus *Helicotapirus* (*T. veroensis* and *T. haysii*). As with maxillary OSA, *T. polkensis* exhibits multiple pairwise significant differences, the only exception being the Pliocene *T. arvernensis*.

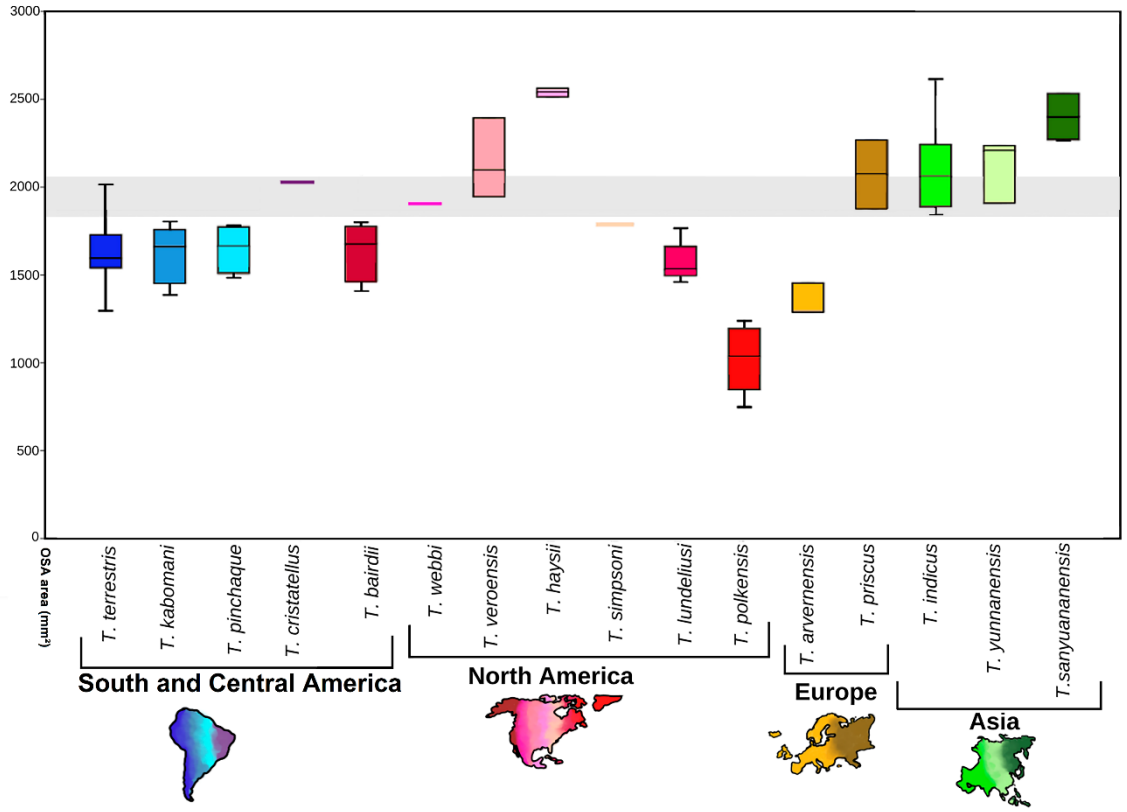

Figure 7. Box plot of occlusal surface area (OSA) for lower dentition. The *y*-axis represents OSA (in square millimetres). *Tapirus* species are listed according to their geographical locality. Species represented by a single coloured line were sampled by a single specimen. The predicted seed predation/dispersion threshold is represented by the grey horizontal region. Box plots were performed in Past v.4.03; all colours, continent shapes and the grey transition threshold were added in Adobe Photoshop and Adobe Sketch programs

Correlation between upper and lower OSA

Upper and lower tooth row OSAs were regressed against one another using an ordinary least squares regression), for species exhibiting full complements of both upper and lower dentition (N = 15), revealing a strong positive correlation (R^2 = 0.762) between upper and lower OSAs (Figure 8). Notable similarities in mean OSA values in the biplot are revealed between the

extant Neotropical tapirs *T. kabomani*, *T. terrestris* and *T. bairdii*, matching results from ANOVA and Tukey's HSD pairwise comparisons on both upper and lower OSA values. Given that the mean OSA values for upper and lower tooth rows are well correlated, and in accordance with the lower tooth row being involved more exclusively in feeding (e.g. Zhou *et al.*, 2019), we posit that (in cases where both lower and upper teeth OSAs are available) focus should be centred on lower tooth row OSA as a better indicator of seed dispersal patterns within the genus *Tapirus*.

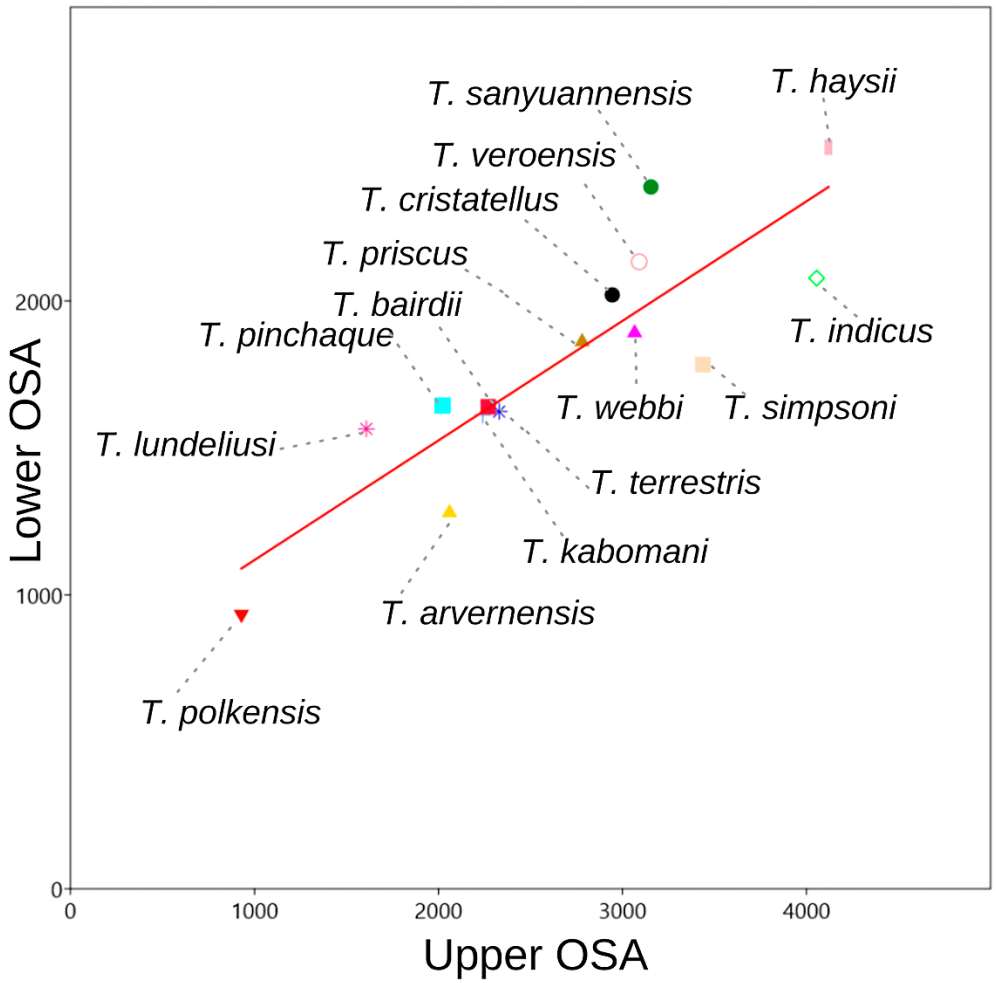

Figure 8. Ordinary least squares regression of species average OSAs for tapir species that presented both upper and lower tooth rows. The regression revealed a strong positive correlation (R^2 = 0.762).

DISCUSSION

In this study, we have assessed tooth shape and size quantitatively in a wide range of tapir species, demonstrating that there is little variability in dental shape (from linear

morphometrics) when size is removed. When we focus on a specific aspect of size (the OSA of the cheek tooth row), we can see clear differences between modern Neotropical and Asiatic species of tapir, and these differences seem to match very well with observed differences in seed dispersal potential. Here, we highlight our findings with respect to known tapir biology and place our conclusions in a palaeoecological framework.

Little variation in tapir tooth shape

Regarding the morphometric shape analysis including complete dentition, it can be concluded that size is the most diagnostic variable for tapir teeth [as shown in previous studies (Perini *et al.*, 2011) and confirmed quantitatively in the present study]. Tooth size seems to track body size in most tapir species, with the notable exception of the modern Central American tapir *T. bairdii*. This species is widely regarded as the second largest tapir in the world (Quse & Fernandes-Santos, 2014) and is the largest herbivore in the Neotropics, yet tooth measurements and OSA box plots (Figs 6, 7) in this study suggest similar size and shape to other Neotropical species, such as *T. pinchaque* (the smallest modern tapir). These data match those on lower dentition in previous studies (Perini *et al.*, 2011). Olmos (1997) found an overall seed dispersion rate of 76.5% for *T. bairdii*; it is possible that small-sized teeth, and consequently low OSAs, might contribute to a considerably high dispersion rate in this large species, which presents an interesting future direction to investigate in the evolution of this lineage with regard to evolutionary pressures favouring selection for proportionally small teeth in a large rainforest ungulate species. Recent biomechanical evidence exploring bite forces and skull strength in tapirs corroborate the OSA results for *T. bairdii*; estimated bite forces for this species are comparable to those for *T. terrestris* and *T. pinchaque* (Van Linden *et al.*, 2022), but the presence of a sagittal table in this species allows for higher mechanical efficiency during mastication (DeSantis *et al.*, 2020), allowing for the processing of larger seeds than *T. terrestris* or *T. pinchaque* (Janzen 1982b; O'Farrill *et al.*, 2013), despite the similar small tooth OSA.

Regarding the differences in tooth shape, the upper teeth seem to be more diagnostic for the species studied. Visually, the upper teeth have a more variable shape between them (and between species) than the lower teeth. This situation is problematic, because lower tooth shape (only) has been used in the past to describe new extinct tapir species (Tong, 2005; Holanda & Cozzuol, 2006; Holanda & Ferrero, 2012). The morphometric data and statistical analyses generated in the present study indicate a lack of interspecific discriminatory power available from studying upper or lower dentition from tapirs; this is exceedingly important for future phylogenetic studies on tapirs, which must turn the focus towards cranial and postcranial material wherever possible, in addition to robust dental characters. Previous literature suggests

that tapirs do not present remarkable craniodental differences when compared with other mammalian genera (Guérin & Eisenmann, 1994; Dumbá *et al.*, 2019); and, apart from some nasal retraction and sagittal crest development, very little morphological change has occurred in the tapir cranium during the course of *Tapirus* evolution (Radinsky, 1965; Dumbá *et al.*, 2019). Thus, it is possible that species currently recognized as *Tapirus* that are morphometrically distinct from modern tapirs in both size (PC1; OSAs) and shape (PC2–PC17) might not represent the genus *Tapirus s.s.* The phylogeny of the Tapiridae is in dire need of revision such that further conclusions about craniodental evolution in these animals can be made within a stable phylogenetic framework. Irrespective of this, our study offers a quantitative warning for research based solely on dental morphological evolution in tapirs (and other animals), which must take into account the poor discriminatory power that dental shape seems to offer and shift focus to more morphofunctional aspects (e.g. dental complexity, food-processing biomechanics and herbivore–plant interactions) in order to gain greater insights.

Occlusal surface area and seed dispersal in modern tapirs

From the evidence of previous studies investigating seed dispersal in tapirs (e.g. Campos-Arceiz *et al.*, 2012), *T. indicus* is not a good disperser of big seeds; this is probably attributable, in part, to the large skull offering greater muscle attachment and higher bite force application (Van Linden *et al.*, 2022), in addition to the size of its dentition and, consequently, the large available occlusal surface to process the seeds. The morphometric analyses carried out here generated quantitative information about the teeth of tapirs with a broad temporal, geographical and phylogenetic scope, much of which has been unavailable until now. Within modern tapirs (*T. bairdii*, *T. terrestris*, *T. kabomani*, *T. pinchaque* and *T. indicus*) there is clearly a disparity in dental size (Figs 4A, 5A, PC1 vs. PC2, Figure 8; tables S13–S15), a disparity in dental shape (Figs 4B, 5B, PC2 vs PC3; tables S7–S10) and a disparity in seed dispersal performance (Figure 3). Given that these modern species appear clearly separated from one another when all these factors are considered, it can be concluded that the large dentition (lower and upper), hence large processing area of modern *T. indicus* plays a key role in predating seeds (particularly small and medium-sized seeds) rather than dispersing them as Neotropical tapirs do (Figure 3; Brooks *et al.*, 1997; Campos-Arceiz *et al.*, 2012). Given the size discrepancy between *T. indicus* OSAs and those of Neotropical species (significantly different areas; $P < 0.01$; tables S12–15), there would appear to be a direct relationship between organism size and OSA. However, the large size of tapirs does not seem to be the only explanation available, as evidenced by the large-bodied, small-toothed *T. bairdii*. Some large herbivores are known to

have small dentition in comparison to their body size (e.g. *Hippopotamus*), seemingly linked to their lower metabolic rate (Owen-Smith, 1988).

The OSA in tapirs represents a proxy for capacity to process food in the oral cavity and might therefore be linked (indirectly) with aspects of feeding physiology and metabolism. It could be argued that a smaller OSA indicates increased digestive efficiency and a longer transit time in the gut, which permits a more efficient absorption of nutrients (Owen-Smith, 1988). In the case of modern tapirs, this would indicate an increased digestive efficiency and, consequently, a lower dispersion rate for *T. bairdii* (76.5% dispersion rate; Olmos 1997) than is shown by *T. terrestris* (90.91% dispersion rate; Brisola, 1989; Bodmer, 1991; Rodrigues *et al.*, 1993) and *T. pinchaque* (98.84% dispersion rate; Downer, 1996). Nevertheless, the dispersion rate remains higher than that exhibited by *T. indicus* (Campos-Arceiz *et al.*, 2012). An increased digestive efficiency could, therefore, have overcome any strong selection for the oral mechanical processing of vegetation (Brooks *et al.*, 1997), which, along with increased mechanical efficiency of the skull (DeSantis *et al.*, 2020), could explain the proportionally small teeth in *T. bairdii*. Future studies relating dental processing capacity to metabolism and digestive efficiency in large herbivores will be required to establish exactly whether small dental dimensions in a large species could be an indicator of higher seed dispersal potential.

Occlusal surface area as a palaeoecological predictor

In this study, we found that average OSAs for upper and lower tooth rows appear well correlated at the species level (table S7); however, owing to the more direct functional utility of the mandible as a food-processing unit (Zhou *et al.*, 2019), we postulate that lower tooth row OSA might influence mastication more acutely compared with the upper OSA. Our discussion will therefore focus predominantly on results of the lower tooth row OSA available for chewing, and the consequences for seed dispersal potential in tapirs (Figure 7).

The OSA analysis performed here shows that, with the exception of *T. cristatellus*, the South American tapirs sampled have much smaller OSAs than *T. indicus* and are therefore interpreted as efficient dispersers (Figs 6, 7). The most effective South American disperser (*T. pinchaque*) is vital for habitat engineering, providing seed dispersal for numerous tree species in its montane habitat (Downer, 1996). Thus, comparing OSA values for this species and for *T. indicus* with OSA values recorded for extinct species will be of particular interest for inferring seed dispersal potential in poorly studied tapirs from modern and past ecosystems. No seed dispersal data are currently known for the recently described extant little black tapir, *T. kabomani*; from the results we have collected for OSA (Figs 6, 7), and based on tooth shape and size information (Figs 4, 5), we can infer that this species is most likely to be a efficient

disperser of small and large seeds. *Tapirus kabomani* exhibits few significant differences from other South American *Tapirus* species and falls below the threshold for dispersion in both Figures 6 and 7. Assuming that OSA calculated in the present study represents a solid proxy for seed dispersal potential in tapirs, our data highlight the immense importance of this species for maintaining the Amazonian forest it inhabits. Clearly, more research is required to observe behaviour and direct feeding ecology in this rarely seen species; however, we feel confident in our inference of *T. kabomani* as a successful and probably pivotal contributor along with *T. terrestris* to the maintenance of the Amazonian plant community.

Following the robust inference of *T. kabomani* as an important and successful seed disperser, we move to extinct tapir species to elaborate on their potential as plant community engineers in past ecosystems. When we consider the North American species, there is the potential for a confounding effect of size. The smallest known member of *Tapirus*, *T. polkensis*, was present in eastern North America (Gibson, 2011) and was part of a diverse Miocene–Pliocene megafaunal assemblage including browsing proboscideans (e.g. *Mammut*) and a range of other herbivorous mammals. Given that both proboscideans and tapirids are known to disperse seeds, it is possible that *T. polkensis* was a highly effective disperser of small seeds within its habitat, whereas the seed predation and large-seed dispersal niches might have been occupied by proboscideans (as they are today in Southeast Asia; Campos-Arceiz *et al.*, 2012).

In other ecosystems at different time periods, other tapirs seem to have adopted different roles. For example, the contemporaneous Late Miocene (Clarendonian–Hemphillian) species *T. webbi* and *Tapirus simpsoni* were both large species and both exhibit similar OSAs (Figs 6–8), whereas the contemporaneous Pleistocene tapir fauna, which included *T. haysii*, *T. veroensis* and *T. merriami* exhibit notable differences in OSA (Figure 6), with *T. merriami* exhibiting significant differences from *T. haysii*, and *T. veroensis* demonstrating a large range of values (tables S12–S15). The range of values recorded for *T. veroensis* might represent a certain amount of plasticity in diet for this species, which was very widespread across southern North America during the Pleistocene epoch (Hulbert *et al.*, 2009); *T. veroensis* is recorded as having the highest bite forces for Nearctic tapir species (Van Linden *et al.*, 2022), lending credence to the dietary plasticity for this taxon, which would have been capable of feeding on a wider range of vegetation than its contemporaries. *Tapirus haysii* is frequently cited as having been a large tapir (e.g. Hulbert, 1995); based on our calculated OSA values, we find this conclusion to be sustained, and it is therefore likely that *T. haysii* (and, to a certain extent, *T. veroensis*) was probably not as effective a seed disperser as the smaller, contemporaneous west-coast *T. merriami* or many of the previous species in North America (including its close phylogenetic

relative, *T. lundeliusi*; Hulbert, 2010). A tantalizing pattern emerged within the data in the present study, suggesting that there might be significant differences in tooth shape between Pliocene and Pleistocene tapirs (table S11), mirroring the patterns of biting mechanics recently exposed in Pleistocene tapirs (Van Linden *et al.*, 2022).

In stark contrast to the North American pattern, the majority of extinct European tapir species appear to have had the potential to be fairly successful seed dispersers (based mostly on upper OSA); this follows the observed pattern of small-sized tapirs being more efficient at dispersing seeds (or less efficient at predating them); consequently, the small OSA available for seed processing suggests that European tapirs would have been comparable habitat engineers to the tapirs of Central and South America today (Figs 6–8; tables S11–S15). The presence of only one widely recognized large tapir in Europe (*T. priscus*) and multiple smaller species (*T. arvernensis*, *Tapirus balkanicus*, *Tapirus telleri*, *Tapiriscus pannonicus*, etc.) seems to indicate that tapirs in Europe were not predominantly seed predators and probably occupied a niche as fruit and leaf eaters and seed dispersers. Previous studies show, through pollen records, that the Miocene Western Europe presented a subtropical–tropical to warm-temperate climate and vegetation (Moreno & Suc, 2007). These palaeoecological records suggest that this scenario was probably maintained by important seed dispersers that were fit for this environment. Given that living tapirs are inhabitants of such tropical–subtropical habitats, it is safe to assume that extinct species might have fed on comparable vegetation to living species (DeSantis, 2011). Our data, based on available OSAs, indicates that European *Tapirus* (with the oldest records described for the Middle Miocene) were good seed dispersers and therefore probably contributed to building and maintaining the Miocene European flora. Throughout the Miocene of Europe, several major climatic and faunal turnovers occurred (Vallesian Crisis turnover event and Messinian Salinity crisis; Casanovas *et al.*, 2014; Madof *et al.*, 2019), with tapirs persisting through the Miocene in Europe after the so-called ‘tapir vacuum’ (18–14 Mya; Van der Made, 2010). The presence of large, forest-based, brachydont herbivores, such as tapirs, performing successful seed dispersal throughout periods of climatic and faunal upheaval might well have facilitated recovery and periods of floral stability, providing an invaluable service for Late Miocene ecosystems in Europe.

Three of the better-known Asiatic tapirs were sampled for the present study (*T. indicus*, *T. sanyuanensis* and *T. yunnanensis*), with the exclusion of *Tapirus* (*Megatapirus*) *augustus* and several species known from very fragmentary remains (e.g. *Tapirus peii*; Ji *et al.*, 2015). All the species sampled fell within the seed-predation feeding bracket defined by *T. indicus* OSAs, irrespective of overall body size, and no significant differences were observed

between extinct species and the modern *T. indicus* (Figs 6, 7; tables S12–S15). This evidence, supported by high bite forces expected for other Asiatic (Indomalayan) tapirs (Van Linden *et al.*, 2022), tentatively suggests that extinct species of *Tapirus* in Asia probably processed seeds more successfully than species with smaller occlusal surfaces in other geographical regions. Subsequently, Asiatic tapirs offered less chance of leaving seeds intact and available for dispersion (unless the seeds were small enough to escape crushing during mastication).

CONCLUSION

Using a broad range of extant and extinct tapir specimens currently available, our morphometric and ecologically informed assessment of tapir dental shape and OSAs leads us to conclude that South American, early North American (Late Miocene–Pliocene) and European *Tapirus* species present high potential for successful seed dispersion and were most probably instrumental in the maintenance of floral communities in their respective habitats. In contrast, Pleistocene North American species and all sampled Asiatic species (Plio-Pleisto-Holocene) exhibit large occlusal surfaces for effective food processing and would probably have been poor dispersers of small seeds and capable predators of larger seeds. The Central American tapir *T. bairdii* presents an intriguing morphological condition, with relatively small OSAs in comparison to other modern species, despite retaining the ability to process some large seed species with its heightened mechanical efficiency during mastication. With the inclusion of more specimens (particularly of the modern *T. bairdii*) and expansive quantitative investigations into digestive physiology/processing, *in vivo* feeding mechanics and seed predation in multiple tropical vertebrate groups, a clearer outlook on the efficacy of tapirs as habitat engineers and floral community stewards throughout their evolution might be achieved. The combined understanding of the ecological interactions between megaherbivores and floral composition through time can better enable us to preserve and conserve current and future tropical forest ecosystems, including the seed dispersers and predators that inhabit them.

ACKNOWLEDGEMENTS

We would like to thank Dr Alexandre Salino for his contributions in the collecting of seed size data. We also thank Drs Ursula Menkveld-Gfeller, Loïc Costeur, Martina Schenkel, Olivier Pauwels and Joséphine Lesur for providing access to museums across Europe. We would like to thank three anonymous reviewers for their constructive comments on the manuscript. This project was funded by Coordenação de Aperfeiçoamento de Pessoal de Nível Superior doctoral funding (L.C.C.S.D.) and Fundação de Amparo à Pesquisa do Estado de Minas Gerais (M.A.C.), with additional funding for data collection from an Fonds

Wetenschappelijk Onderzoeken grant number 11Y7615N doctoral fellowship (J.A.M.). We have no conflicts of interest to declare.

DATA AVAILABILITY

Supplemental material is available in the Supporting Information. Other data underlying this chapter are available under reasonable request to the first author.

REFERENCES

Bodmer RE (1990). Fruit patch size and frugivory in the lowland tapir (Tapirus terrestris). Journal of Zoology 222: 121–128.

Bodmer RE (1991). Strategies of seed dispersal and seed predation in Amazonian ungulates. Biotropica 23: 255–261.

Brisola LM (1989). Estudo do hábito alimentar de Tapirus terrestris (Lineu 1778, Ordem Perissodactyla) e sua atuação como dispersor de sementes no Parque Estadual do Morro do diabo. B.Sc. Thesis, Universidade Estadual Paulista.

Brooks DM Bodmer ER Matola (1997). Tapirs: status survey and conservation action plan. Gland: IUCN.

Campos-Arceiz A, Traeholt C, Jaffar R, Santamaria L, Corlett RT (2012). Asian tapirs are no elephants when it comes to seed dispersal. Biotropica 44: 220–227.

Casanovas-Vilar I, van den Hoek Ostende LW, Furió M, Madern PA (2014). The range and extent of the Vallesian Crisis (Late Miocene): new prospects based on the micromammal record from the Vallès-Penedès basin (Catalonia, Spain). Journal of Iberian Geology 40: 29–48.

Cozzuol MA, Clozato CL, Holanda EC, Rodrigues FHG, Nienow S, de Thoisy B, Redondo RAF, Santos FR (2013). A new species of tapir from the Amazon. Journal of Mammalogy 94: 1331–1345.

Cozzuol MA, de Thoisy B, Fernandes-Ferreira H, Rodrigues FHG, Santos FR (2014). How much evidence is enough evidence for a new species? Journal of Mammalogy 95: 899–905.

Damuth J, Janis C (2011). On the relationship between hypsodonty and feeding ecology in ungulate mammals, and its utility in palaeoecology. Biological Reviews of the Cambridge Philosophical Society 86: 733–758.

Demment M, Van Soest PV (1985). A nutritional explanation for body-size patterns of ruminant and nonruminant herbivores. The American Naturalist 125: 641–672.

DeSantis LRG, MacFadden BJ (2007). Identifying forested environments in deep time using fossil tapirs: evidence from evolutionary morphology and stable isotopes. Courier-Forschungsinstitut Senckenberg 258: 147–157.

DeSantis LRG (2011). Stable isotope ecology of extant tapirs from the Americas. Biotropica 43: 746–754.

DeSantis LRG, Sharp AC, Schubert BW, Colbert MW, Wallace SC, Grine FE (2020). Clarifying relationships between cranial form and function in tapirs, with implications for the dietary ecology of early hominins. Science Reports 10: 8809.

Downer CC (1996). The mountain tapir, endangered ‘flagship’ species of the high Andes. Oryx 30: 45–58.

Dumbá LCCS, Parisi Dutra R, Cozzuol MA (2019). Cranial geometric morphometric analysis of the genus Tapirus (Mammalia, Perissodactyla). Journal of Mammal Evolution 26: 545–555.

Eisenberg JF, Groves CP, MacKinnon K (1990). Tapirs, p. 598 - 608. In Parker, SB (ed.), Grzimek's Encyclopedia of Mammals, volume 4. New York: McGraw-Hill, Inc.

Famoso NA, Feranec RS, Davis EB (2013). Occlusal enamel complexity and its implications for lophodonty, hypsodonty, body mass and diet in extinct and extant ungulates. Palaeogeography, Palaeoclimatology, Palaeoecology 387: 211–216.

Fragoso JMV (1997). Tapir-generated seed shadows: scale-dependent patchiness in the Amazon rain forest. Journal of Ecology 85: 519–529.

Gibson ML (2011). Population structure based on age-class distribution of Tapirus polkensis from the gray fossil site Tennessee. MSc. Thesis, East Tennessee State University. Paper 1267.

Giombini MI, Bravo SP, Martínez MF (2009). Seed dispersal of the palm Syagrus romanzoffiana by tapirs in the semi-deciduous Atlantic forest of Argentina. Biotropica 41: 408–413.

Guérin C, Eisenmann V (1994). Les tapirs (Mammalia, Perissodactyla) du Miocène supérieur d'Europe occidentale. Geobios 27: 113–127.

Hammer Ø, Harper DAT, Ryan PD (2001). PAST: Paleontological statistics software package for education and data analysis. Palaeontologia Electronica 4: 9.

Holanda EC, Cozzuol MA (2006). New records of Tapirus from the late Pleistocene of southwestern Amazonia, Brazil. Revista Brasileira de Paleontologia 9: 93–200.

Holanda EC, Ferrero B (2012). Reappraisal of the genus Tapirus (Perissodactyla, Tapiridae): systematics and phylogenetic affinities of the South American tapirs. Journal of Mammalian Evolution 20: 33–44.

Holland BS, Copenhaver MD (1988). Improved Bonferroni-type multiple testing procedures. Psychological Bulletin 104: 145–149.

Holm S (1979). A simple sequentially rejective multiple test procedure. Scandinavian Journal of Statistics 6: 65–70.

Hulbert RC Jr (1995). The giant tapir, Tapirus haysii, from Leisey Shell Pit lA and other Florida Irvingtonian localities. Bulletin of the Florida Museum of Natural History 37: 515–551.

Hulbert RC Jr. (2005). Late Miocene Tapirus (Mammalia, Perissodactyla) from Florida, with description of a new species, Tapirus webbi. Bulletin of the Florida Museum of Natural History 45: 465–494.

Hulbert RC Jr (2010). A new early Pleistocene tapir (Mammalia: Perissodactyla) from Florida, with a review of Blancan tapirs from the State. Florida Museum of Natural History Bulletin 49: 67–126.

Hulbert RC Jr, Wallace SC, Klippel WE, Parmalee PW (2009). Cranial morphology and systematics of an extraordinary sample of the late Neogene dwarf tapir, Tapirus polkensis (Olsen). Journal of Paleontology 8: 238–262.

Janis CM (1988). An estimation of tooth volume and hypsodonty indices in ungulate mammals, and the correlation of these factors with dietary preference. In: Russell DE, Santoro JP, Sigogneau-Russell D (eds). Teeth revisited: proceedings of the seventh international symposium on dental morphology, Paris 1986. Paris: Mémoires du Muséum national d'Histoire naturelle, 367–387.

Janis CM (1995). Correlations between craniodental morphology and feeding behavior in ungulates: reciprocal illumination between living and fossil taxa. In: Thomason JJ (ed). Functional morphology in vertebrate paleontology, 76–98. Cambridge: Cambridge University Press, 76–98.

Janzen DH (1981). Digestive seed predation by a Costa Rican Baird's tapir (Tapirus bairdii). Biotropica 13: 59–63.

Janzen DH (1982a). Wild plant acceptability to a captive Costa Rican Baird's tapir. Brenesia 19/20: 99–128.

Janzen DH (1982b). Seeds in tapir dung in Santa Rosa National Park, Costa Rica. Brenesia 19/20: 129–135.

Ji XP, Jablonski NG, Tong HW (2015). Tapirus yunnanensis from Shuitangba, a terminal Miocene hominoid site in Zhaotong, Yunnan Province of China. Vertebrata PalAsiatica 53: 177–192.

Jiménez-Moreno G, Suc J-P (2007). Middle Miocene latitudinal climatic gradient in western Europe : evidence from pollen records. Palaeogeography, Palaeoclimatology, Palaeoecology 253: 224–241.

MacLaren JA, Hulbert RC, Wallace SC, Nauwelaerts S (2018). A morphometric analysis of the forelimb in the genus Tapirus (Perissodactyla: Tapiridae) reveals influences of habitat, phylogeny and size through time and across geographical space. Zoological Journal of the Linnean Society 184: 499–515.

Madof AS, Bertoni C, Lofi J (2019). Discovery of vast fluvial deposits provides evidence for drawdown during the late Miocene Messinian salinity crisis. Geology 47: 171–174.

Moyano SR, Giannini NP (2017). Comparative cranial ontogeny of Tapirus (Mammalia: Perissodactyla: Tapiridae). Journal of Anatomy 231:665–682.

O'Farrill G, Galetti M, Campos-Arceiz A (2013). Frugivory and seed dispersal by tapirs: an insight on their ecological role. Integrative Zoology 8: 4–17.

Olmos F (1997). Tapirs as seed dispersers and predators. In: Brooks DM, Bodmer RE, Matola S (compilers). Tapirs—status survey and conservation action plan. IUCN/SSC Tapir Specialist Group. Gland and Cambridge: IUCN, 3–9.

Owen-Smith N (1988). Megaherbivores: the influence of very large body size on ecology. Cambridge: Cambridge University Press.

Pérez-Barbería F, Gordon I (1998). The influence of molar occlusal surface area on the voluntary intake, digestion, chewing behaviour and diet selection of red deer (Cervus elaphus). Journal of Zoology 245: 307–316.

Perini FA, Oliveira JA, Salles LO, Moraes CR, Neto PG, Guedes LFB, Oliveira M (2011). New fossil records of Tapirus (Mammalia, Perissodactyla) from Brazil, with a critical analysis of intra-generic diversity assessments based on lower molar size variability. Geobios 44: 609–619.

Quse V, Fernandes-Santos RC (2014). Tapir Veterinary Manual (RC Quse, V., Fernandes-Santos, Ed.). IUCN/SSC Tapir Specialist Group.

Radinsky LB (1965). Evolution of the tapiroid skeleton from Heptodon to Tapirus. Bulletin of the Museum of Comparative Zoology 134: 69–106.

Rodrigues M, Olmos F, Galetti M (1993). Seed dispersal by tapir in southeastern Brazil. Mammalia 57: 460–461.

Rojas RR, Mora WV, Lozano EP, Herrera ERT, Heymann EW, Bodmer R (2021). Ontogenetic skull variation in an Amazonian population of lowland tapir, Tapirus terrestris (Mammalia: Perissodactyla) in the department of Loreto, Peru. Acta Amazonica 51: 311–322.

Schneider CA, Rasband WS, Eliceiri KW (2012). NIH Image to ImageJ: 25 years of image analysis. Nature Methods 9: 671–675.

Schwarm A, Ortmann S, Wolf C, Streich WJ, Clauss M (2009). More efficient mastication allows increasing intake without compromising digestibility or necessitating a larger gut: comparative feeding trials in banteng (Bos javanicus) and pygmy hippopotamus

(Hexaprotodon liberiensis). Comparative Biochemistry Physiology, A-Molecular and Integrative Physiology 152: 504–512.

Tong HW (2005). Dental characters of Quaternary tapirs in China, their significance in classification and phylogenetic assessment. Geobios 38: 139–150.

Ungar PS (2015). Mammalian dental function and wear: a review. Biosurface and Biotribology 1: 25–41.

Van der Made J (2010). Els macrovertebrats del Camp dels Ninots i el seu context: canvis ambientals, evolució i estructura social. In: Campeny Vall-llosera, G., Gómez de Soler B, ed. El Camp dels Ninots - Restres de l'Evolució. Tarragona: Ayuntament de Caldes de Malavella, Caldes de Malavella, & Institut Català de Paleoecologia Humana i Evolució Social 105–128.

Van Linden L, Stoops K, Dumbá LCCS, Cozzuol MA, MacLaren JA (2022). Sagittal crest morphology decoupled from relative bite performance in Pleistocene tapirs (Perissodactyla: Tapiridae). Integrative Zoology: 1–24. doi: 10.1111/1749-4877.12627.

Williams KD (1984). The entral American tapir (Tapirus bairdii) in northwestern Costa Rica. Dissertation Abstracts International, B (Sciences and Engineering) 45: 1075.

Williams KD, Petrides GA (1980). Browse use, feeding behavior, and management of the Malayan tapir. The Journal of Wildlife Management 44: 489–494.

Winkler DE, Kaiser TM (2015). Structural morphology of molars in large mammalian herbivores: enamel content varies between tooth positions. PLoS One 10: e0135716.

Zhou Z, Winkler DE, FortunyI J, Kaiser TM, Marcé-Nogué J (2019). Why ruminating ungulates chew sloppily: biomechanics discern a phylogenetic pattern. PLoS One 14: e0214510.

Supporting Information

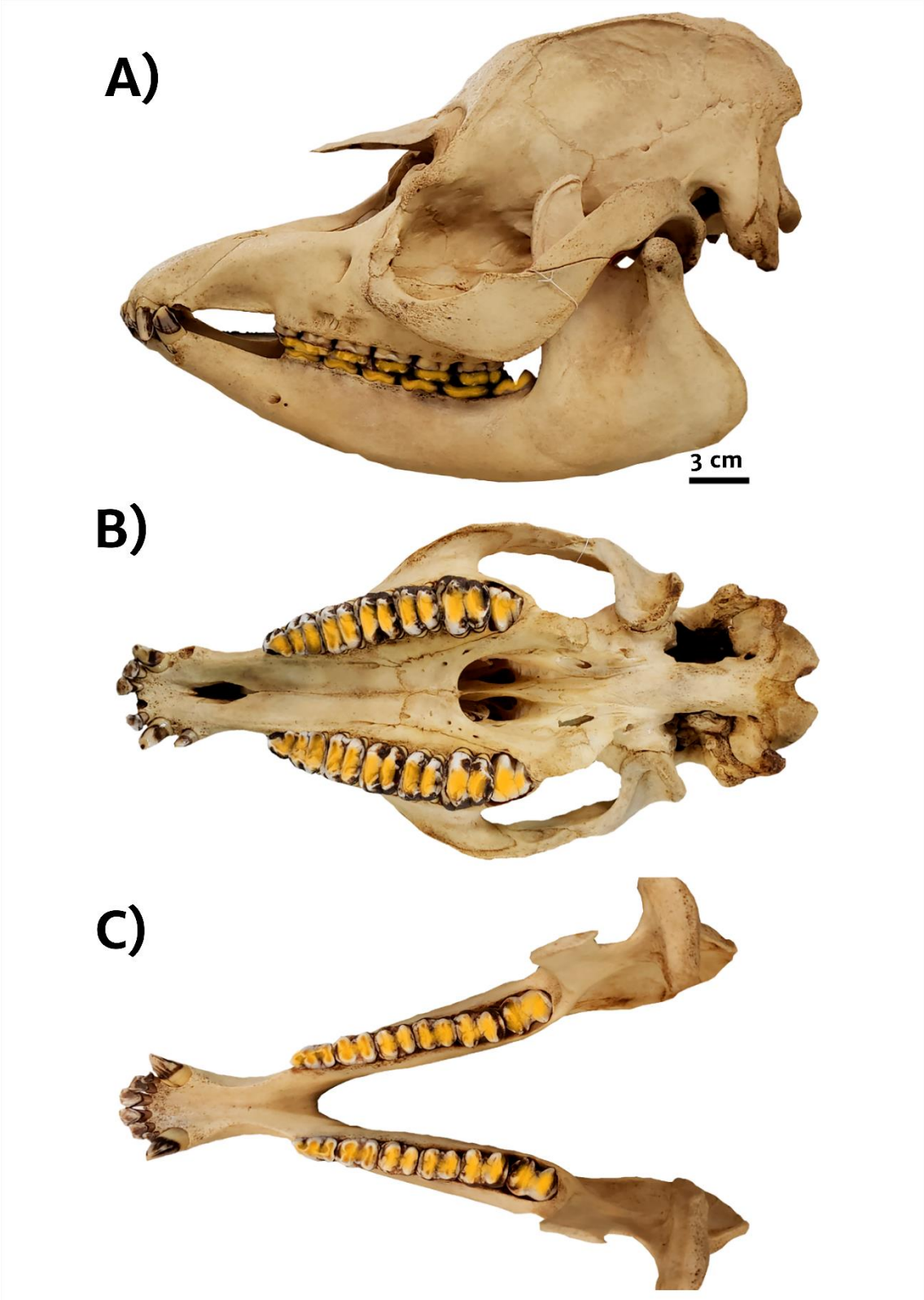

Figure S1. *Tapirus kabomani* holotype *UFMG 3177* illustrates the object of study of the present work: occlusal surface area (in yellow) of premolars and molars in adults (with M2/m2 fully grown). A, lateral view of the skull. B, ventral view of the skull. C, ventral mandibular view. In Figures S1–S7, 'Comp' means length, 'Lant' means anterior width and 'Lpos' means posterior width.

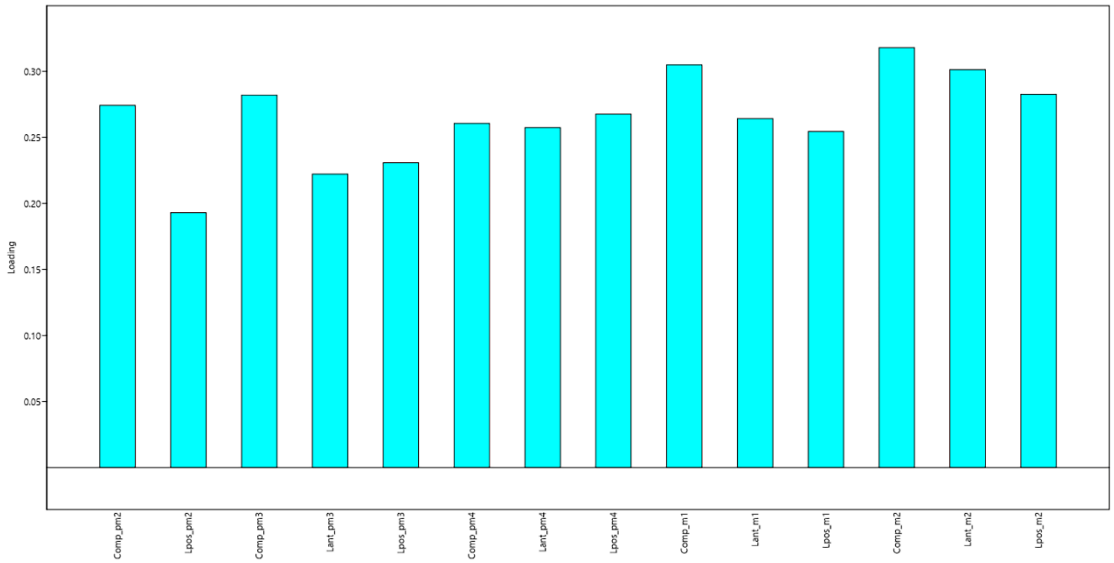

Figure S2. Loadings for principal component (PC)1 (representing size), in the lower teeth principal components analysis.

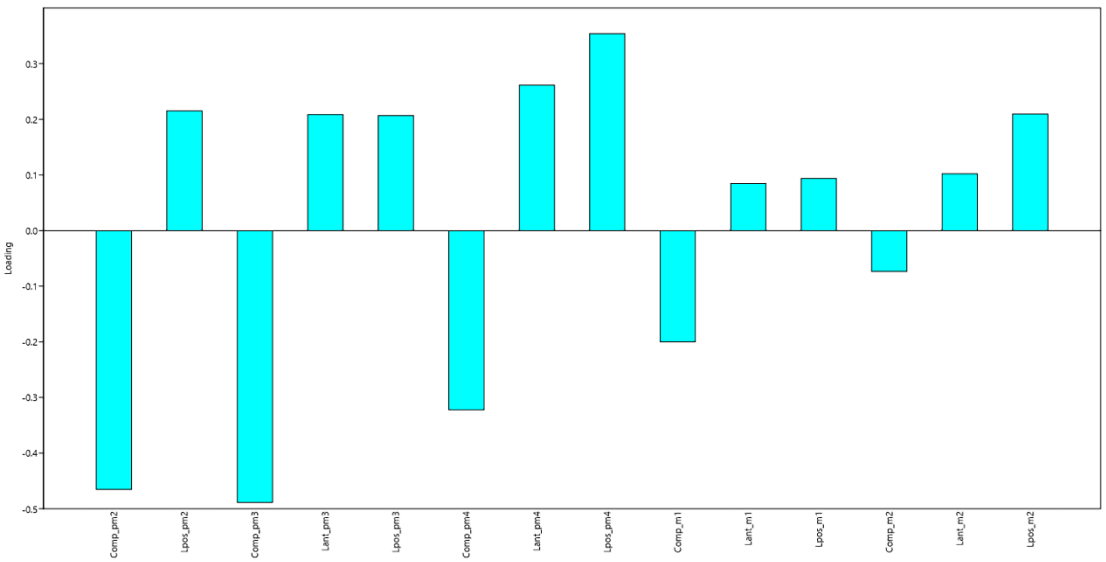

Figure S3. Loadings for principal component (PC)2 (mostly representing shape), in the lower teeth principal components analysis.

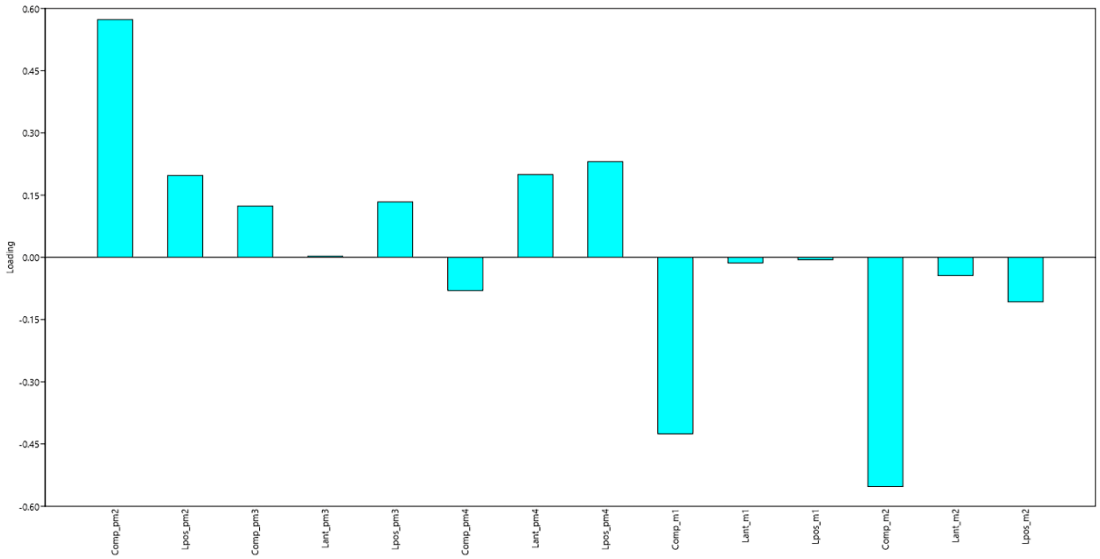

Figure S4. Loadings for principal component (PC)3 (mostly representing shape), in the lower teeth principal components analysis.

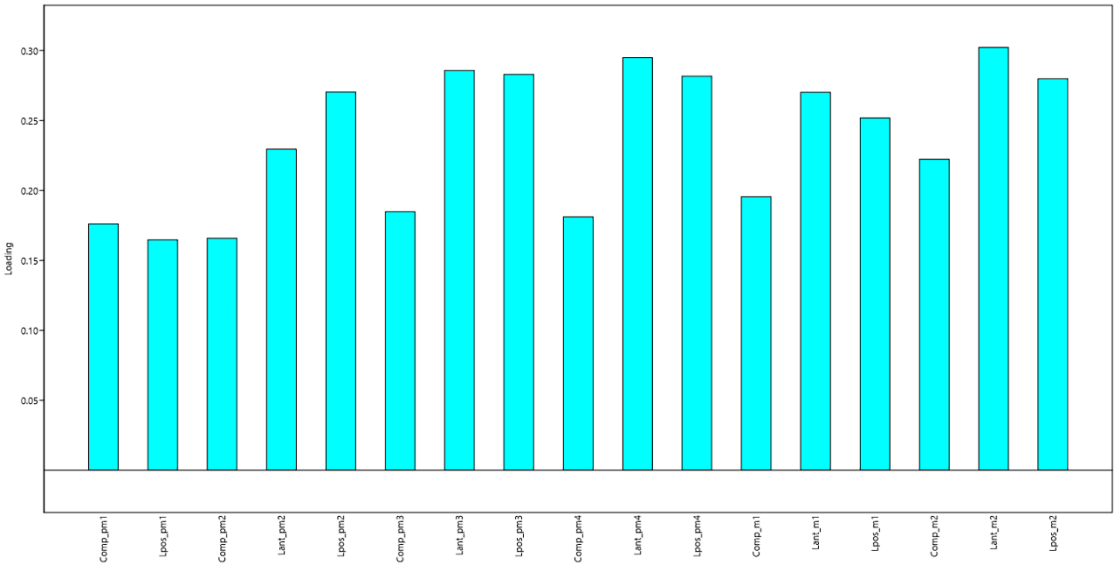

Figure S5. Loadings for principal component (PC)1 (representing size), in the upper teeth principal components analysis.

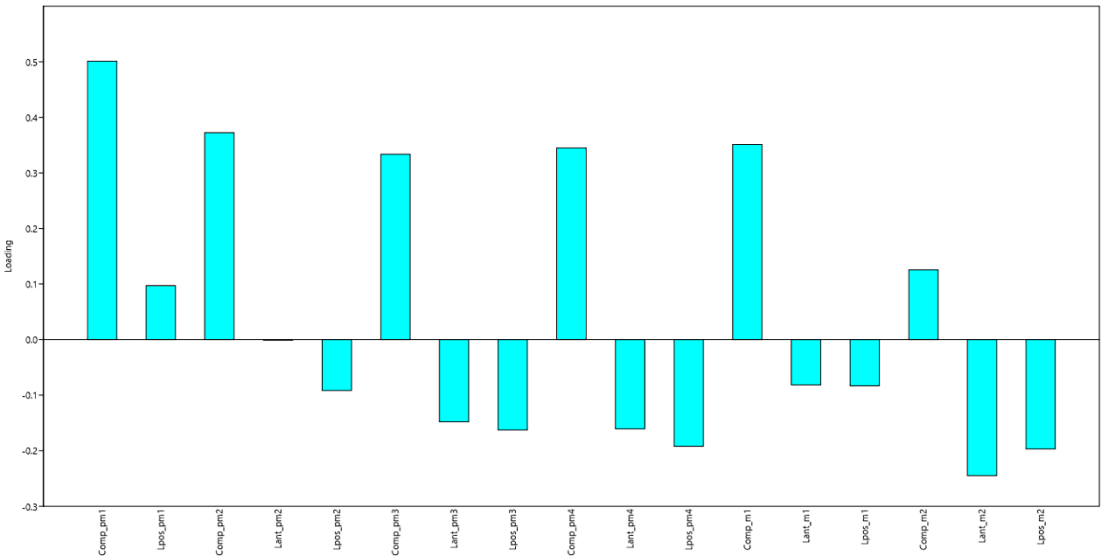

Figure S6. Loadings for principal component (PC)2 (mostly representing shape), in the upper teeth principal components analysis.

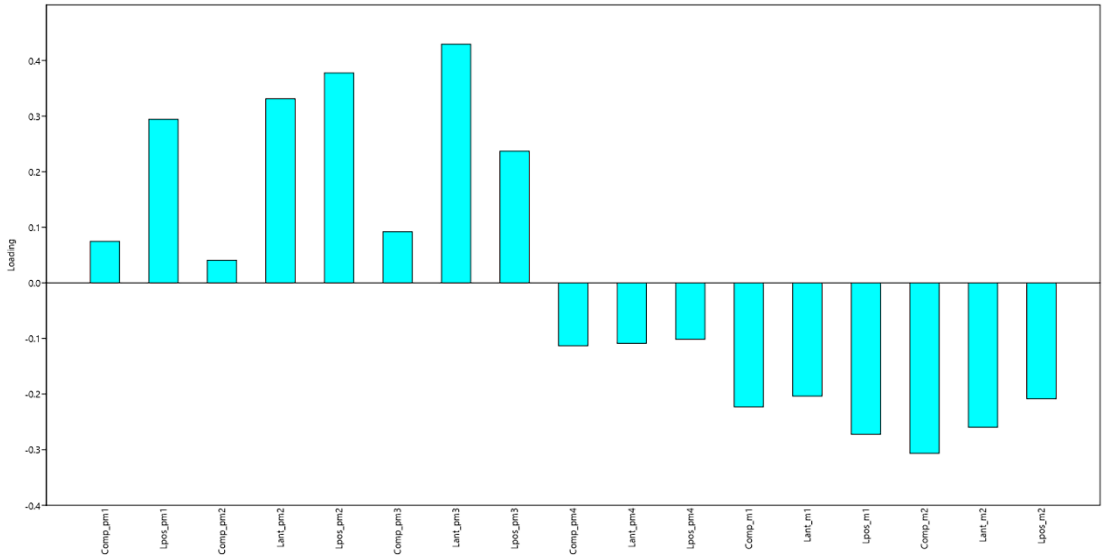

Figure S7. Loadings for principal component (PC)3 (mostly representing shape), in the upper teeth principal components analysis.

Table S1 - List of the 24 tapir species used in the PCA analysis. Genus and species are listed with age, locality, number of specimens (N), and presence/absence of upper and lower toothrow specimens.

Species	**Age**	**Location**	**Lower toothrow (n =127)**	**Upper toothrow (n =80)**
Tapirus terrestris	Holocene	South America	70	17
Tapirus kabomani	Holocene	South America	9	15
Tapirus bairdii	Holocene	South America	7	2
Tapirus pinchaque	Holocene	Central / South America	4	3
Tapirus indicus	Pleist. - Holocene	South-East Asia	9	7
Tapirus rondoniensis	Pleistocene	South America	0	1
Tapirus cristatellus	Pleistocene	South America	1	1
Tapirus veroensis	Pleistocene	North America	3	1
Tapirus sanyuannensis	Pleistocene	Asia	1	1
Tapirus arvernensis	Plio. - Pleistocene	Europe	3	2
Tapirus haysii	Plio. - Pleistocene	North America	2	3
Tapirus jeanpiveteaui	Pliocene	Europe	0	1

Tapirus lundeliusi	Pliocene	North America	4	4
Tapirus yunnanensis	Miocene	Asia	3	1
Tapirus webbi	Miocene	North America	1	5
Tapirus simpsoni	Miocene	North America	1	1
Tapirus priscus	Miocene	Europe	1	1
Tapirus polkensis	Miocene	North America	8	9
Tapirus johnsoni	Miocene	North America	0	1
Tapirus telleri	Miocene	Europe	0	1
Tapirus balkanicus	Miocene	Europe	0	1
Tapirus merriami	Miocene	North America	0	1
Tapirus tarijensis	Pleistocene	South America	0	1

Table S2 - List of the 24 tapir species used in the Boxplot analysis. Genus and species are listed with age, locality, number of specimens (N), and presence/absence of upper and lower toothrow specimens.

Species	**Age**	**Location**	**Lower toothrow (n = 130)**	**Upper toothrow (n =80)**
Tapirus terrestris	Holocene	South America	68	17
Tapirus kabomani	Holocene	South America	9	15
Tapirus bairdii	Holocene	Central / South America	7	2
Tapirus pinchaque	Holocene	South America	4	3
Tapirus indicus	Pleist. – Holocene	South-East Asia	11	7
Tapirus rondoniensis	Pleistocene	South America	0	1
Tapirus mesopotamicus	Pleistocene	South America	0	1
Tapirus cristatellus	Pleistocene	South America	1	1
Tapirus veroensis	Pleistocene	North America	3	1
Tapirus sanyuannensis	Pleistocene	Asia	2	0
Tapirus arvernensis	Plio. – Pleistocene	Europe	3	2
Tapirus haysii	Plio. – Pleistocene	North America	2	4
Tapirus jeanpiveteaui	Pliocene	Europe	0	1

Tapirus lundeliusi	Pliocene	North America	5	0
Tapirus yunnanensis	Miocene	Asia	3	0
Tapirus webbi	Miocene	North America	1	5
Tapirus simpsoni	Miocene	North America	1	1
Tapirus priscus	Miocene	Europe	1	1
Tapirus polkensis	Miocene	North America	8	9
Tapirus johnsoni	Miocene	North America	0	1
Tapirus telleri	Miocene	Europe	0	1
Tapirus balkanicus	Miocene	Europe	0	1
Tapirus merriami	Miocene	North America	0	1
Tapirus tarijensis	Pleistocene	South America	0	1

Table S3 - Traditional morphometry dental data acquired for PCA analysis - Lower teeth (n = 123). Specimen Age based on the eruption of molar teeth (tooth listed represents the last tooth to be fully erupted; derived from Hulbert 2010 age categories for tapirs).

Specimen	**Species**	**Collection**	**Age**	**Locality**
Perucho Verna	*T. terrestris*	unknown	m3	Perucho Verna, Entre Rios, Argentina
MN 57062	*T. terrestris*	Museu Nacional do Rio de Janeiro	m2	No locality data
MN 865	*T. terrestris*	Museu Nacional do Rio de Janeiro	m3	Porto Esperidião, MT, Brazil
MN 11976	*T. terrestris*	Museu Nacional do Rio de Janeiro	m3	Jacaré, Rio 7 de setembro, MT, Brazil

MN 32708	*T. terrestris*	Museu Nacional do Rio de Janeiro	m3	Xavantina, Rio das Mortes, MT, Brazil
MN 1605	*T. terrestris*	Museu Nacional do Rio de Janeiro	m2	No locality data
MN 1601	*T. terrestris*	Museu Nacional do Rio de Janeiro	m2	No locality data
MN 866	*T. terrestris*	Museu Nacional do Rio de Janeiro	m2	No locality data
MN 64572	*T. terrestris*	Museu Nacional do Rio de Janeiro	m3	Estância Ecológica SESC Pantanal, Barão de Melgaço, MT, Brazil
MN 70698	*T. terrestris*	Museu Nacional do Rio de Janeiro	m3	Parque Nacional Viruá, RR, Brazil
MN 57067	*T. terrestris*	Museu Nacional do Rio de Janeiro	m2	No locality data
MN 57071	*T. terrestris*	Museu Nacional do Rio de Janeiro	m3	No locality data
MN 71598	*T. terrestris*	Museu Nacional do Rio de Janeiro	m2	No locality data
MZUSP 22421	*T. terrestris*	Museu de Zoologia da Universidade de São Paulo	m2	No locality data
MZUSP 9714	*T. terrestris*	Museu de Zoologia da Universidade de São Paulo	m2	Varjão do Guaratuba, SP, Brazil
MZUSP 3269	*T. terrestris*	Museu de Zoologia da Universidade de São Paulo	m3	RS, Brazil
MZUSP 20034	*T. terrestris*	Museu de Zoologia da Universidade de São Paulo	m3	Boraceia, SP, Brazil
MZUSP 3728	*T. terrestris*	Museu de Zoologia da Universidade de São Paulo	m3	Rio das Cinzas, PR, Brazil
MZUSP 106	*T. terrestris*	Museu de Zoologia da Universidade de São Paulo	m3	São Lourenço, RS, Brazil
MZUSP 3266	*T. terrestris*	Museu de Zoologia da Universidade de São Paulo	m2	Piracicaba, SP, Brazil
MZUSP 6575	*T. terrestris*	Museu de Zoologia da Universidade de São Paulo	m3	Barra do Mosquito, SP, Brazil
MZUSP 3268	*T. terrestris*	Museu de Zoologia da Universidade de São Paulo	m3	Rio Claro, SP, Brazil

MZUSP 5701	*T. terrestris*	Museu de Zoologia da Universidade de São Paulo	m3	Ilha Seca, SP, Brazil
MZUSP 3758	*T. terrestris*	Museu de Zoologia da Universidade de São Paulo	m3	Vanuire, SP, Brazil
MZUSP 31983	*T. terrestris*	Museu de Zoologia da Universidade de São Paulo	m2	Estação Ecologica de Caetetus, SP, Brazil
MZUSP 9712	*T. terrestris*	Museu de Zoologia da Universidade de São Paulo	m2	Marilia, SP, Brazil
MZUSP 6139	*T. terrestris*	Museu de Zoologia da Universidade de São Paulo	m3	Rio Verde, GO, Brazil
MZUSP 7007	*T. terrestris*	Museu de Zoologia da Universidade de São Paulo	m3	Das Mortes River, MT, Brazil
MZUSP 7006	*T. terrestris*	Museu de Zoologia da Universidade de São Paulo	m2	Das Mortes River, MT, Brazil
MZUSP 22422	*T. terrestris*	Museu de Zoologia da Universidade de São Paulo	m2	No locality data
MZUSP 3727	*T. terrestris*	Museu de Zoologia da Universidade de São Paulo	m3	Pardo River, MT, Brazil
MZUSP 10715	*T. terrestris*	Museu de Zoologia da Universidade de São Paulo	m3	Trombetas River, PA, Brazil
AMNH 217150	*T. terrestris*	American Museum of Natural History	m3	Cochabamba, Bolivia
AMNH 246974	*T. terrestris*	American Museum of Natural History	m3	Chuquisaca, Bolivia
AMNH 394	*T. terrestris*	American Museum of Natural History	m2	Chapada dos Guimaraes, MT, Brazil
AMNH 36663	*T. terrestris*	American Museum of Natural History	m3	Porto do Campo, MT, Brazil
AMNH 95132	*T. terrestris*	American Museum of Natural History	m3	Piquiatuba, Tapajos River, PA, Brazil
AMNH 95133	*T. terrestris*	American Museum of Natural History	m3	Caxiricatuba, Tapajos River, PA, Brazil
AMNH 95755	*T. terrestris*	American Museum of Natural History	m2	Tapajos River, Limontuba, PA, Brazil
AMNH 96131	*T. terrestris*	American Museum of Natural History	m3	Xingu River, PA, Brazil

AMNH 120996	*T. terrestris*	American Museum of Natural History	m3	Fazenda Alegre, Paraguai River, MS, Brazil
AMNH 14690	*T. terrestris*	American Museum of Natural History	m3	Bonda, Cacagualito Plantation, Colombia
AMNH 142280	*T. terrestris*	American Museum of Natural History	m2	Serrania de La Macarena, Colombia
AMNH 140493	*T. terrestris*	American Museum of Natural History	m3	Guiana
AMNH 117646	*T. terrestris*	American Museum of Natural History	m2	Bonda, Los Naranjos, Colombia
AMNH 71728	*T. terrestris*	American Museum of Natural History	m2	Napo River, Curaray River mouth, Peru
AMNH 71729	*T. terrestris*	American Museum of Natural History	m3	Napo River, Curaray River mouth, Peru
AMNH 71730	*T. terrestris*	American Museum of Natural History	m3	Napo River, Curaray River mouth, Peru
AMNH 75328	*T. terrestris*	American Museum of Natural History	m3	Sarayacu, Ucayali River, Peru
AMNH 76149	*T. terrestris*	American Museum of Natural History	m3	Urubamba River mouth, Peru
AMNH 76452	*T. terrestris*	American Museum of Natural History	m2	Sarayacu, Ucayali River, Peru
Manacá	*T. terrestris*	Universidade Federal de Minas Gerais, Coleção de Mastozoologia	m2	SP, Brazil
MCN-MZ 95	*T. terrestris*	Museu de Ciências Naturais PUC Minas	m2	Zoológico de Belo Horizonte, MG, Brazil
MCN-MZ 92	*T. terrestris*	Museu de Ciências Naturais PUC Minas	m3	Zoológico de Belo Horizonte, MG, Brazil
MN 79096	*T. terrestris*	Museu Nacional do Rio de Janeiro	m2	No locality data
MN 69101	*T. terrestris*	Museu Nacional do Rio de Janeiro	m3	No locality data
MN 69114	*T. terrestris*	Museu Nacional do Rio de Janeiro	m2	No locality data
MN 64652	*T. terrestris*	Museu Nacional do Rio de Janeiro	m3	Estância Ecológica SESC Pantanal, MT, Brazil
MN 57138	*T. terrestris*	Museu Nacional do Rio de Janeiro	m2	No locality data

MN 57071	*T. terrestris*	Museu Nacional do Rio de Janeiro	m3	No locality data
MN 64806	*T. terrestris*	Museu Nacional do Rio de Janeiro	m3	Barão de Melgaço, MT, Brazil
MN 64437	*T. terrestris*	Museu Nacional do Rio de Janeiro	m3	Estância Ecológica SESC Pantanal, MT, Brazil
MN 83550	*T. terrestris*	Museu Nacional do Rio de Janeiro	m3	No locality data
MN 1605	*T. terrestris*	Museu Nacional do Rio de Janeiro	m2	No locality data
M 017	*T. terrestris*	unknown	m3	No locality data
M 020	*T. terrestris*	unknown	m2	No locality data
M 068	*T. terrestris*	unknown	m2	No locality data
M 083	*T. terrestris*	unknown	m2	No locality data
M 017	*T. terrestris*	unknown	m3	No locality data
M 020	*T. terrestris*	unknown	m2	No locality data
UFMG 4560	*T. kabomani*	Universidade Federal de Minas Gerais, Coleção de Mastozoologia	m3	Lábrea, AM, Brazil
Brasília 1	*T. kabomani*	Universidade Federal de Minas Gerais, Coleção de Mastozoologia	m2	Brasília, Distrito Federal, GO, Brazil
UFMG 3177	*T. kabomani*	Universidade Federal de Minas Gerais, Coleção de Mastozoologia	m2	Porto Velho, RO, Brazil
UFMG 4583	*T. kabomani*	Universidade Federal de Minas Gerais, Coleção de Mastozoologia	m2	No locality data
Brasília 2	*T. kabomani*	Universidade Federal de Minas Gerais, Coleção de Mastozoologia	m3	Brasília, Distrito Federal, GO, Brazil

MN 600	*T. kabomani*	Museu Nacional do Rio de Janeiro	m2	No locality data
MN 57069	*T. kabomani*	Museu Nacional do Rio de Janeiro	m2	No locality data
MN 1607	*T. kabomani*	Museu Nacional do Rio de Janeiro	m3	No locality data
MN 869	*T. kabomani*	Museu Nacional do Rio de Janeiro	m3	No locality data
AMNH 80075	*T. bairdii*	American Museum of Natural History	m3	Atlantida, Honduras
AMNH 206834	*T. bairdii*	American Museum of Natural History	m3	Santo Domingo Zanatapec, Mexico
AMNH 208259	*T. bairdii*	American Museum of Natural History	m3	Santo Domingo Zanatapec, Mexico
AMNH 29455	*T. bairdii*	American Museum of Natural History	m3	El Tuma, Nicaragua
AMNH 29526	*T. bairdii*	American Museum of Natural History	m3	El Tuma, Nicaragua
AMNH 35000	*T. bairdii*	American Museum of Natural History	m3	El Tuma, Nicaragua
AMNH 130104	*T. bairdii*	American Museum of Natural History	m3	No locality data
AMNH 54960	*T. indicus*	American Museum of Natural History	m3	Chaiing, Burma
AMNH 80077	*T. indicus*	American Museum of Natural History	m3	India
AMNH 54657	*T. indicus*	American Museum of Natural History	m3	Me Wung River, Thailand
AMNH 130108	*T. indicus*	American Museum of Natural History	m3	Asia
RBINS 1184E	*T. indicus*	Royal Belgian Institute of Natural Sciences	m2	Asia
RBINS 1188D	*T. indicus*	Royal Belgian Institute of Natural Sciences	m3	Asia
RBINS 13492	*T. indicus*	Royal Belgian Institute of Natural Sciences	m3	Asia

NMB C.3761.3	*T. indicus*	National History Museum Basel	m3	Asia
NMB 8125.3	*T. indicus*	National History Museum Basel	m2	Asia
AMNH 149332	*T. pinchaque*	American Museum of Natural History	m2	Paletara, Colombia
AMNH 70521	*T. pinchaque*	American Museum of Natural History	m2	Papallacta, Ecuador
AMNH 149424	*T. pinchaque*	American Museum of Natural History	m2	No locality data
RBINS 1186i	*T. pinchaque*	Royal Belgian Institute of Natural Sciences	m3	South America
UF 221720	*T. lundeliusi*	Florida Museum of Natural History, Florida	m2	Haile 7C, Alachua Co., Florida, USA
UF 160715	*T. lundeliusi*	Florida Museum of Natural History, Florida	m3	Haile 7C, Alachua Co., Florida, USA
UF 206878	*T. lundeliusi*	Florida Museum of Natural History, Florida	m3	Haile 7C, Alachua Co., Florida, USA
UF 224680	*T. lundeliusi*	Florida Museum of Natural History, Florida	m3	Haile 7C, Alachua Co., Florida, USA
ZT-2010-03-063	*T. yunnanensis*	Yunnan Institute of Cultural Relics and Archaeology	m2	Gansu, China
ZT-2007-03-184	*T. yunnanensis*	Yunnan Institute of Cultural Relics and Archaeology	m3	Gansu, China
ZT-2007-01-294	*T. yunnanensis*	Yunnan Institute of Cultural Relics and Archaeology	m3	Gansu, China
CM 159	*T. veroensis*	Central Missouri State College, Warrensburg, Missouri	m2	Crankshaft Cave, Missouri
OMNH 59528	*T. veroensis*	Oklahoma Museum of Natural History	m2	Sassafras Cave, Ozark Highlands, Oklahoma
Mean of Florida sample (Hulbert 1995)	*T. veroensis*	Florida Museum of Natural History, Florida	m3	Rancholabrean sites across Florida
Mean of Florida sample (Hulbert 1995)	*T. haysii*	Florida Museum of Natural History, Florida	m3	Multiple localities (mostly Leisey Shell Pit 1A, Florida)
Mean of Port Kennedy	*T. haysii*	Academy of Natural Sciences, Drexel	m3	Port Kennedy, Pennsylvania

sample (Hulbert 1995)		University, Philadelphia		
MCL 23.333/1	*T. cristatellus*	Museu de Ciências Naturais da Pontifícia Universidade Católica de Minas Gerais, Brazil	m3	Poço Azul, BA, Brazil
UF 26191	*T. webbi*	Florida Museum of Natural History, Florida	m3	Love Bone Bed, Alachua County, Florida
NMB VT. 573.3	*T. arvernensis*	National History Museum Basel	m3	Switzerland
NMB VT. 661	*T. arvernensis*	National History Museum Basel	m3	Switzerland
MNHN F PET 232a	*T. arvernensis*	Muséum National d'Histoire Naturelle Paris	m2	Perrier-le-Étouaires, Puy-de-Dôme, France
NHMUK PV M 2627	*T. priscus*	Natural History Museum London	m3	Eppelsheim, Germany
Unlabelled	*T. simpsoni*	Unknown	m3	Nebraska
ETMNH 3699	*T.polkensis*	General Shale Brick Museum of Natural History	m2	Gray Fossil Site, Tennessee
ETMNH 3426	*T. polkensis*	General Shale Brick Museum of Natural History	m2	Gray Fossil Site, Tennessee
ETMNH 3719	*T. polkensis*	General Shale Brick Museum of Natural History	m3	Gray Fossil Site, Tennessee
ETMNH 682	*T. polkensis*	General Shale Brick Museum of Natural History	m3	Gray Fossil Site, Tennessee
ETMNH 5285	*T. polkensis*	General Shale Brick Museum of Natural History	m3	Gray Fossil Site, Tennessee
ETMNH 3519	*T. polkensis*	General Shale Brick Museum of Natural History	m3	Gray Fossil Site, Tennessee
ETMNH 608	*T.polkensis*	General Shale Brick Museum of Natural History	m3	Gray Fossil Site, Tennessee
ETMNH 3717	*T. polkensis*	General Shale Brick Museum of Natural History	m3	Gray Fossil Site, Tennessee
V 12578.03	*T. sanyuanensis*	Institute of Vertebrate Paleontology and Paleoanthropology	m2	Fanchang, Anhui, China

Table S4 - Traditional morphometry dental data acquired for PCA analysis - upper teeth (n = 80). Specimen Age based on the eruption of molar teeth (tooth listed represents the last tooth to be fully erupted; derived from Hulbert 2010 age categories for tapirs).

Specimen	Species	Collection	Age	Locality
UFMG 4558	*T. terrestris*	Universidade Federal de Minas Gerais, Coleção de Mastozoologia	m3	Comodoro, MT, Brazil
UFMG 4559	*T. terrestris*	Universidade Federal de Minas Gerais, Coleção de Mastozoologia	m2	Lábrea, AM, Brazil
UFMG 4557	*T. terrestris*	Universidade Federal de Minas Gerais, Coleção de Mastozoologia	m2	Floresta do Jamari, RO, Brazil
MN 79096	*T. terrestris*	Museu Nacional do Rio de Janeiro	m2	No locality data
MN 64572	*T. terrestris*	Museu Nacional do Rio de Janeiro	m3	Estância Ecológica SESC Pantanal (RPPN), Barão de Melgaço, MT, Brazil
MN 57138	*T. terrestris*	Museu Nacional do Rio de Janeiro	m2	No locality data
MN 57071	*T. terrestris*	Museu Nacional do Rio de Janeiro	m3	No locality data
MN 64437	*T. terrestris*	Museu Nacional do Rio de Janeiro	m3	Estância Ecológica SESC Pantanal (RPPN), Barão de Melgaço, MT, Brazil
MN 1605	*T. terrestris*	Museu Nacional do Rio de Janeiro	m2	No locality data
UFMG 4588	*T. terrestris*	Universidade Federal de Minas Gerais, Coleção de Mastozoologia	m3	Parna Amazônia, Tapajós, PA, Brazil
UFMG 6028	*T. terrestris*	Universidade Federal de Minas Gerais, Coleção de Mastozoologia	m2	No locality data
UFMG 4591	*T. terrestris*	Universidade Federal de Minas Gerais, Coleção de Mastozoologia	m2	No locality data
UFMG 6027	*T. terrestris*	Universidade Federal de Minas Gerais, Coleção de Mastozoologia	m2	Parque Estadual Chandless, AC, Brazil
MCN-MZ 95	*T. terrestris*	Museu de Ciências Naturais PUC Minas	m2	Zoológico de Belo Horizonte, MG, Brazil
MN 1606	*T. terrestris*	Museu Nacional do Rio de Janeiro	m2	No locality data

Manacá	*T. terrestris*	Universidade Federal de Minas Gerais, Coleção de Mastozoologia	m2	SP, Brazil
UFMG4197	*T. terrestris*	Universidade Federal de Minas Gerais, Coleção de Mastozoologia	m2	RO, Brazil
CP 01	*T. terrestris*	unknown	m3	No locality data
CP 02	*T. terrestris*	unknown	m3	No locality data
M 017	*T. terrestris*	unknown	m3	No locality data
M 020	*T. terrestris*	unknown	m2	No locality data
M 068	*T. terrestris*	unknown	m2	No locality data
M 083	*T. terrestris*	unknown	m2	No locality data
MCN M1315	*T. terrestris*	unknown	m2	No locality data
MCN M2532	*T. terrestris*	unknown	m2	No locality data
MCN M2750	*T. terrestris*	unknown	m2	No locality data
MCN M2848	*T. terrestris*	unknown	m2	No locality data
UFMG 3176	*T. kabomani*	Universidade Federal de Minas Gerais, Coleção de Mastozoologia	m2	Rio Madeira, RO, Brazil
UFMG 3182	*T. kabomani*	Universidade Federal de Minas Gerais, Coleção de Mastozoologia	m2	RO, Brazil
UFMG 4561	*T. kabomani*	Universidade Federal de Minas Gerais, Coleção de Mastozoologia	m2	Reserva Karitiana, RO, Brazil
UFMG 4547	*T. kabomani*	Universidade Federal de Minas Gerais, Coleção de Mastozoologia	m3	Reserva Karitiana, RO, Brazil
UFMG 3178	*T. kabomani*	Universidade Federal de Minas Gerais, Coleção de Mastozoologia	m3	Reserva Karitiana, RO, Brazil
UFMG 3183	*T. kabomani*	Universidade Federal de Minas Gerais, Coleção de Mastozoologia	m3	Lábrea, AM, Brazil

UFMG 3181	*T. kabomani*	Universidade Federal de Minas Gerais, Coleção de Mastozoologia	m2	Reserva Karitiana, RO, Brazil
UFMG 3177	*T. kabomani*	Universidade Federal de Minas Gerais, Coleção de Mastozoologia	m2	AM, Brazil
UFMG 4543	*T. kabomani*	Universidade Federal de Minas Gerais, Coleção de Mastozoologia	m2	Reserva Karitiana, RO, Brazil
MN 57069	*T. kabomani*	Museu Nacional do Rio de Janeiro	m2	No locality data
MN 1700	*T. kabomani*	Museu Nacional do Rio de Janeiro	m3	GO, Brazil
MN 1607	*T. kabomani*	Museu Nacional do Rio de Janeiro	m3	No locality data
MN 869	*T. kabomani*	Museu Nacional do Rio de Janeiro	m3	No locality data
Brasília 2	*T. kabomani*	Universidade Federal de Minas Gerais, Coleção de Mastozoologia	m3	Brasília, Distrito Federal, GO, Brazil
Brasília 1	*T. kabomani*	Universidade Federal de Minas Gerais, Coleção de Mastozoologia	m2	Brasília, Distrito Federal, GO, Brazil
P1070255	*T. pinchaque*	unknown	m2	No locality data
RBINS 1186D	*T. pinchaque*	Royal Belgian Institute of Natural Sciences, Brussels	m3	South America
Tpinchaque-Ecuador	*T. pinchaque*	Museo Nacional da Escola Politécnica de Quito, Ecuador	m3	No locality data
bairdii1	*T. bairdii*	unknown	m2	No locality data
bairdii2	*T. bairdii*	unknown	m2	No locality data
Ti 29926	*T. indicus*	Museo Argentino de Ciencias Naturales	m2	Asia
NMB C.3761.2	*T. indicus*	National History Museum Basel	m3	Asia
RBINS 1184E	*T. indicus*	Royal Belgian Institute of Natural Sciences	m2	Asia
RBINS 13492	*T. indicus*	Royal Belgian Institute of Natural Sciences	m3	Asia

NMB8125.2	*T. indicus*	National History Museum Basel	m2	Asia
F:AM 37403	*T. webbi*	American Museum of Natural History, NY	m2	Mixon's Bone Bed, Todd County, Florida
UF26179	*T. webbi*	Florida Museum of Natural History, Florida	m2	Love Bone Bed, Alachua Co., Florida, USA
UF11007	*T. webbi*	Florida Museum of Natural History, Florida	m2	McGehee Farm, Alachua Co., Florida, USA
UF11005	*T. webbi*	Florida Museum of Natural History, Florida	m2	McGehee Farm, Alachua Co., Florida, USA
UF28014	*T. webbi*	Florida Museum of Natural History, Florida	m2	Love Bone Bed, Alachua Co., Florida, USA
UF121736	*T. lundeliusi*	Florida Museum of Natural History, Florida	m2	Haile 7C, Alachua Co., Florida, USA
UF 224674	*T. lundeliusi*	Florida Museum of Natural History, Florida	m3	Haile 7G, Alachua Co., Florida, USA
UF 224680	*T. lundeliusi*	Florida Museum of Natural History, Florida	m3	Haile 7G, Alachua Co., Florida, USA
UF 160715	*T. lundeliusi*	Florida Museum of Natural History, Florida	m3	Haile 7C, Alachua Co., Florida, USA
Mean of Port Kenedy sample (Hulbert 1995)	*T. haysii*	Academy of Natural Sciences, Drexel University, Philadelphia	m3	Port Kenedy, Pennsylvania
UF 84190	*T. haysii*	Florida Museum of Natural History, Florida	m3	Leisey Shell Pit 1A, Hillsborough Co., Florida
Mean of Florida sample (Hulbert 1995)	*T. haysii*	Florida Museum of Natural History, Florida	m3	Multiple localities (mostly Leisey Shell Pit 1A, Florida)
Mean of Florida sample (Hulbert 1995)	*T. veroensis*	Florida Museum of Natural History, Florida	m3	Rancholabrean sites across Florida
MCL 23.333/1	*T. cristatellus*	Museu de Ciências Naturais da Pontifícia Universidade Católica de Minas Gerais, Brazil	m3	Poço Azul, BA, Brazil
MNHN F PET 233a	*T. arvernensis*	Muséum National d'Histoire Naturelle Paris	m3	Perrier-le-Étouaires, Puy-de-Dôme, France
NMB VT. 573	*T. arvernensis*	National History Museum Basel	m2	Switzerland
UNSM 45106	*T. simpsoni*	University of Nebraska State Museum	m3	Kimball Formation, Frontier Co., Nebraska

AMNH 37302	*T. johnsoni*	American Museum of Natural History	m3	Nebraska, USA
V 12576	*T. sanyuannensis*	Institute of Vertebrate Paleontology and Paleoanthropology	mm3	Fanchang Co., Anhui, China
Unlabelled	*T. jeanpiveteaui*	Unknown (France?)	m2	Barro, Charente, France
UNIR-PLV-M009	*T. rondoniensis*	Coleção de Paleovertebrados do Laboratório de Biologia Evolutiva e da Conservação, UNIR	m2	Madeira River, RO, Brazil
ETMNH 3719	*T. polkensis*	General Shale Brick Museum of Natural History	m3	Gray Fossil Site, Tennessee
ETMNH 3426	*T. polkensis*	General Shale Brick Museum of Natural History	m2	Gray Fossil Site, Tennessee
ETMNH 3843	*T. polkensis*	General Shale Brick Museum of Natural History	m3	Gray Fossil Site, Tennessee
ETMNH 680	*T. polkensis*	General Shale Brick Museum of Natural History	m3	Gray Fossil Site, Tennessee
ETMNH 682	*T. polkensis*	General Shale Brick Museum of Natural History	m3	Gray Fossil Site, Tennessee
ETMNH 606	*T. polkensis*	General Shale Brick Museum of Natural History	m3	Gray Fossil Site, Tennessee
ETMNH 5285	*T. polkensis*	General Shale Brick Museum of Natural History	m3	Gray Fossil Site, Tennessee
ETMNH 611	*T. polkensis*	General Shale Brick Museum of Natural History	mm3	Gray Fossil Site, Tennessee
ETMNH 3699	*T. polkensis*	General Shale Brick Museum of Natural History	2	Gray Fossil Site, Tennessee
NMB O.E. 15	*T. telleri*	National History Museum Basel	m3	Switzerland
Unlabelled	*T. balkanicus*	Museum of Paleontology and Historical Geology Sofia	m3	Hrabarsko, Bulgaria
UTEP 118	*T. merriami*	University of Texas at El Paso Biodiversity Collections	m3	North America
MNPA-V 006038	*T. tarijensis*	Museo Nacional Paleontológico-Arqueológico, Universidad Autónoma Juan Misael Saracho, Tarija, Bolivia	m3	Tarija Valley, Bolivia

YICRA ZT-2013-05-001	*T. yunnanensis*	Yunnan Institute of Cultural Relics and Archaeology	m2	Zhaotong, Yunnan Province, China
NHMUK PV M 40633	*T. priscus*	Natural History Museum London	m3	Eppelsheim, Germany

Table S5 - OSA dental data acquired for Box Plot analysis - Lower Teeth (n = 130). Specimen Age based on the eruption of molar teeth (tooth listed represents the last tooth to be fully erupted; derived from Hulbert 2010 age categories for tapirs).

Specimen	Species	Collection	Age	Locality
Perucho Verna	*T. terrestris*	unknown	m3	Perucho Verna, Entre Rios, Argentina
MN 57062	*T. terrestris*	Museu Nacional do Rio de Janeiro	m2	No locality data
MN 865	*T. terrestris*	Museu Nacional do Rio de Janeiro	m3	Porto Esperidião, MT, Brazil
MN 11976	*T. terrestris*	Museu Nacional do Rio de Janeiro	m3	Jacaré, Rio 7 de setembro, MT, Brazil
MN 32708	*T. terrestris*	Museu Nacional do Rio de Janeiro	m3	Xavantina, Rio das Mortes, MT, Brazil
MN 1605	*T. terrestris*	Museu Nacional do Rio de Janeiro	m2	No locality data
MN 1601	*T. terrestris*	Museu Nacional do Rio de Janeiro	m2	No locality data
MN 866	*T. terrestris*	Museu Nacional do Rio de Janeiro	m2	No locality data
MN 64572	*T. terrestris*	Museu Nacional do Rio de Janeiro	m3	Estância Ecológica SESC Pantanal, Barão de Melgaço, MT, Brazil
MN 70698	*T. terrestris*	Museu Nacional do Rio de Janeiro	m3	Parque Nacional Viruá, RR, Brazil
MN 57067	*T. terrestris*	Museu Nacional do Rio de Janeiro	m2	No locality data
MN 57071	*T. terrestris*	Museu Nacional do Rio de Janeiro	m3	No locality data
MN 71598	*T. terrestris*	Museu Nacional do Rio de Janeiro	m2	No locality data
MZUSP 22421	*T. terrestris*	Museu de Zoologia da Universidade de São Paulo	m2	No locality data
MZUSP 9714	*T. terrestris*	Museu de Zoologia da Universidade de São Paulo	m2	Varjão do Guaratuba, SP, Brazil
MZUSP 3269	*T. terrestris*	Museu de Zoologia da Universidade de São Paulo	m3	RS, Brazil
MZUSP 20034	*T. terrestris*	Museu de Zoologia da Universidade de São Paulo	m3	Boraceia, SP, Brazil
MZUSP 3728	*T. terrestris*	Museu de Zoologia da Universidade de São Paulo	m3	Rio das Cinzas, PR, Brazil

MZUSP 106	*T. terrestris*	Museu de Zoologia da Universidade de São Paulo	m3	São Lourenço, RS, Brazil
MZUSP 3266	*T. terrestris*	Museu de Zoologia da Universidade de São Paulo	m2	Piracicaba, SP, Brazil
MZUSP 6575	*T. terrestris*	Museu de Zoologia da Universidade de São Paulo	m3	Barra do Mosquito, SP, Brazil
MZUSP 3268	*T. terrestris*	Museu de Zoologia da Universidade de São Paulo	m3	Rio Claro, SP, Brazil
MZUSP 5701	*T. terrestris*	Museu de Zoologia da Universidade de São Paulo	m3	Ilha Seca, SP, Brazil
MZUSP 3758	*T. terrestris*	Museu de Zoologia da Universidade de São Paulo	m3	Vanuire, SP, Brazil
MZUSP 31983	*T. terrestris*	Museu de Zoologia da Universidade de São Paulo	m2	Estação Ecologica de Caetetus, SP, Brazil
MZUSP 9712	*T. terrestris*	Museu de Zoologia da Universidade de São Paulo	m2	Marilia, SP, Brazil
MZUSP 6139	*T. terrestris*	Museu de Zoologia da Universidade de São Paulo	m3	Rio Verde, GO, Brazil
MZUSP 7007	*T. terrestris*	Museu de Zoologia da Universidade de São Paulo	m3	Das Mortes River, MT, Brazil
MZUSP 7006	*T. terrestris*	Museu de Zoologia da Universidade de São Paulo	m2	Das Mortes River, MT, Brazil
MZUSP 22422	*T. terrestris*	Museu de Zoologia da Universidade de São Paulo	m2	No locality data
MZUSP 3727	*T. terrestris*	Museu de Zoologia da Universidade de São Paulo	m3	Pardo River, MT, Brazil
MZUSP 10715	*T. terrestris*	Museu de Zoologia da Universidade de São Paulo	m3	Trombetas River, PA, Brazil
AMNH 217150	*T. terrestris*	American Museum of Natural History	m3	Cochabamba, Bolivia
AMNH 246974	*T. terrestris*	American Museum of Natural History	m3	Chuquisaca, Bolivia
AMNH 394	*T. terrestris*	American Museum of Natural History	m2	Chapada dos Guimaraes, MT, Brazil
AMNH 36663	*T. terrestris*	American Museum of Natural History	m3	Porto do Campo, MT, Brazil
AMNH 95132	*T. terrestris*	American Museum of Natural History	m3	Piquiatuba, Tapajos River, PA, Brazil
AMNH 95133	*T. terrestris*	American Museum of Natural History	m3	Caxiricatuba, Tapajos River, PA, Brazil

AMNH 95755	*T. terrestris*	American Museum of Natural History	m2	Tapajos River, Limontuba, PA, Brazil
AMNH 96131	*T. terrestris*	American Museum of Natural History	m3	Xingu River, PA, Brazil
AMNH 120996	*T. terrestris*	American Museum of Natural History	m3	Fazenda Alegre, Paraguai River, MS, Brazil
AMNH 14690	*T. terrestris*	American Museum of Natural History	m3	Bonda, Cacagualito Plantation, Colombia
AMNH 142280	*T. terrestris*	American Museum of Natural History	m2	Serrania de La Macarena, Colombia
AMNH 140493	*T. terrestris*	American Museum of Natural History	m3	Guyana
AMNH 117646	*T. terrestris*	American Museum of Natural History	m2	Bonda, Los Naranjos, Colombia
AMNH 71728	*T. terrestris*	American Museum of Natural History	m2	Napo River, Curaray River mouth, Peru
AMNH 71729	*T. terrestris*	American Museum of Natural History	m3	Napo River, Curaray River mouth, Peru
AMNH 71730	*T. terrestris*	American Museum of Natural History	m3	Napo River, Curaray River mouth, Peru
AMNH 75328	*T. terrestris*	American Museum of Natural History	m3	Sarayacu, Ucayali River, Peru
AMNH 76149	*T. terrestris*	American Museum of Natural History	m3	Urubamba River mouth, Peru
AMNH 76452	*T. terrestris*	American Museum of Natural History	m2	Sarayacu, Ucayali River, Peru
Manacá	*T. terrestris*	Universidade Federal de Minas Gerais, Coleção de Mastozoologia	m2	SP, Brazil
MCN-MZ 95	*T. terrestris*	Museu de Ciências Naturais PUC Minas	m2	Zoológico de Belo Horizonte, MG, Brazil
MCN-MZ 92	*T. terrestris*	Museu de Ciências Naturais PUC Minas	m3	Zoológico de Belo Horizonte, MG, Brazil
MN 79096	*T. terrestris*	Museu Nacional do Rio de Janeiro	m2	No locality data
MN 69101	*T. terrestris*	Museu Nacional do Rio de Janeiro	m3	No locality data
MN 69114	*T. terrestris*	Museu Nacional do Rio de Janeiro	m2	No locality data
MN 64652	*T. terrestris*	Museu Nacional do Rio de Janeiro	m3	Estância Ecológica SESC Pantanal, MT, Brazil
MN 57138	*T. terrestris*	Museu Nacional do Rio de Janeiro	m2	No locality data
MN 57071	*T. terrestris*	Museu Nacional do Rio de Janeiro	m3	No locality data
MN 64806	*T. terrestris*	Museu Nacional do Rio de Janeiro	m3	Barão de Melgaço, MT, Brazil
MN 64437	*T. terrestris*	Museu Nacional do Rio de Janeiro	m3	Estância Ecológica SESC Pantanal, MT, Brazil
MN 83550	*T. terrestris*	Museu Nacional do Rio de Janeiro	m3	No locality data
MN 1605	*T. terrestris*	Museu Nacional do Rio de Janeiro	m2	No locality data

M 017	*T. terrestris*	unknown	m3	No locality data
M 020	*T. terrestris*	unknown	m2	No locality data
M 068	*T. terrestris*	unknown	m2	No locality data
M 017	*T. terrestris*	unknown	m3	No locality data
M 020	*T. terrestris*	unknown	m2	No locality data
UFMG 4560	*T. kabomani*	Universidade Federal de Minas Gerais, Coleção de Mastozoologia	m3	Lábrea, AM, Brazil
Brasília 1	*T. kabomani*	Universidade Federal de Minas Gerais, Coleção de Mastozoologia	m2	Brasília, Distrito Federal, GO, Brazil
UFMG 3177	*T. kabomani*	Universidade Federal de Minas Gerais, Coleção de Mastozoologia	m2	Porto Velho, RO, Brazil
UFMG 4583	*T. kabomani*	Universidade Federal de Minas Gerais, Coleção de Mastozoologia	m2	No locality data
Brasília 2	*T. kabomani*	Universidade Federal de Minas Gerais, Coleção de Mastozoologia	m3	Brasília, Distrito Federal, GO, Brazil
MN 600	*T. kabomani*	Museu Nacional do Rio de Janeiro	m2	No locality data
MN 57069	*T. kabomani*	Museu Nacional do Rio de Janeiro	m2	No locality data
MN 1607	*T. kabomani*	Museu Nacional do Rio de Janeiro	m3	No locality data
MN 869	*T. kabomani*	Museu Nacional do Rio de Janeiro	m3	No locality data
AMNH 80075	*T. bairdii*	American Museum of Natural History	m3	Atlantida, Honduras
AMNH 206834	*T. bairdii*	American Museum of Natural History	m3	Santo Domingo Zanatapec, Mexico
AMNH 208259	*T. bairdii*	American Museum of Natural History	m3	Santo Domingo Zanatapec, Mexico
AMNH 29455	*T. bairdii*	American Museum of Natural History	m3	El Tuma, Nicaragua
AMNH 29526	*T. bairdii*	American Museum of Natural History	m3	El Tuma, Nicaragua
AMNH 35000	*T. bairdii*	American Museum of Natural History	m3	El Tuma, Nicaragua
AMNH 130104	*T. bairdii*	American Museum of Natural History	m3	No locality data
AMNH 54960	*T. indicus*	American Museum of Natural History	m3	Chaiing, Burma
MN57063	*T. indicus*	Museu Nacional do Rio de Janeiro	m3	Asia
AMNH 80077	*T. indicus*	American Museum of Natural History	m3	India

AMNH 54657	*T. indicus*	American Museum of Natural History	m3	Me Wung River, Thailand
AMNH 130108	*T. indicus*	American Museum of Natural History	m3	Asia
MN57063	*T. indicus*	Museu Nacional do Rio de Janeiro	m3	Asia
Ti 30351[e]	*T. indicus*	Museo Argentino de Ciencias Naturales	m3	Asia
Ti 29926[g]	*T. indicus*	Museo Argentino de Ciencias Naturales	m2	Asia
RBINS 1184E	*T. indicus*	Royal Belgian Institute of Natural Sciences	m2	No locality data
RBINS 1188D	*T. indicus*	Royal Belgian Institute of Natural Sciences	m3	No locality data
NMB C.3761.3	*T. indicus*	National History Museum Basel	m3	Asia
AMNH 149332	*T. pinchaque*	American Museum of Natural History	m2	Paletara, Colombia
AMNH 70521	*T. pinchaque*	American Museum of Natural History	m2	Papallacta, Ecuador
AMNH 149424	*T. pinchaque*	American Museum of Natural History	m2	No locality data
RBINS 1186	*T. pinchaque*	Royal Belgian Institute of Natural Sciences	m3	No locality data
MCL 23.333/1	*T. cristatellus*	Museu de Ciências Naturais da Pontifícia Universidade Católica de Minas Gerais, Brazil	m3	Poço Azul, BA, Brazil
CM 159	*T. veroensis*	Central Missouri State College, Warrensburg, Missouri	m2	Crankshaft Cave, Missouri
OMNH 59528	*T. veroensis*	Oklahoma Museum of Natural History	m2	Sassafras Cave, Ozark Highlands, Oklahoma
Mean of Florida sample (Hulbert 1995)	*T. veroensis*	Florida Museum of Natural History, Florida	m3	Rancholabrean sites across Florida
Mean of Florida sample (Hulbert 1995)	*T. haysii*	Florida Museum of Natural History, Florida	m3	Multiple localities (mostly Leisey Shell Pit 1A, Florida)
Mean of Port Kenedy sample (Hulbert 1995)	*T. haysii*	Academy of Natural Sciences, Drexel University, Philadelphia	m3	Port Kenedy, Pennsylvania

Unlabelled	*T. arvernensis*	Museum of Natural History, University of Florence, Italy	m3	Lower Valdarno Basin, Tuscany, Italy
NMB VT. 573.3	*T. arvernensis*	National History Meseum Basel	m3	Switzerland
NMB VT. 661	*T. arvernensis*	National History Museum Basel	m3	Switzerland
UF 26191	*T. webbi*	Florida Museum of Natural History, Florida	m3	Love Bone Bed, Alachua County, Florida
Unlabelled	*T. simpsoni*	Unknown	m3	Nebraska
CV 858	*T. sanyuanensis*	Institute of Vertebrate Paleontology and Paleoanthropology	m3	Damiao,Wushan in Chongqing, China
V 12578.03	*T. sanyuannensis*	Institute of Vertebrate Paleontology and Paleoanthropology	m2	Fanchang, Anhui, China
NHMUK PV M 2627	*T. priscus*	Natural History Museum London	m3	Eppelsheim, Germany
UF 121736	*T. lundeliusi*	Florida Museum of Natural History, Florida	m2	Haile 7C, Alachua Co., Florida, USA
UF 221720	*T. lundeliusi*	Florida Museum of Natural History, Florida	m3	Haile 7C, Alachua Co., Florida, USA
UF 160715	*T. lundeliusi*	Florida Museum of Natural History, Florida	m3	Haile 7C, Alachua Co., Florida, USA
UF 207868	*T. lundeliusi*	Florida Museum of Natural History, Florida	m3	Haile 7C, Alachua Co., Florida, USA
UF 224680	*T. lundeliusi*	Florida Museum of Natural History, Florida	m3	Haile 7C, Alachua Co., Florida, USA
ZT-2010-03-063	*T. yunnanensis*	Yunnan Institute of Cultural Relics and Archaeology	m2	Shuitangba, China
ZT-2007-03-184	*T. yunnanensis*	Yunnan Institute of Cultural Relics and Archaeology	m2	Shuitangba, China
T-2007-01-294	*T. yunnanensis*	Yunnan Institute of Cultural Relics and Archaeology	m2	Shuitangba, China
ETMNH 3699	*T. polkensis*	General Shale Brick Museum of Natural History	m2	Gray Fossil Site, Tennessee
ETMNH 3719	*T. polkensis*	General Shale Brick Museum of Natural History	m3	Gray Fossil Site, Tennessee

ETMNH 3426	*T. polkensis*	General Shale Brick Museum of Natural History	m2	Gray Fossil Site, Tennessee
ETMNH 682	*T. polkensis*	General Shale Brick Museum of Natural History	m3	Gray Fossil Site, Tennessee
ETMNH 5285	*T. polkensis*	General Shale Brick Museum of Natural History	m3	Gray Fossil Site, Tennessee
ETMNH 3519	*T. polkensis*	General Shale Brick Museum of Natural History	m3	Gray Fossil Site, Tennessee
ETMNH 608	*T.polkensis*	General Shale Brick Museum of Natural History	m3	Gray Fossil Site, Tennessee
ETMNH 3717	*T. polkensis*	General Shale Brick Museum of Natural History	m3	Gray Fossil Site, Tennessee

Table S6 - OSA dental data acquired for Box Plot analysis - Upper Teeth (n = 80). Specimen Age based on the eruption of molar teeth (tooth listed represents the last tooth to be fully erupted; derived from Hulbert 2010 age categories for tapirs).

Specimen	Species	Collection	Age	Locality
UFMG 4558	*T. terrestris*	Universidade Federal de Minas Gerais, Coleção de Mastozoologia	M3	Comodoro, MT, Brazil
UFMG 4559	*T. terrestris*	Universidade Federal de Minas Gerais, Coleção de Mastozoologia	M2	Lábrea, AM, Brazil
UFMG 4557	*T. terrestris*	Universidade Federal de Minas Gerais, Coleção de Mastozoologia	M2	Floresta do Jamari, RO, Brazil
MN 79096	*T. terrestris*	Museu Nacional do Rio de Janeiro	M2	No locality data
MN 64572	*T. terrestris*	Museu Nacional do Rio de Janeiro	M3	Estância Ecológica SESC Pantanal (RPPN), Barão de Melgaço, MT, Brazil
MN 57138	*T. terrestris*	Museu Nacional do Rio de Janeiro	M2	No locality data
MN 57071	*T. terrestris*	Museu Nacional do Rio de Janeiro	M3	No locality data
MN 64437	*T. terrestris*	Museu Nacional do Rio de Janeiro	M3	Estância Ecológica SESC Pantanal (RPPN), Barão de Melgaço, MT, Brazil
MN 1605	*T. terrestris*	Museu Nacional do Rio de Janeiro	M2	No locality data
UFMG 4588	*T. terrestris*	Universidade Federal de Minas Gerais, Coleção de Mastozoologia	M3	Parna Amazônia, Tapajós, PA, Brazil

UFMG 6028	*T. terrestris*	Universidade Federal de Minas Gerais, Coleção de Mastozoologia	M2	No locality data
UFMG 4591	*T. terrestris*	Universidade Federal de Minas Gerais, Coleção de Mastozoologia	M2	No locality data
UFMG 6027	*T. terrestris*	Universidade Federal de Minas Gerais, Coleção de Mastozoologia	M2	Parque Estadual Chandless, AC, Brazil
MCN-MZ 95	*T. terrestris*	Museu de Ciências Naturais PUC Minas	M2	Zoológico de Belo Horizonte, MG, Brazil
MN 1606	*T. terrestris*	Museu Nacional do Rio de Janeiro	M2	No locality data
Manacá	*T. terrestris*	Universidade Federal de Minas Gerais, Coleção de Mastozoologia	M2	SP, Brazil
UFMG 4197	*T. terrestris*	Universidade Federal de Minas Gerais, Coleção de Mastozoologia	M2	RO, Brazil
Brasília 1	*T. kabomani*	Universidade Federal de Minas Gerais, Coleção de Mastozoologia	M2	Brasília, Distrito Federal, GO, Brazil
UFMG 3176	*T. kabomani*	Universidade Federal de Minas Gerais, Coleção de Mastozoologia	M2	Rio Madeira, RO, Brazil
UFMG 3182	*T. kabomani*	Universidade Federal de Minas Gerais, Coleção de Mastozoologia	M2	RO, Brazil
UFMG 4561	*T. kabomani*	Universidade Federal de Minas Gerais, Coleção de Mastozoologia	M2	Reserva Karitiana, RO, Brazil
UFMG 4547	*T. kabomani*	Universidade Federal de Minas Gerais, Coleção de Mastozoologia	M3	Reserva Karitiana, RO, Brazil
UFMG 3178	*T. kabomani*	Universidade Federal de Minas Gerais, Coleção de Mastozoologia	M3	Reserva Karitiana, RO, Brazil
UFMG 3183	*T. kabomani*	Universidade Federal de Minas Gerais, Coleção de Mastozoologia	M3	Lábrea, AM, Brazil
UFMG 3181	*T. kabomani*	Universidade Federal de Minas Gerais,	M2	Reserva Karitiana, RO, Brazil

		Coleção de Mastozoologia		
UFMG 3177	*T. kabomani*	Universidade Federal de Minas Gerais, Coleção de Mastozoologia	M2	AM, Brazil
UFMG 4543	*T. kabomani*	Universidade Federal de Minas Gerais, Coleção de Mastozoologia	M2	Reserva Karitiana, RO, Brazil
MN 57069	*T. kabomani*	Museu Nacional do Rio de Janeiro	M2	No locality data
MN 1700	*T. kabomani*	Museu Nacional do Rio de Janeiro	M3	GO, Brazil
MN 1607	*T. kabomani*	Museu Nacional do Rio de Janeiro	M3	No locality data
MN 869	*T. kabomani*	Museu Nacional do Rio de Janeiro	M3	No locality data
Brasília 2	*T. kabomani*	Universidade Federal de Minas Gerais, Coleção de Mastozoologia	M3	Brasília, Distrito Federal, GO, Brazil
MN 75063	*T. indicus*	Museu Nacional do Rio de Janeiro	M2	Asia
Ti 29926	*T. indicus*	Museo Argentino de Ciencias Naturales	M2	Asia
Ti 30351[j]	*T. indicus*	Museo Argentino de Ciencias Naturales	M3	Asia
RBINS 13492s	*T. indicus*	Royal Belgian Institute of Natural Sciences	M3	Asia
NMB C.3761.3	*T. indicus*	National History Museum Basel	M3	Asia
NMB 8125.3	*T. indicus*	National History Museum Basel	M2	Asia
RBINS 1184E	*T. indicus*	Royal Belgian Institute of Natural Sciences	M2	Asia
MLP 1451	*T. bairdii*	Coleção de Mastozoologia do Museo de La Plata	M1	No locality data
AMNH 80076	*T. bairdii*	American Museum of Natural History	M2	No locality data
Unlabelled	*T. pinchaque*	Museo Nacional da Escola Politécnica de Quito, Ecuador	M3	No locality data
UF/C6110	*T. pinchaque*	Florida Museum of Natural History	M2	No locality data
RBINS 1186	*T. pinchaque*	Royal Belgian Institute of Natural Sciences	M3	No locality data
MCL 23.333/1	*T. cristatellus*	Museu de Ciências Naturais da Pontifícia Universidade Católica	M3	Poço Azul, BA, Brazil

		de Minas Gerais, Brazil		
Mean of Florida sample (Hulbert 1995)	*T. haysii*	Florida Museum of Natural History, Florida	M3	Multiple localities (mostly Leisey Shell Pit 1A, Florida)
Mean of Port Kenedy sample (Hulbert 1995)	*T. haysii*	Academy of Natural Sciences, Drexel University, Philadelphia	M3	Port Kenedy, Pennsylvania
UF 84190	*T. haysii*	Florida Museum of Natural History, Florida	M3	Leisey Shell Pit 1A, Hillsborough Co., Florida
F:AM 37403	*T. webbi*	American Museum of Natural History, NY	M2	Mixon's Bone Bed, Todd County, Florida
UF 26179	*T. webbi*	Florida Museum of Natural History, Florida	M2	Love Bone Bed, Alachua Co., Florida, USA
UF 11007	*T. webbi*	Florida Museum of Natural History, Florida	M2	McGehee Farm, Alachua Co., Florida, USA
UF 11005	*T. webbi*	Florida Museum of Natural History, Florida	M2	McGehee Farm, Alachua Co., Florida, USA
UF 28014	*T. webbi*	Florida Museum of Natural History, Florida	M2	Love Bone Bed, Alachua Co., Florida, USA
Mean of Florida sample (Hulbert 1995)	*T. veroensis*	Florida Museum of Natural History, Florida	M3	Rancholabrean sites across Florida
Unlabelled	*T. jeanpivetaui*	Unknown (France?)	M2	Barro, Charente, France
Unlabelled	*T. arvernensis*	Museum of Natural History, University of Florence, Italy	M3	Lower Valdarno Basin, Tuscany, Italy
NMB VT. 661	*T. arvernensis*	National History Museum Basel	M3	Switzerland
NHMUK PV M 40633	*T. priscus*	Natural History Museum London	M3	Eppelsheim, Germany
UNIR-PLV-M009	*T. rondoniensis*	Coleção de Paleovertebrados do Laboratório de Biologia Evolutiva e da Conservação, UNIR	M2	Madeira River, RO, Brazil
AMNH 37302	*T. johnsoni*	American Museum of Natural History, NY	M3	Nebraska, USA
UNSM 45106	*T. simpsoni*	University of Nebraska State Museum	M3	Kimball Formation, Frontier Co., Nebraska
UF 121736	*T. lundeliusi*	Florida Museum of Natural History, Florida	M2	Haile 7C, Alachua Co., Florida, USA
UF 224674	*T. lundeliusi*	Florida Museum of Natural History, Florida	M3	Haile 7G, Alachua Co., Florida, USA

UF 224680	*T. lundeliusi*	Florida Museum of Natural History, Florida	M3	Haile 7G, Alachua Co., Florida, USA
UF 160715	*T. lundeliusi*	Florida Museum of Natural History, Florida	M3	Haile 7C, Alachua Co., Florida, USA
ETMNH 3699	*T. polkensis*	General Shale Brick Museum of Natural History	M2	Gray Fossil Site, Tennessee
ETMNH 3426	*T. polkensis*	General Shale Brick Museum of Natural History	M2	Gray Fossil Site, Tennessee
ETMNH 3843	*T. polkensis*	General Shale Brick Museum of Natural History	M2	Gray Fossil Site, Tennessee
ETMNH 3719	*T. polkensis*	General Shale Brick Museum of Natural History	M3	Gray Fossil Site, Tennessee
ETMNH 680	*T. polkensis*	General Shale Brick Museum of Natural History	M3	Gray Fossil Site, Tennessee
ETMNH 682	*T. polkensis*	General Shale Brick Museum of Natural History	M3	Gray Fossil Site, Tennessee
ETMNH 606	*T. polkensis*	General Shale Brick Museum of Natural History	M3	Gray Fossil Site, Tennessee
ETMNH 5285	*T. polkensis*	General Shale Brick Museum of Natural History	M3	Gray Fossil Site, Tennessee
ETMNH 611	*T. polkensis*	General Shale Brick Museum of Natural History	M3	Gray Fossil Site, Tennessee
CICYTTP-PV-M-1-23	*T. mesopotamicus*	Centro de Investigaciones Científicas y Transferencia de Tecnología a la Producción, Diamante, Argentina	M2	Província Entre Ríos, Formação Arroyo Feliciano, Argentina.
V 12578.03	*T. sanyuannensis*	Institute of Vertebrate Paleontology and Paleoanthropology	M2	Fanchang, Anhui, China
YICRA ZT-2013-05-001	*T. yunnanensis*	Yunnan Institute of Cultural Relics and Archaeology	M2	Zhaotong, Yunnan Province, China
NMB O.E. 15	*T. telleri*	National History Museum Basel	M3	Switzerland
Unlabeled	*T. balkanicus*	Museum of Paleontology and Historical Geology Sofia	M3	Hrabarsko, Bulgaria

UTEP 118	*T. merriami*	University of Texas at El Paso Biodiversity Collections	M3	California
MNPA-V 006038	*T. tarijensis*	Museo Nacional Paleontológico-Arqueológico, Universidad Autónoma Juan Misael Saracho, Tarija, Bolivia	M3	Tarija Valley, Bolivia

CHAPTER 2 - Phylogeny and historical biogeography of Tapiridae (Mammalia, Perissodactyla).

LARISSA COSTA COIMBRA SANTOS DUMBÁ1, DANIEL DE MELO CASALI2, and MARIO ALBERTO COZZUOL3.

1*Programa de Pós Graduação, Zoologia/Departamento de Zoologia, Instituto de Ciências Biológicas, Universidade Federal de Minas Gerais, Avenida Antônio Carlos 6627, Belo Horizonte, Minas Gerais, Brazil*

2Departamento de Biologia, Faculdade de Filosofia, Ciências e Letras, Universidade de São Paulo, R. do Lago 717, São Paulo, São Paulo, Brazil

3*Departamento de Zoologia, Instituto de Ciências Biológicas, Universidade Federal de Minas Gerais, Avenida Antônio Carlos 6627, Belo Horizonte, Minas Gerais, Brazil*

ABSTRACT

Family Tapiridae comprises perissodactyl herbivorous mammals, including 5 extant and 50 extinct species. Although many previous studies have been conducted for the genus *Tapirus*, little is known about the phylogenetic and biogeographic history of Tapiridae and important gaps remain regarding our knowledge of *Tapirus* as well. For instance, European *Tapirus* have never been studied in a phylogenetic and/or formal biogeographic framework. Here, based on a revised and expanded morphological dataset, we conducted phylogenetic and divergence times estimations using maximum parsimony and Bayesian approaches, and reconstructed the biogeographic history of Tapiridae applying statistical models. Non-*Tapirus* Tapiridae are recovered as monophyletic (excepting for *Nexuotapirus*) in non-clock BI and MP analysis and as paraphyletic and clock-BI analysis. The genus *Tapirus* was recovered as monophyletic as well. The Miocene *T. johnsoni* is sister to all *Tapirus*. North American tapirs are polyphyletic. *T. lundeliusi* is sister to all South American tapirs, which form a clade. Tapiridae diverged at some point from the Middle Eocene to the Late Oligocene, in North America. *Tapirus* originated in the same continent, later, with divergence times ranging from the latest Oligocene/Early Miocene to the Late Miocene. Tapirids dispersed many times from North America to Eurasia, and tapirs dispersed from North America to Eurasia and South America, becoming isolated and forming new species by vicariant events. Most of our dispersion biogeographic inferences are consistent with the presence of transient or permanent land bridges, such as the Bering passage and the Panama bridge. The present study contributes to our understanding of the phylogenetic relationships, temporal and spatial dynamics of tapirids. Biogeographic patterns and the extinction of tapirids in North America and in Europe are associated with climate changes and set an alert for the preservation of living species of tapirs that were more diverse in the past.

KEYWORDS: Morphological evolution. Tapiridae. Maximum Parsimony. Bayesian analysis. Divergence times. Biogeography.

INTRODUCTION

The family Tapiridae Burnett, 1830 comprises perissodactyl mammals belonging to the superfamily Tapiroidea Burnet, 1830 (Holbrook 1998). Tapiroidea has been recovered as a monophyletic group in most previous studies (Holbrook 1998, Holbrook 2001, Bai et al. 2020), and the same applies to family Tapiridae (Holbrook 1998, Holbrook 2001, Colbert 2005, Bai et al. 2020). They are herbivorous mammals, which were more diverse in the past, until the Late Pleistocene (Cozzuol et al. 2013, 2014). Fifty seven extinct species have been described for the family, a number that could be higher depending on the definition of Tapiridae. Many fossil species descriptions were based only on dental and/or fragmentary cranial specimens (Perini et al. 2011). Since its first descriptions, Tapiridae taxonomy was plagued by numerous synonymies (Scherler et al. 2011) and several species were described based on dental and/or fragmented cranial remains, which is problematic (Perini et al. 2011, Scherler et al. 2011, Dumbá et al. 2022). The oldest fossil records from Tapiridae are from the Early Eocene (~48 Ma). The oldest records for *Tapirus* come from North America, Europe and Asia, and are from the Middle Miocene (~13.8 Ma). Tapirs reached South America after the formation of the Isthmus of Panama, through The Great American Biotic Interchange (Woodburne 2010; Cione et al. 2015; O'Dea et al. 2016), and the oldest South American records are from the Plio-Pleistocene (2.6 Ma) (Holanda et al. 2011).

Inside Tapiridae, only the genus *Tapirus* has living representatives: *T. pinchaque* Roulin, 1829 of the Andes mountains, *T. terrestris* Linnaeus, 1758 the lowland tapir, *T. bairdii* Gill, 1865 of Central and northern South America, *T. indicus* Desmarest, 1819 which inhabits fragmented regions in southeastern Asia and *T. kabomani* Cozzuol et al., 2013, described for the Amazon (Cozzuol et al., 2013, 2014).

Tapirus has been inferred as a monophyletic group (Hulbert 2010, Holanda and Ferrero 2012, Cozzuol et al. 2013, 2014). Species of the genus are recognized by the presence of a short mobile proboscis (Radinsky 1965; Padilla and Dowler 1994; Olmos 1997), which is present in all *Tapirus sensu strictu* (Cozzuol et al. 2013, 2014) evidenced in extinct species by osteological traits such as the nasal retraction, nasal fossae extended backward (Rustioni and Mazza 2001) and enlargement of the nasal notch (Wall 1980; Holbrook 1998). The proboscis, nonetheless, may also have been present, even if less developed,in some non-*Tapirus* Tapiridae (Albright 1998), and appears to be a trait responsible for most of the cranial differences between *Tapirus* and primitive Tapiroidea (Dumbá et al. 2019).

Although *Tapirus* is well studied in the literature (Dumbá et al. 2022), little is known about the phylogenetic and biogeographic history of the family they belong to. Albright (1998), who originally described the genus *Nexuotapirus,* did not resolve its phylogenetic relations in Tapiridae, showing a non computer-assisted tree including a few tapiroids and tapirids. Most recent works have focused on *Tapirus* and studied the phylogenetic history of South American, North American and Asian tapirs (Hulbert 2010, Holanda and Ferrero 2012, Cozzuol et al. 2013, 2014). Cerdeño and Ginsburg (1988) described the new European genus, *Eotapirus*. Spassov and Ginsburg 1999 described the species *T. balkanicus*. More recently, Rustioni and Mazza 2001 described remains of *T. arvernensis* and Scherler et al. 2011 provided a detailed taxonomic description and a biogeographic range study of many European tapirid species. Boev (2017) briefly described recent findings of European tapirs in Bulgaria. Those works, amongst other literature regarding European Tapiridae, were only descriptive/taxonomic. European tapirs have never been included in a phylogenetic study.

Until the relationships between European and other tapirid species are understood, the exact geographical origin and appearance of the family and genus *Tapirus* cannot be estimated. There is no phylogeny including tapirids from all continents.

Biogeographic assessments for Tapiridae in the past were mostly purely discursive and/or based in biostratigraphic information (Janis 1984, Guérin and Eisenmann 1994, McKenna and Bell 1997, Albright 1998, Holanda and Ferrero 2012, Kerber and Oliveira 2008, Scherler et al. 2011 and Ferrero et al. 2013), not based on formal biogeographic analysis. One exception is the study conducted by Eberle (2005), which performed a biogeographic analysis for a few Tapiroidea genera based on ancestral states estimation using maximum-parsimony. This study has the problem of a restricted taxonomic sampling, coding of taxa for the oldest record of the genus, ignoring "polymorphic" ranges and not relying on a method that disregard the possibility of cladogenetic biogeographical events.

The present work intends to review the phylogeny of Tapiridae based on cranial, dental and postcranial morphological qualitative and quantitative characters. Based on the phylogenetic and divergence times' results, we performed biogeographic analysis to infer ancestral areas and paleogeographic events that could have shaped the distribution of the species.

MATERIAL AND METHODS

Discrete and geometric morphometrics' character matrices

We obtained and revised discrete cranial, dental and postcranial characters from the matrices of Cozzuol et al. 2013, 2014 (See Supporting Information S1), previously adapted from Hulbert and Wallace (2005). *Heptodon*, a non-Tapiridae genus belonging to the super

family Tapiroidea Burnett, 1830 was chosen as novelty as the most external outgroup due to its extensive fossil record. Terminal taxa were scored at species (*Tapirus*) or genus (non-*Tapirus* Tapiridae) levels to maximize the character coverage. Only taxa with at least 70% of coded cells were further considered for phylogenetic analyses. Taxonomic sampling information of newly added species, in comparison to Cozzuol et al. 2013, 2014 discrete matrices, are included in Supporting Information S2.

Landmarks for 2D cranial geometric morphometric data were obtained through TpsDig version 2.3. Hereafter, landmarked pictures were exported to Past Program version 3.14 (Hammer et al. 2001) and aligned using Generalized Procrustes Analysis (GPA, Rohlf and Slice 1990). GPA eliminates effects of scale, position, and orientation by generating a common centroid size for all configurations, leaving only shape as cause of variation between species (Bookstein 1991). 18 lateral and 13 dorsal views' landmark configurations considered in the present study were adapted from Dumbá et al. 2019 and are available in Supporting Information S3 and S4. Only specimens that exhibited no missing landmarks in the configurations proposed were retained for phylogenetic analyses. *T. hungaricus* was not coded for morphometric data, as the only specimen available is dorsoventrally flattened and therefore was not a fit for landmark attainment. As morphometric dental data were previously inferred to carry low phylogenetic information (Perini et al. 2011, Dumbá et al. 2022), they were not included in the present work. We selected landmarks avoiding dependency between qualitative and quantitative data. A list of specimens used for the attainment of landmarks is available in Supporting Information S5 and S6.

Both discrete and morphometric data obtained from photos were produced from direct observations in museum collections and from the literature. Only adults (with at least m2/M2 erupted) were included in the morphometric sample.

Maximum parsimony phylogenetic analyses

We conducted maximum parsimony (MP) phylogenetic analyses in the software TNT 1.5 (Goloboff and Catalano 2016). We considered two datasets, one exclusively composed of discrete characters and another combining discrete with geometric morphometric data. For both analyses, we used implied weighs (Goloboff 1993), setting the concavity constant to 12. This value has been shown to be more reasonable than the stronger weights originally proposed as the default in TNT (Goloboff et al. 2018), and corresponds to roughly half the number of taxa in the dataset, which has been shown to be a reasonable value, considering the fitting of implied weight parsimony when treated as a model in a likelihood framework (Goloboff and Arias 2019). Different k values were tested, but topologies did not change or produced unresolved

phylogenetic hypothesis. For the analysis of the discrete character matrix, we used a combination of sectorial searches and tree fusing, in their default configurations. We considered we have found the most parsimonious tree after ten hits of the minimum tree length. These searches considered ten initial random addition sequences (RAS), holding 100,000 trees in memory, and collapsing branch lengths equal to zero. We set the driver to check the level of the analysis at every hit to improve the efficiency of the searches. We further ran an additional search in the trees from memory using tree bisection and reconnection (TBR) to ensure we recovered all most parsimonious trees (MPTs).

For the combined analysis, which required greater computation effort given the geometric morphometric data, we applied two rounds of TBR, after 10 RAS, holding a single tree per replication. Each landmark configuration was considered to have the same weight of a discrete character. We explored the sensitivity of the resulting topology to alternative settings used in the calculations of ancestral states for morphometric geometric characters (number of cells per grid – 6, 8 and 10; number of nesting grid levels – 1 and 2), alternative alignment of landmarks (GPA and RFTRA), and also considered using 100 RAS instead of 10. Since none of these changes affected the obtained topology, we conducted the final analyses with the default configurations for all settings.

For both datasets (discrete only and combined), node supports were evaluated with Poisson bootstrap (PB) resampling, a metric that is not distorted when weights are applied during searches (Goloboff et al. 2003). Synapomorphies were evaluated with unambiguous optimizations in TNT.

Bayesian phylogenetic inference and divergence times' estimations

Bayesian inferences (BI) were performed with the software MrBayes 3.2.7a (Ronquist et al. 2012a), in CIPRES Science Gateway (Miller et al. 2010).

Firstly, a non-clock Bayesian phylogenetic inference was conducted. For that, we employed the Mkv model of morphological character evolution (Lewis 2001), and partitioned characters by the degree of homoplasy they showed in the most parsimonious tree, measured by the number of extra steps (Rosa et al. 2019; Casali et al. 2022). Partition absolute rates were independently estimated, ensuring that relative branch lengths were proportional across partitions (i.e., linked branch lengths). As shown in recent studies (Rosa et al. 2019; Casali et al. 2022), this partitioning approach better-fit the data than alternative strategies to model rate heterogeneity among characters and partitions in morphological datasets. The Markov chain Monte Carlo (MCMC) analysis considered four independent runs, with four chains each, through 5M generations, and sampling at each 500^{th}. A relative burn-in consisting of the 25%

initial samples was discarded before summarizing the results. The topology was summarized using a Maximum Compatibility Tree (*contype = allcompat*). We considered analyses to have converged if ESS > 200, PRSF ~ 1.0 and ASDSF < 0.01, also inspecting the likelihood trace plots in MrBayes. Node supports were assessed with posterior probabilities (PP).

We also employed a tip-dated Bayesian inference, co-estimating the topology and divergence times. The substitution model and partitioning scheme were the same as employed in non-clock Bayesian analyses. Fossil tip-dates were obtained from the literature (Supporting Information S7), and applied as uniform distributions in order to consider the stratigraphic uncertainty of fossil records, following best practices (Barido-Sottani et al. 2019). For the diversification prior, we employed the Fossilized Birth-Death (FBD) process (Heath et al. 2014; Zhang et al. 2016), considering all fossils as tips, since preliminary runs sampling ancestors failed to converge even after increasing generations and adjusting other MCMC settings. The prior for the base clock rate followed a lognormal distribution (M=-1.96, SD=0.65), being these values obtained using the median and upper limit of the 95% HPD tree length of the non-clock Bayesian analysis, and considering the approximate root age of 55 mya for Tapiroidea (Bai et al. 2020), following the procedure proposed in Ronquist et al. (2012b). The root age prior was set using a uniform distribution (50.3–62,0), ranging from the First Appearance Datum of the oldest sampled fossil Tapiroidea (*Heptodon*), to the upper limit of the 95% HPD obtained for Ceratomorpha (Bai et al. 2020).

For the prior of the variance of the clock rates, we tested the relative fit of two relaxed clock models: one assuming uncorrelated rates across branches (IGR) and another assuming autocorrelated rates (TK02), and the latter performed as best-fitting clock model. Four independent MCMC runs with 20M generations were employed, sampling at each 2000th. All other setting and convergence criteria were performed as described for the previous analyses. Node supports were assessed with posterior probabilities (PP).

Lastly, we conducted two additional tip-dating analyses fixing the topologies obtained with MP and non-clock BI analyses, with all other settings unchanged. In total, we obtained three time-calibrated trees, to be applied in biogeographical analyses.

Synapomorphies for Bayesian topologies were obtained after ancestral states estimations conducted with the Mk model, following the protocol presented in Casali et al. (2022), but considering a threshold of 0.25 to collapse ancestral state estimates to the most likely state in the R package *Claddis* (Lloyd 2016), rendering estimates of synapomorphies more conservative than the default (0.01).

Historical biogeography

For each of the three time-calibrated trees, we conducted ancestral range estimations, and inferred the biogeographic events that generated the current spatial distribution of tapirids. The most external outgroup and sole representative of non-tapirid Tapiroidea, *Heptodon* was removed from the trees for biogeographical analyses. The geographic distribution of tapirids was obtained from the literature (Supporting Information S7), considering four areas: Europe (E), Asia (A), North America (N, including Central America), and South America (S). The maximum number of areas in ancestral ranges was limited by the maximum number observed for the tips (=3) and null ranges were allowed. We applied the widely used likelihood implementations of the models DIVA (Ronquist 1997) and DEC (Ree and Smith 2008), available in the package BioGeoBEARS (Matzke 2013) in the R programming environment (R Core Team 2022). Models with founder-event speciation (Matzke 2014) and the model BayArea (Landis et al. 2013) were not considered, since modern species of *Tapirus* are known for having a relatively restricted home-range (Foerster and Vaughan 2002, Ferreguetti et al. 2017), whereas the latter model disregard vicariance, which is also unreasonable for the group being studied. Evaluated models were compared using sample-size corrected Akaike Information Criteria (AICc, Burnham and Anderson 2002), applying a four AICc units threshold to consider models effectively different (Harmon 2018).

The complete set of dispersion events and ancestral biographic areas along with R scripts are available in the Chapter 2 apprendix, file “inputs_BIOGEO.rar”.

RESULTS

Topologies

A single MPT was obtained during maximum parsimony analyses, with the same topology being recovered when discrete characters were analyzed alone, or along with geometric morphometric data.

Results obtained with all three analytical approaches—MP non-clock BI and clock BI—showed a general consistency regarding the main phylogenetic relationships of the group, with all of them recovering a monophyletic *Tapirus*, and three main tapir clades, to be detailed below (Figures 1, 2 and 3). Also, MP and non-clock BI, which disregard temporal information during topological inference, were in a slightly greater agreement when compared to the clock BI topology.

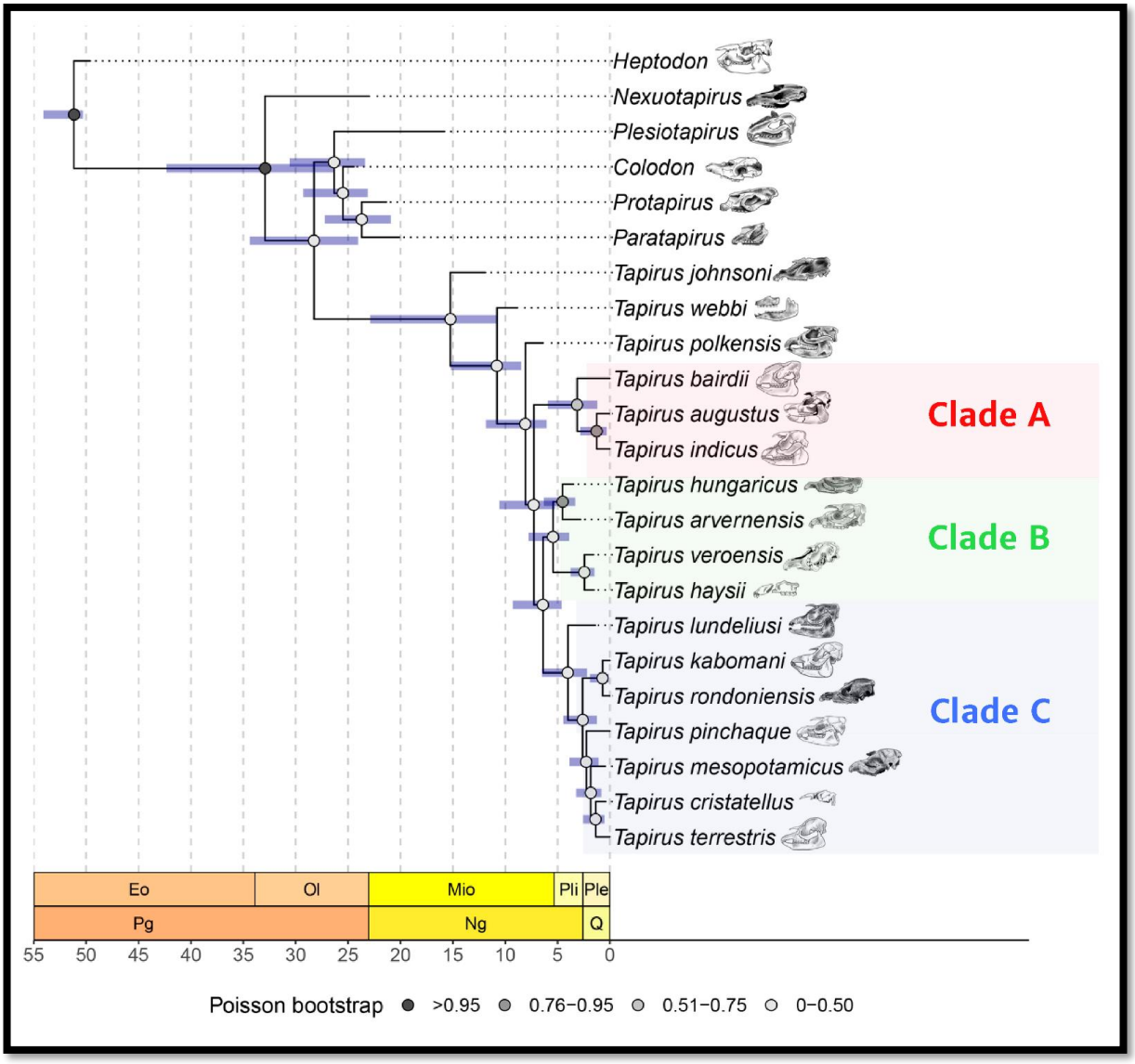

Figure 1. Tip-dating Bayesian chronogram depicting the phylogeny and divergence times of Tapiridae, inferred with the fossilized birth-death diversification prior and an autocorrelated clock prior (TK02), fixing the maximum parsimony topology (MP topology). Node points depict the support for clades and shaded bars depict uncertainty in estimates of node ages. Time scale in millions of years ago.

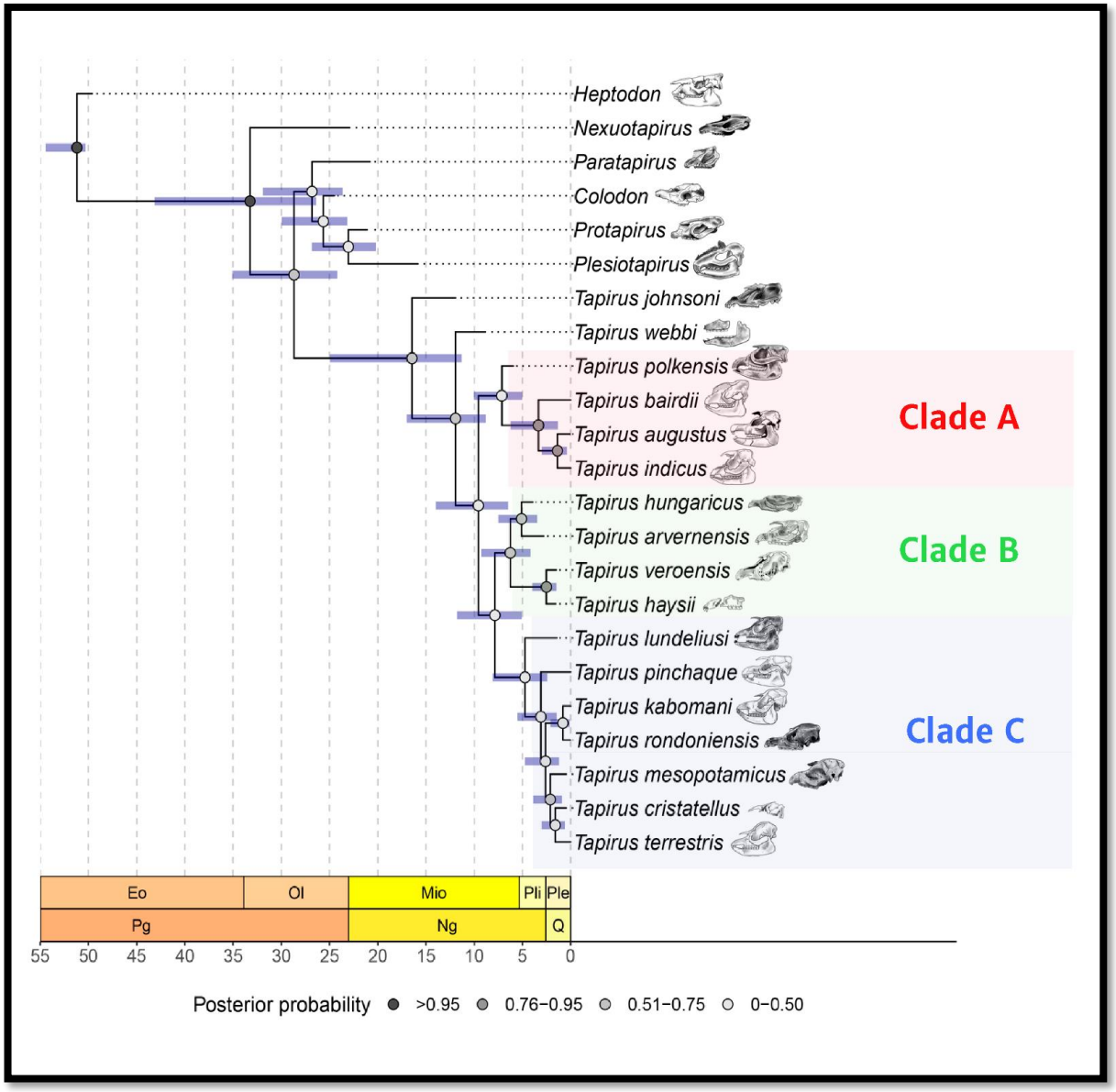

Figure 2. Tip-dating Bayesian chronogram depicting the phylogeny and divergence times of Tapiridae, inferred with the fossilized birth-death diversification prior and an autocorrelated clock prior (TK02), fixing the non-clock Bayesian topology (non-clock BI). Node points depict the support for clades and shaded bars depict uncertainty in estimates of node ages. Time scale in millions of years ago.

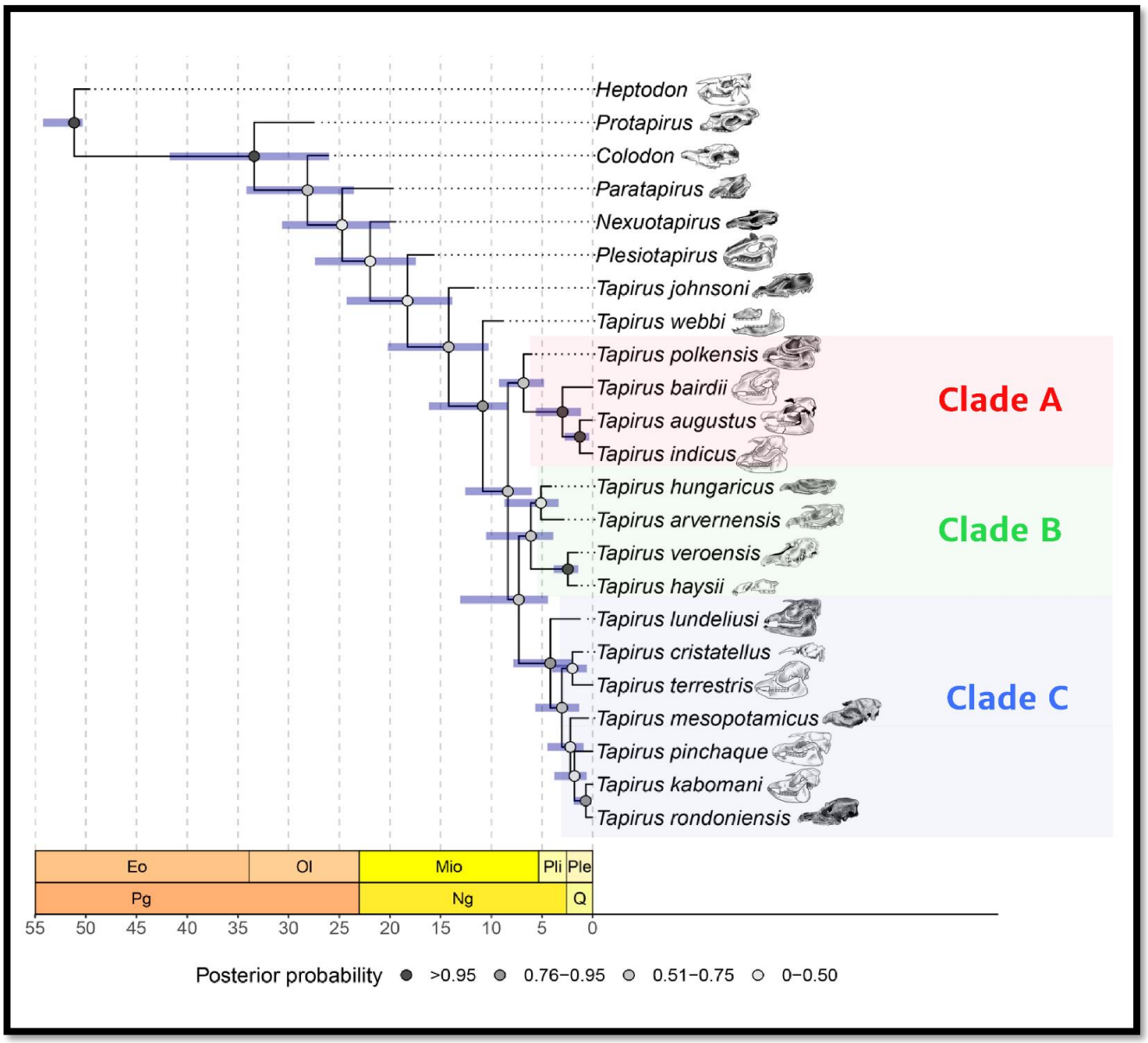

Figure 3. Tip-dating Bayesian chronogram depicting the phylogeny and divergence times of Tapiridae, inferred with the fossilized birth-death diversification prior and an autocorrelated clock prior (TK02), with the topology being co-estimated (clock BI) along with divergence times and other parameters. Node points depict the support for clades and shaded bars depict uncertainty in estimates of node ages. Time scale in millions of years ago.

To the exclusion of *Nexuotapirus*, all other non-*Tapirus* Tapiridae formed a clade in MP (Figure 1) and non-clock BI topology (Figure 2) (despite their different arrangement regarding *Paratapirus* and *Plesiotapirus* positions), whereas in the clock BI tree, in which the topology and divergences times were co-estimated, the non-*Tapirus* tapirids were recovered as successive stem groups of the genus *Tapirus* (Figure 3). The position of *Nexuotapirus* was also variable, being recovered as the first lineage of tapirids to diverge in MP and non-clock BI topologies, whereas in the clock BI topology, it was recovered more nested among non-*Tapirus* tapirids and closer to *Tapirus*.

In all three phylogenetic hypotheses, *T. johnsoni* and *T. webbi* occupied a stem position among tapirs, successivelly diverging before all other lineages (Figures 1, 2 and 3). Following them, *T. polkensis* diverged in the MP tree, whereas in trees from both BI inferences, this taxon was placed among one of the main three clades of *Tapirus* recovered (see Figures 1, 2 and 3), which together comprise the crown group of *Tapirus*. The first to diverge among these three clades was that composed of *T. bairdi*, and the asian tapirs, *T. augustus* and *T. indicus*, and to *T. polkensis* in BI analyses (Clade A), with a consistent arrangement of the first three taxa across phylogenetic hypotheses (see Figures 1, 2 and 3). Sister to clade A, is a major clade composed of the other two main groups of tapirs. One of them comprises species from North America and Europe—T. *veroensis*, *T. haysii*, *T. hungaricus* and *T. arvernensis* (Clade B)—whereas the other clade is almost exclusively composed of the South American species (Clade C, Figures 1, 2 and 3). In this last clade, there is some minor disagreement among inferences regarding the position of *T. mesopotamicus* and *T. pinchaque*, but the rest of the taxa—T. *lundeliusi*, *T. kabomani*, *T. rondoniensis*, *T. cristatellus* and *T. terrestris* - were recovered in more consistent phylogenetic positions (see Figures 1, 2 and 3).

Node supports were generally very low (PB/PP <0.5) or low (<0.75) in parsimony and Bayesian inferences. In the MP (Figure 1) and non-clock BI topology (Figure 2), only the node of Tapiridae was well-supported (> 0.95), whereas in the clock BI topology (Figure 3), the node of Clade A, that of Asian tapirs (*T. augustus* and *T. indicus*), and that of a clade uniting *T. veroensis* and *T. haysii* were also well-supported. These same three clades received moderate support (0.76−0.95) in non-clock BI topology. In the MP topology, the Asian clade and the European clade (*T. arvernensis* and *T. hungaricus*) also received moderate support. In the clock BI topology, other three clades showed moderate support, specifically, Tapiridae minus *Protapirus*, *Tapirus* minus *T. johnsoni* and *T. kabomani* plus *T. rondoniensis*.

Synapomorphies for major clades (*Tapirus* total, *Tapirus* crown group, clade A, clade B+C, clade B and clade C are available in Supporting Information S8. A complete list of synapomorphies and the ancestral states estimated with the Mk model for Bayesian topologies and the discrete character matrix with characters states attained are available under reasonable request to the first author.

Divergence times

The divergence times estimates were also in great agreement in all analyses conducted here (Figures 1, 2 and 3, Table 1). Tapiridae lineages diverged at some point from the Middle Eocene to the Late Oligocene, with the median estimate in the Early Oligocene, close to the limit with the Late Eocene (Figures 1, 2 and 3, Table 1).

For the total group of genus *Tapirus*, divergence times range from the latest Oligocene/Early Miocene to the Late Miocene, with the median estimate indicating a Middle Miocene age for the initial divergence of tapirs (Figures 1, 2 and 3, Table 1). The crown group probably diverged in the Late Miocene, but older ages, in the Middle Miocene, are also included in the 95% highest posterior density interval.

The median estimated divergence of clade A lineages indicates a Late Pliocene age, with the uncertainty ranging from the Late Miocene to the Early Pleistocene, and the separation of this clade from all other tapirs would have happened in the Late Miocene, with the end of Middle Miocene being the oldest estimate and the Early Pliocene the most recent (Figures 1, 2 and 3, Table 1). Similarly, Clade B median and maximum estimated divergence time were also placed in Late Miocene, with the estimates ranging to the Early Pliocene (Table 1). Lineages of Clade C would have diverged at some point from the Late Miocene to the Early Pleistocene, with a median estimate at the Early Pliocene (Figures 1, 2 and 3, Table 1).

A temporal gap was inferred, separating non-*Tapirus* Tapiridae and *Tapirus* in estimates fixing MP and non-clock BI topologies, resulting in a ghost lineage of more than 10 million years (Figures 1 and 2, Table 1). On the other hand, in the clock BI inference, all the divergence ages were recovered at much more regular intervals and major ghost lineages are absent (Figure 3, Table 1).

Table 1 - Divergence times for selected clades in the three phylogenetic hypotheses. Ages informed as median and the 95% highest posterior density interval.

Nodes	**MP**	**non-clock BI**	**clock BI**
Root	51.15 [50.30 - 54.08]	51.20 [50.30 - 54.43]	51.14 [50.30 - 54.22]
Tapiridae	32.91 [26.37 - 42.34]	33.24 [26.40 - 43.13]	33.39 [26.01 - 41.71]
Tapirus (total)	15.23 [10.84 - 22.88]	16.46 [11.31 - 24.94]	14.21 [10.28 - 20.21]
Tapirus (crown group)*	7.27 [5.24 - 10.57]	9.58 [6.51 - 13.97]	8.37 [6.01 - 12.58]
Clade A	3.14 [1.21 - 5.91]	3.35 [1.32 - 6.24]	2.99 [1.17 - 5.60]
Clade B + C	6.40 [4.62 - 9.28]	7.85 [5.08 - 11.78]	7.30 [4.40 - 13.05]

Clade B	5.44 [3.91 - 7.77]	6.27 [4.16 - 9.29]	6.10 [3.91 - 10.52]
Clade C	4.03 [2.21 - 6.51]	4.74 [2.44 - 8.08]	4.19 [2.08 - 7.84]

* This clade excludes *T. polkensis* in MP topology and is not strictly comparable to the clade present in topologies of the BI inferences.

Biogeography

The biogeographic scenarios observed for the non-*Tapirus* Tapiridae differ both related to the tree and biogeographical model (DIVA and DEC) applied during analyses, whereas for the genus *Tapirus*, estimates were consistent across topologies, with only minor disagreements associated with the models. For the analyses using MP and non-clock BI topologies, DIVA and DEC could not be differentiated due to their similar values of AICc (Table 2). On the contrary, in the clock-BI analyses, DEC outperformed DIVA, despite the much similar qualitative patterns and quantitative parameter estimates returned by both models (Table 2).

The most likely ancestral area for Tapiridae is North America in the topologies in which *Neuxuotapirus* is the first lineage to diverge from all other Tapiridae (MP and non-clock BI, Figures 4-7), but in clock BI, in which this taxon is found on a more nested position, the most likely ancestral area is on including North America, Asia, and Europe (Figures 8 and 9). There is much uncertainty regarding the ancestral distribution for the other non-*Tapirus* Tapiridae taxa, irrespective of them forming a clade or not, with North America, North America + Asia, Asia + Europe and North America + Asia + Europe being recovered across topologies and models (Figures 4-9). This uncertainty hampers a clear estimate of the events shaping the distribution of these clades.

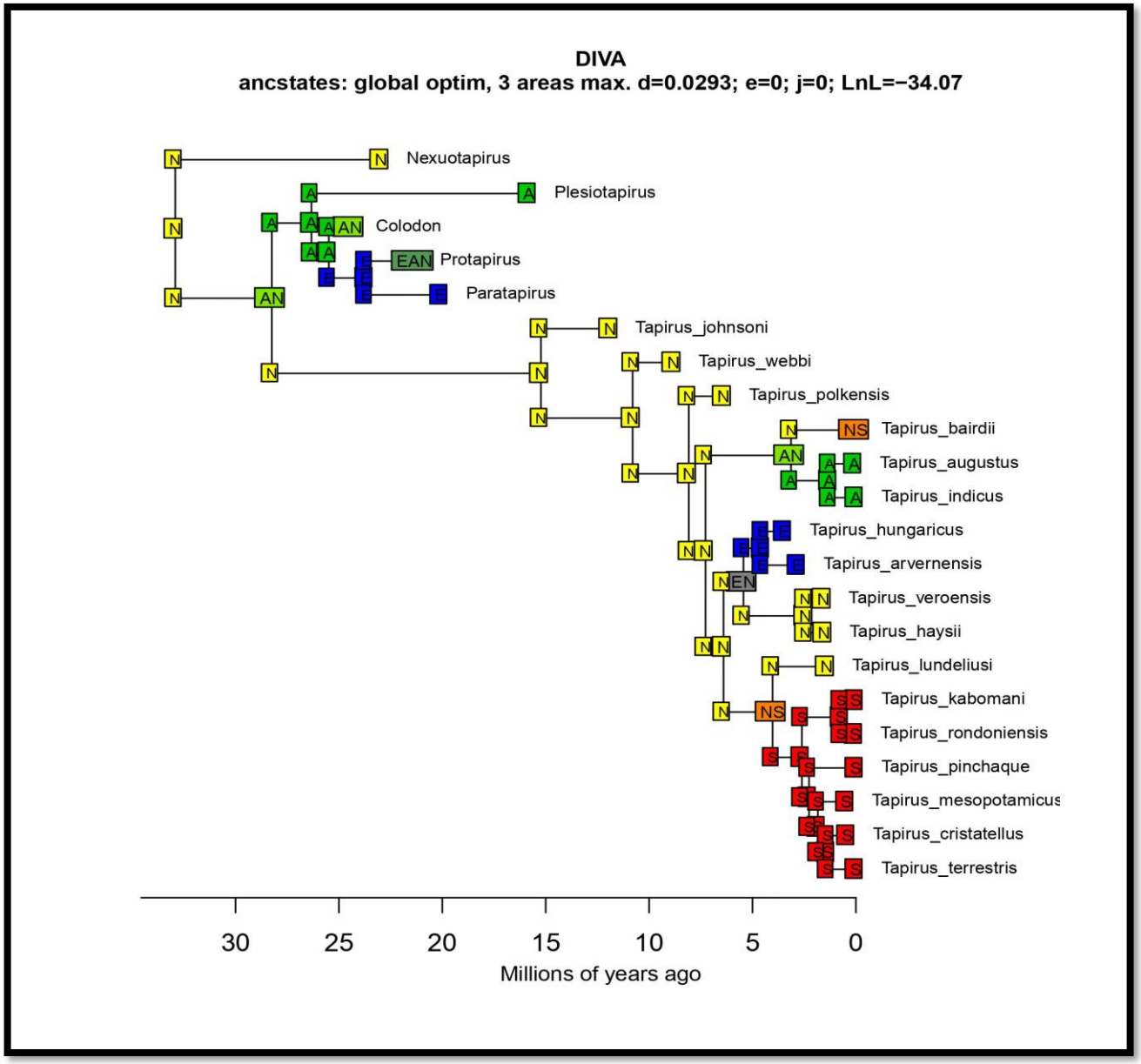

Figure 4. Ancestral range estimation for Tapiridae, based on the model DIVA and the topology from maximum parsimony analysis. Node pies depict marginal likelihoods for each area: Europe (E), Asia (A), North America (N) and South America (S) and their combinations. Time scale in millions of years ago.

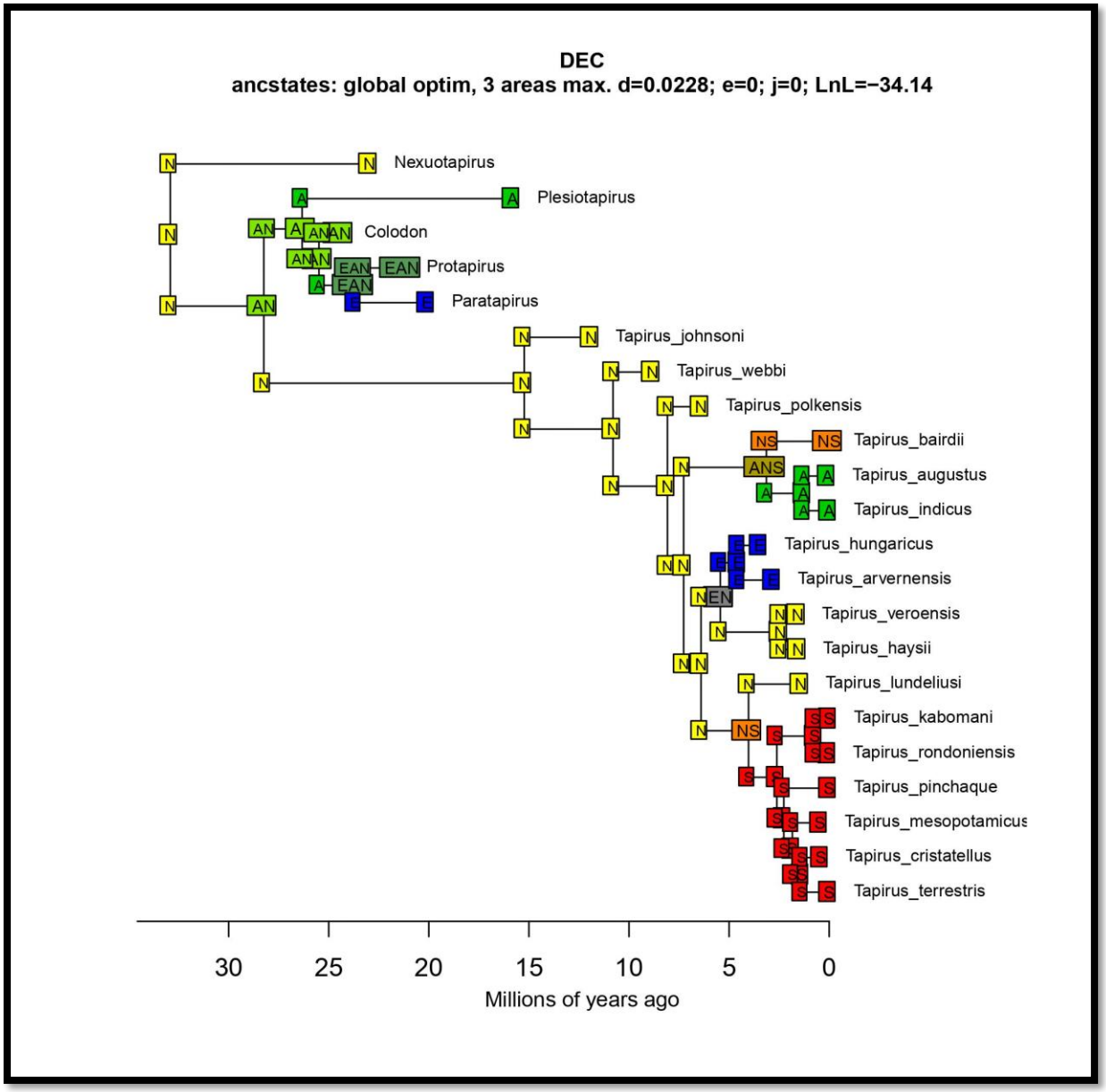

Figure 5. Ancestral range estimation for Tapiridae, based on the model DEC and the topology from maximum parsimony analysis. Node pies depict marginal likelihoods for each area: Europe (E), Asia (A), North America (N) and South America (S) and their combinations. Time scale in millions of years ago.

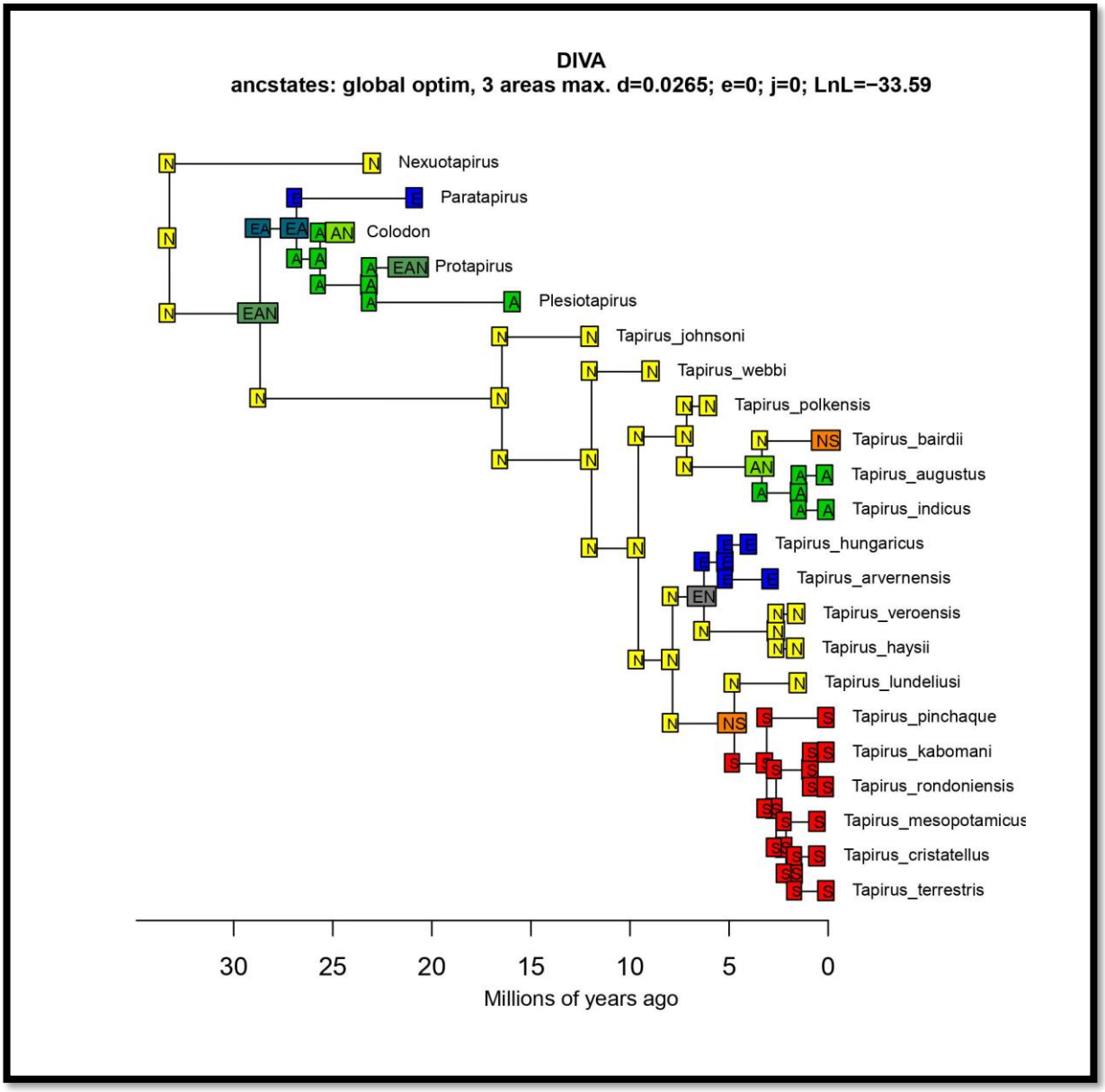

Figure 6. Ancestral range estimation for Tapiridae, based on the model DIVA and the topology from non-clock Bayesian analysis. Node pies depict marginal likelihoods for each area: Europe (E), Asia (A), North America (N) and South America (S) and their combinations. Time scale in millions of years ago.

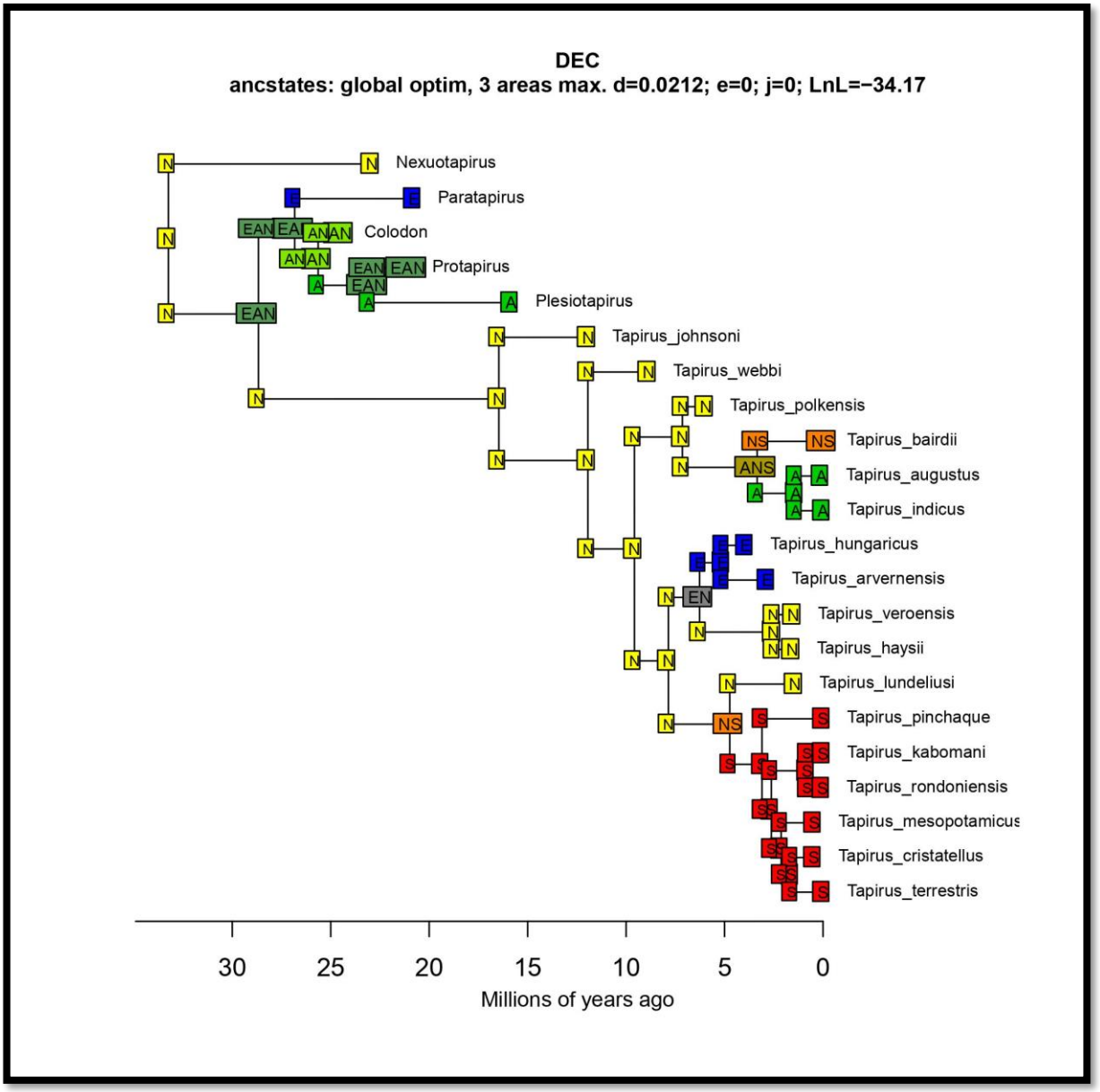

Figure 7. Ancestral range estimation for Tapiridae, based on the model DEC and the topology from non-clock Bayesian analysis. Node pies depict marginal likelihoods for each area: Europe (E), Asia (A), North America (N) and South America (S) and their combinations. Time scale in millions of years ago.

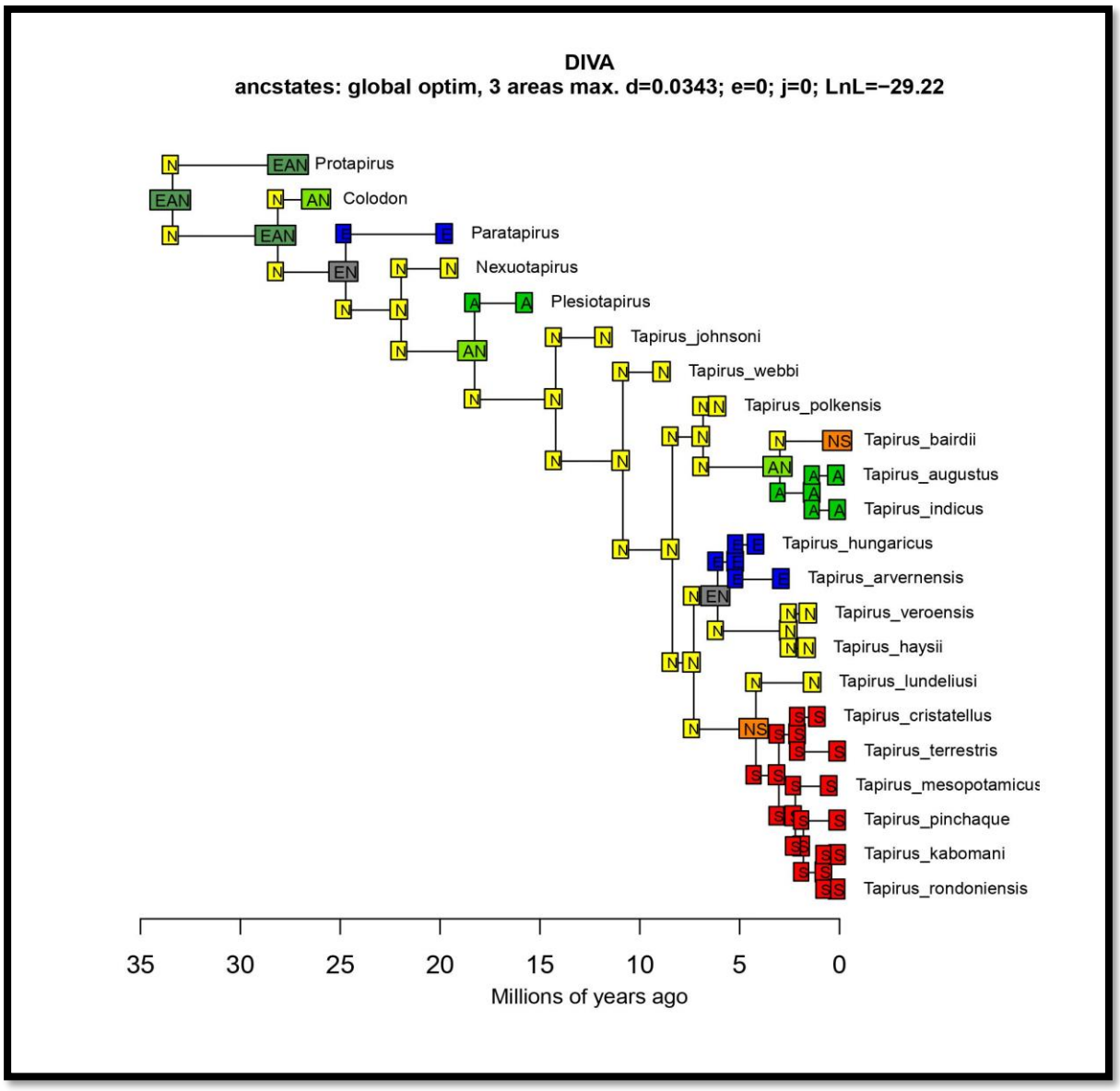

Figure 8. Ancestral range estimation for Tapiridae, based on the model DIVA and the topology from clock Bayesian analysis. Node pies depict marginal likelihoods for each area: Europe (E), Asia (A), North America (N) and South America (S) and their combinations. Time scale in millions of years ago.

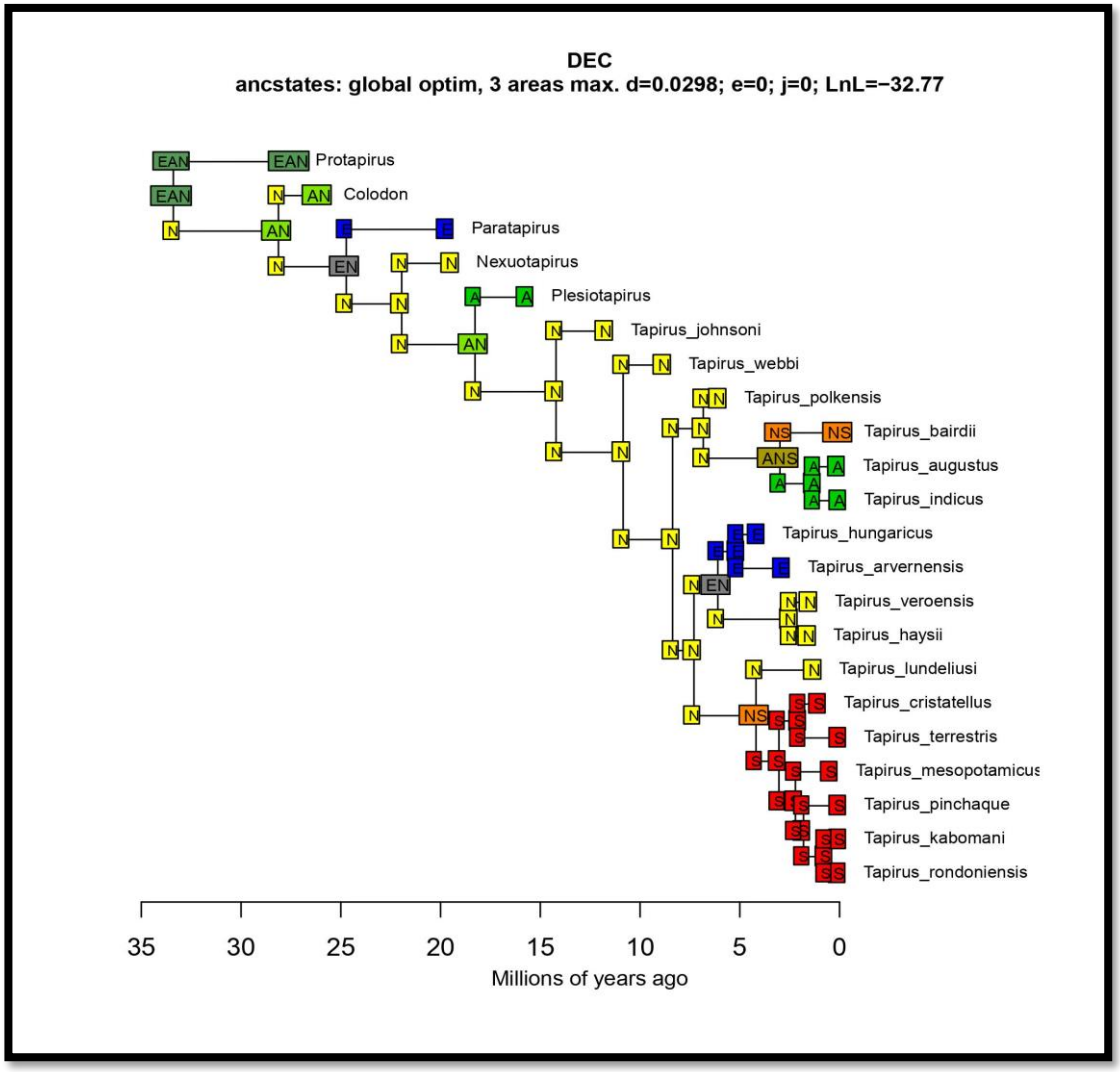

Figure 9. Ancestral range estimation for Tapiridae, based on the model DEC and the topology from clock Bayesian analysis. Node pies depict marginal likelihoods for each area: Europe (E), Asia (A), North America (N) and South America (S) and their combinations. Time scale in millions of years ago.

For genus *Tapirus*, on the other hand, a consistent estimation of North America as the most likely ancestral area was recovered for both the total and the crown group tapirs, irrespective of the tree or model considered, and this estimate is highly supported (Figures 4-9). North America is also recovered as the ancestral distribution for each of the three major clades of *Tapirus* (i.e., clades A, B and C), and for all of them, a sequence of dispersal events expanding the geographic range followed by vicariant speciation defined the recent distribution of these clades (Figures 4-9). For clade A, going from North America, the dispersal event expanded its ancestral distribution to Asia or Asia + South America, and a vicariant event restricted *T. bairdi* to the Americas, and the clade formed by *T. augustus* and *T. indicus* to Asia (Figures 4-9). For clade B, the expanded distribution occupied Europe, and a vicariant event restricted the clade with

T. veroensis and *T. haysii* to North America, and the clade formed by *T. hungaricus* and *T. arvernesnis* to Europe (Figures 4-9). Finally, regarding clade C, a dispersal to South America preceded the vicariant event that restricted *T. lundeliusi* to North America, and all other tapir species to South America (Figures 4-9).

Table 2 - Summary of the results of fitting two biogeographic models (DIVA and DEC) to each of the three topologies evaluated.

Topology	Model	LnL	params	d	e	AICc
MP	DEC	-34.14	2	0.023	1.0e-12	72.92
MP	DIVA	-34.07	2	0.029	1.0e-12	72.78
non-clock BI	DEC	-34.17	2	0.021	1.0e-12	72.98
non-clock BI	DIVA	-33.59	2	0.026	2.0e-09	71.82
clock BI	DEC	-32.77	2	0.030	1.0e-12	70.18
clock BI	DIVA	-29.22	2	0.034	1.0e-12	63.08

LnL - log-likelihood, params. - number of parameters, d - dispersal
- extinction rates, AICc - Sample-size corrected Akaike information
n.

DISCUSSION

Topologies

Topologies that will discussed based on the results obtained in the present work are represented in Figures 10 to 23.

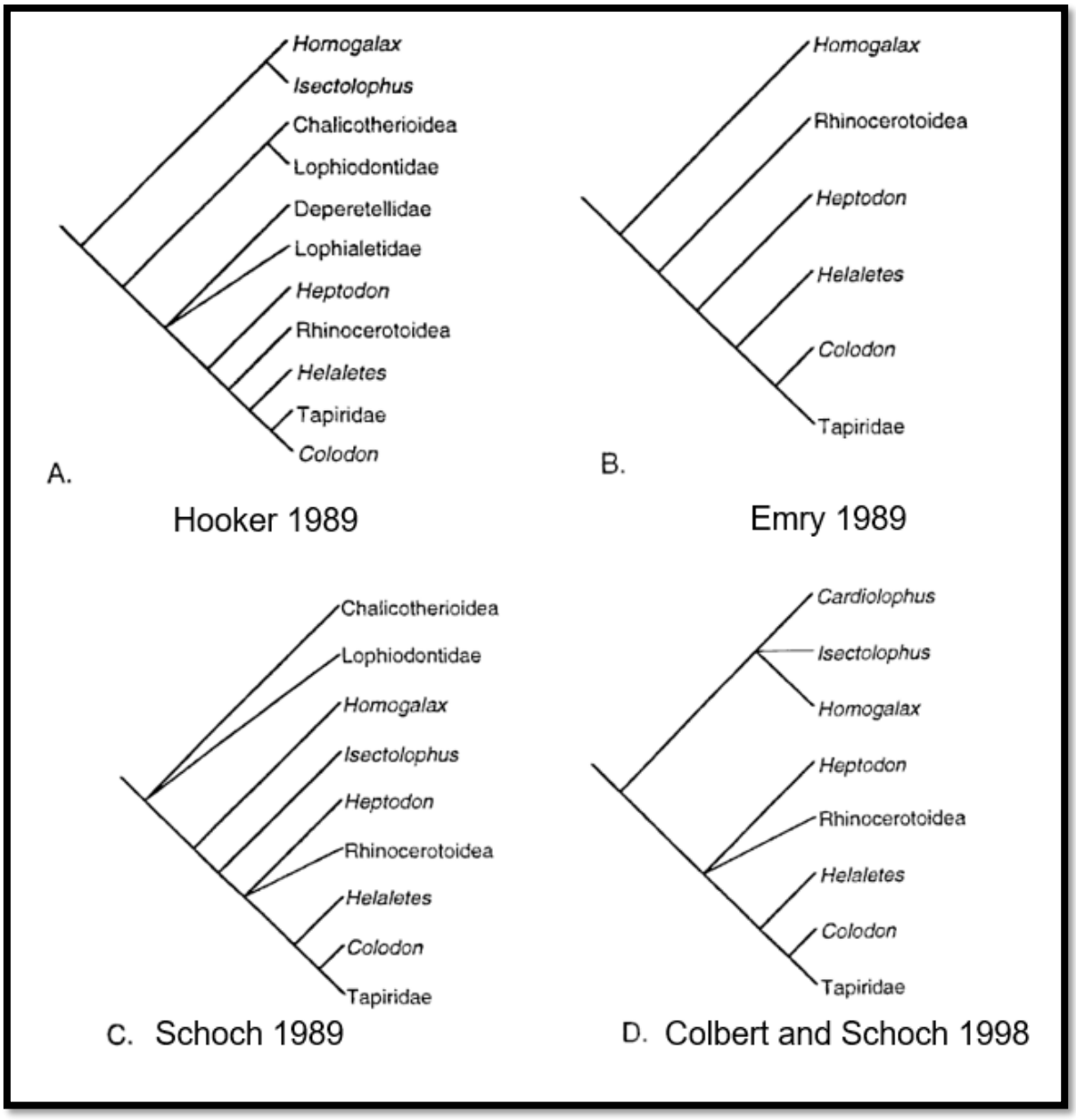

Fig 10. Holbrook 1998 citing Hooker 1989, Emry 1989, Schoch 1989 and Colbert and Schoch 1998.

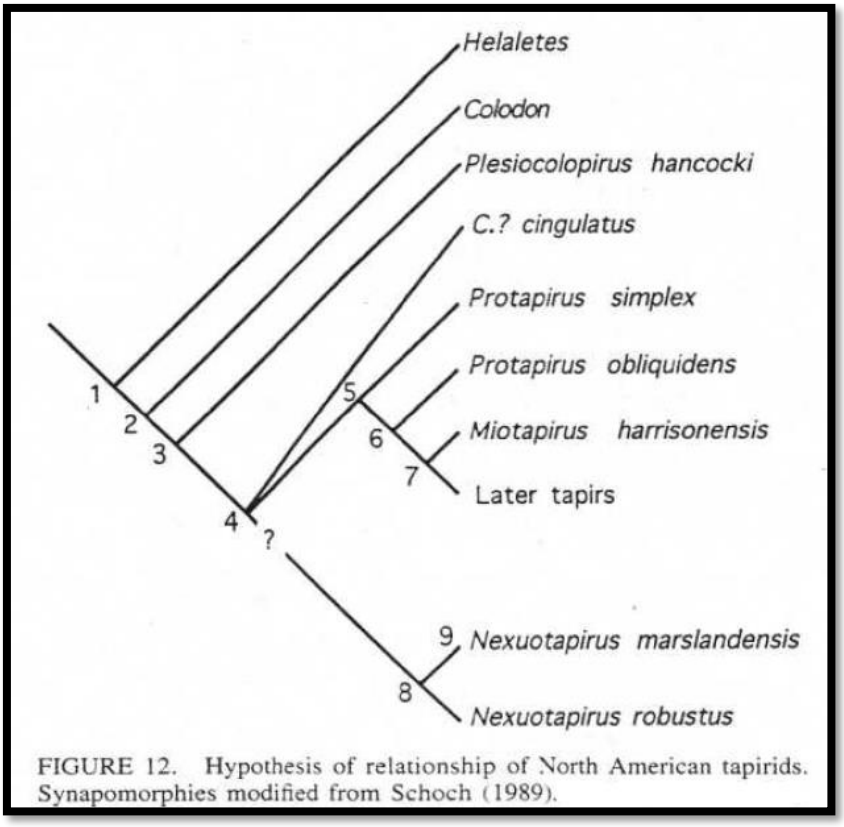

FIGURE 12. Hypothesis of relationship of North American tapirids. Synapomorphies modified from Schoch (1989).

Fig 11. Albright 1998

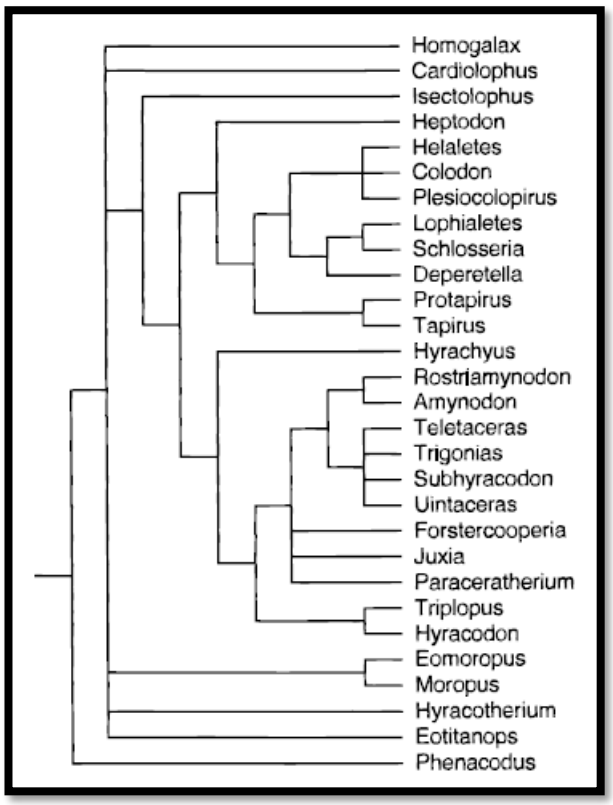

Fig 12. Strict consensus tree, Holbrook 1998

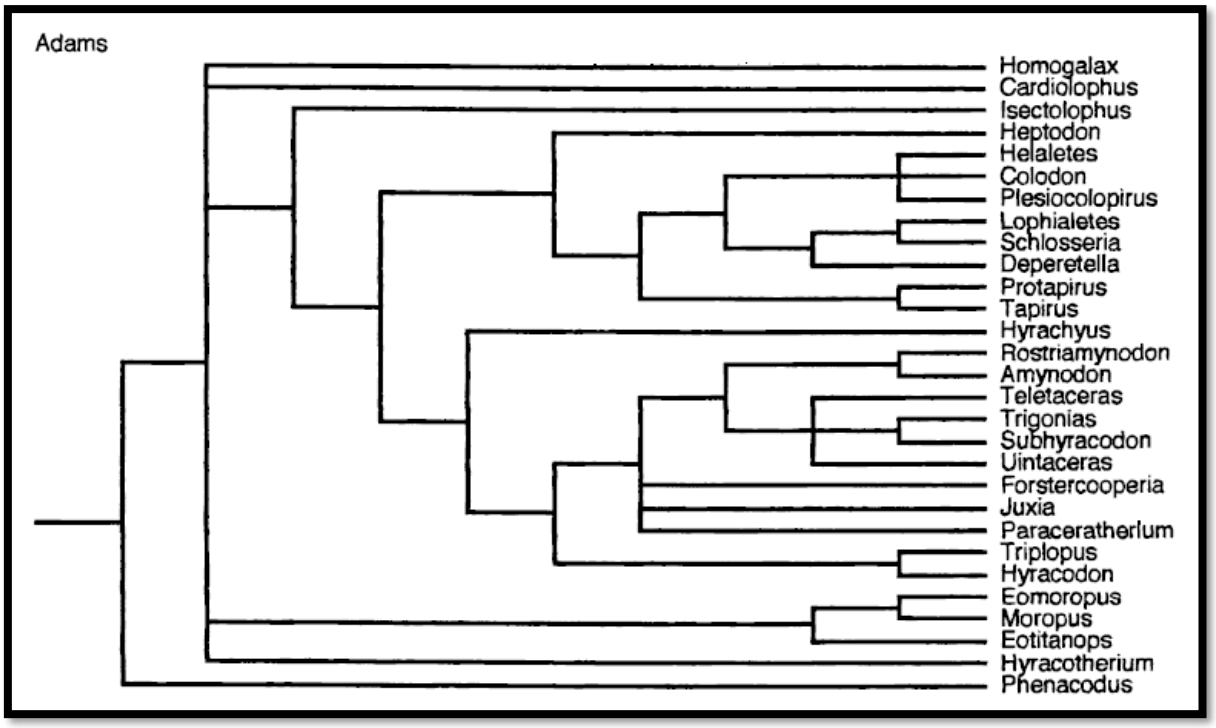

Figure 13 Holbrook 1998 Adam's consensus tree

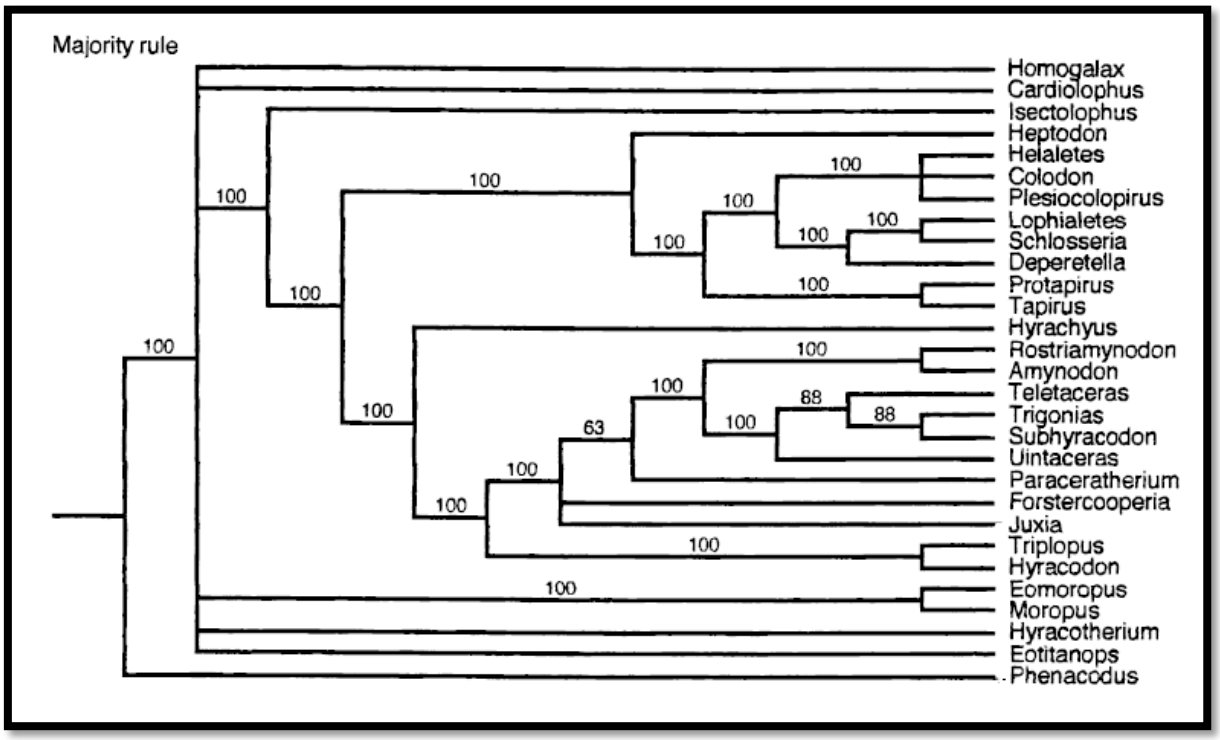

Figure 14 Holbrook 1998 majority rule tree

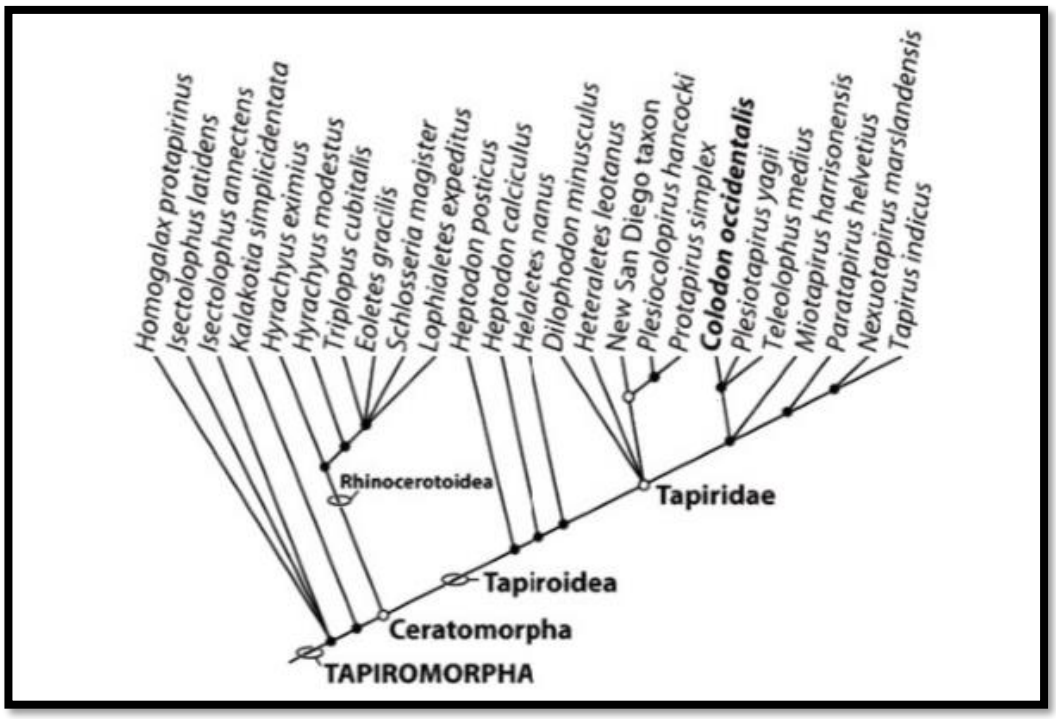

Figure 15. Adam's consensus, Colbert et al. 2005

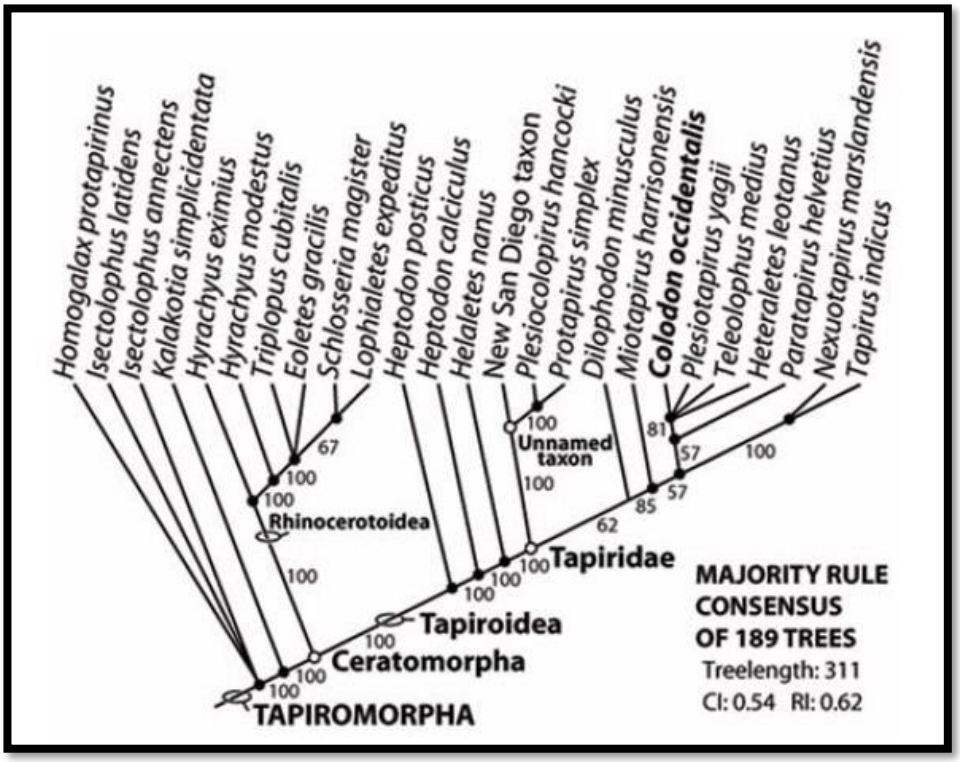

Figure 16. Majority rule consensus, Colbert et al. 2005

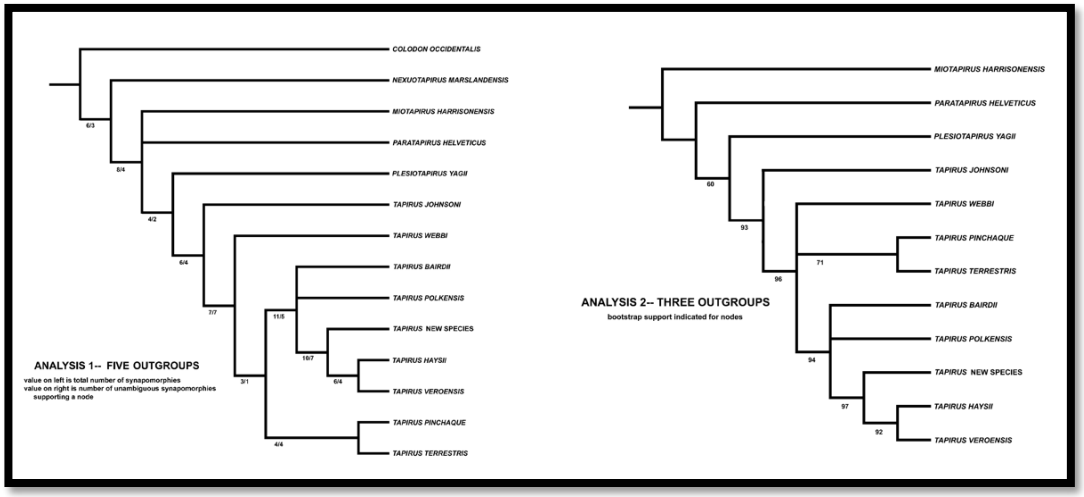

Figure 17. Hulbert and Wallace 2005

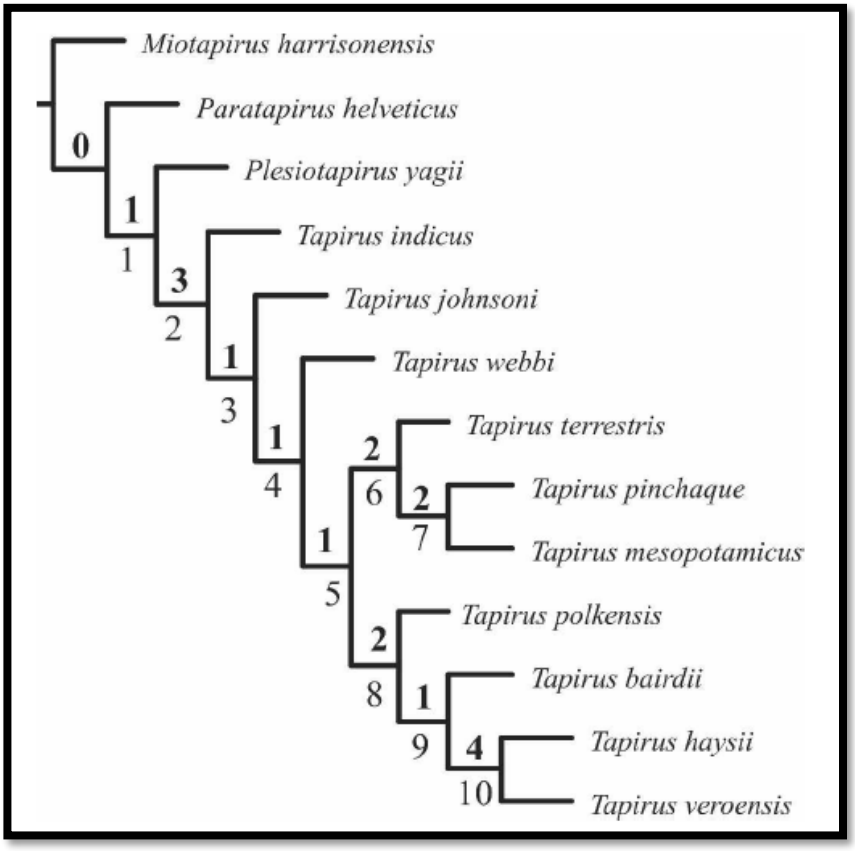

Figure 18. Ferrero and Noriega 2007

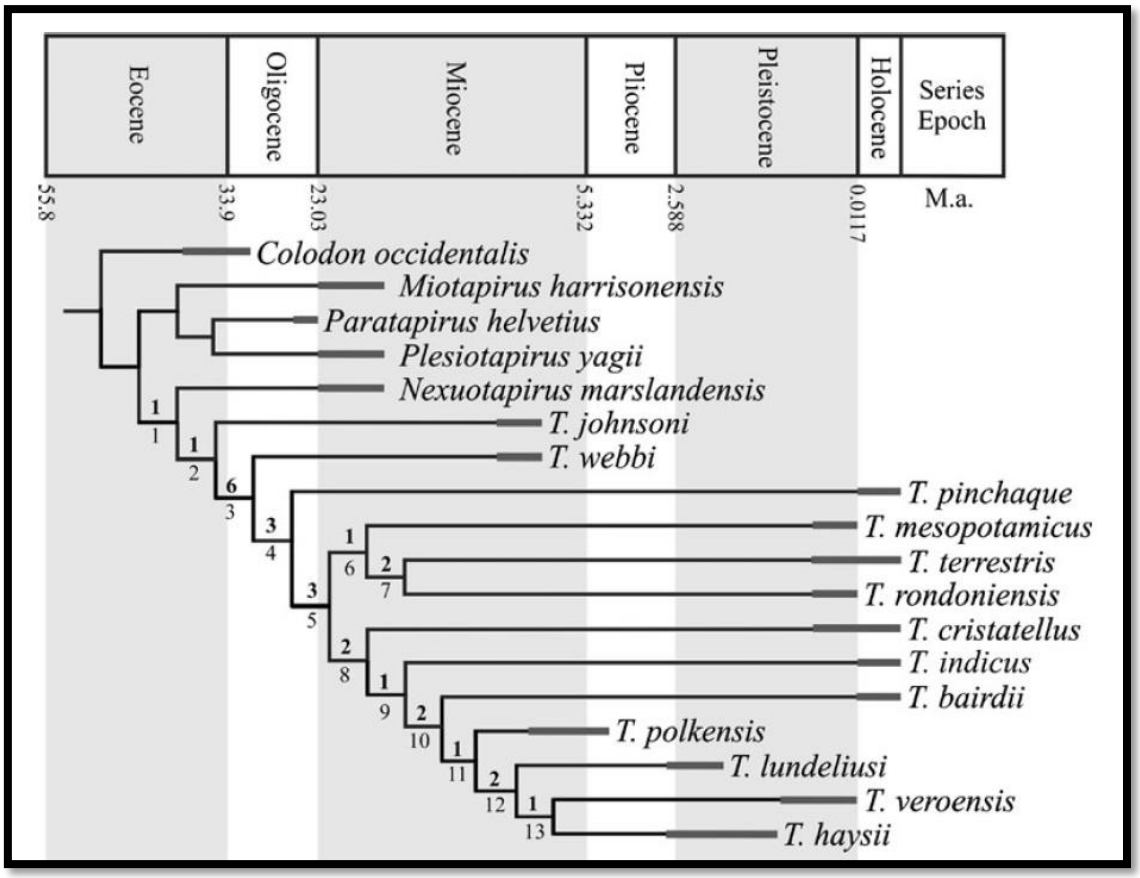

Figure 19. Holanda and Ferrero 2012

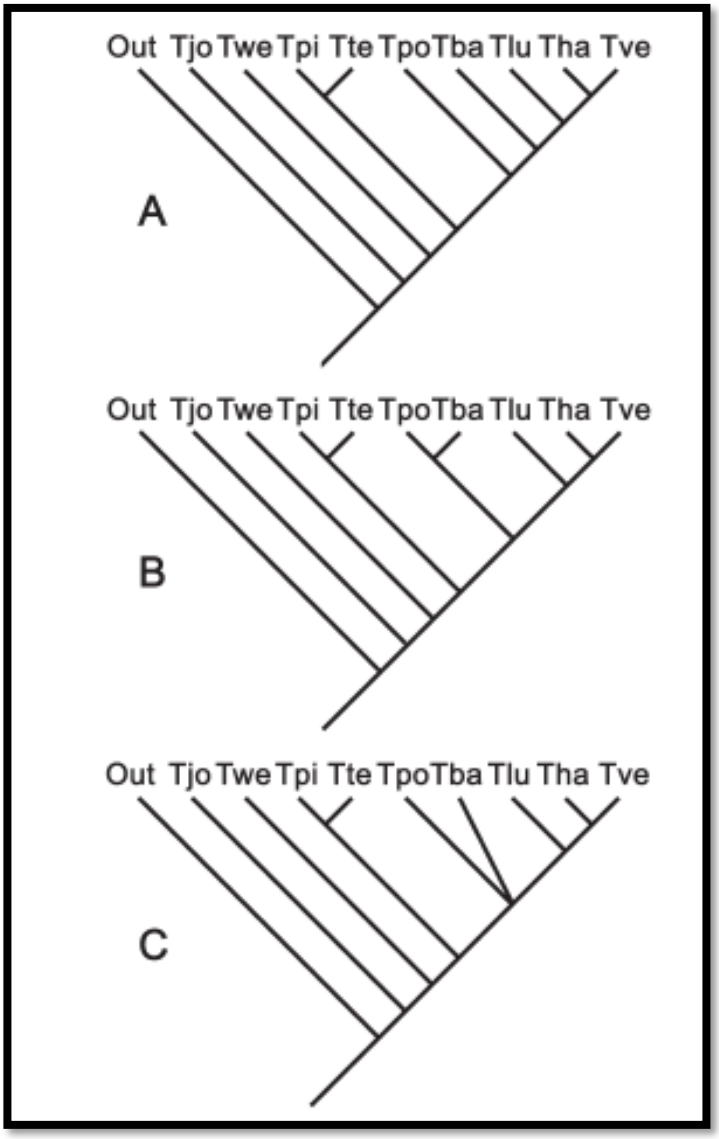

Figure 20. Hulbert 2010, Equally most parsimonious arrangements (A and B), and the strict consensus tree (C) excluding T. *hezhengensis*

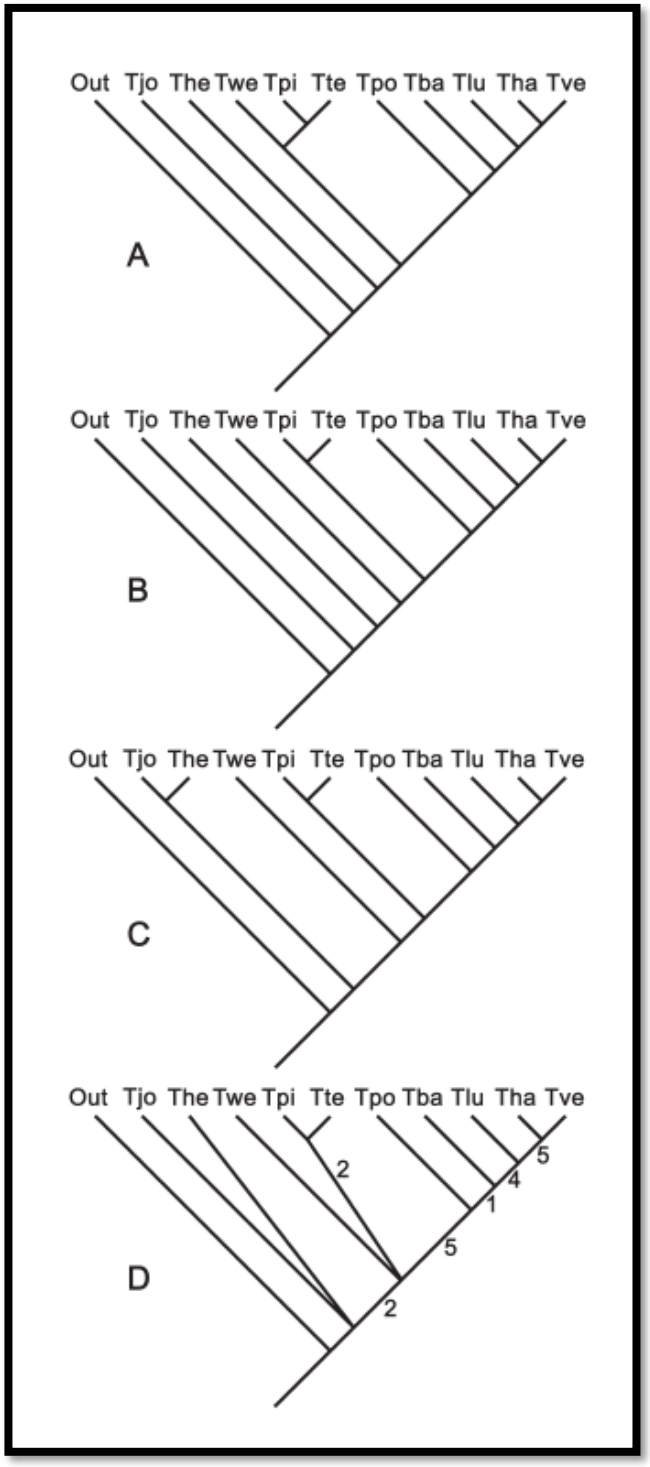

Figure 21. Hulbert 2010, equally most parsimonious arrangements (A, B and C), and the strict consensus tree (D) including T. *hezhengensis*

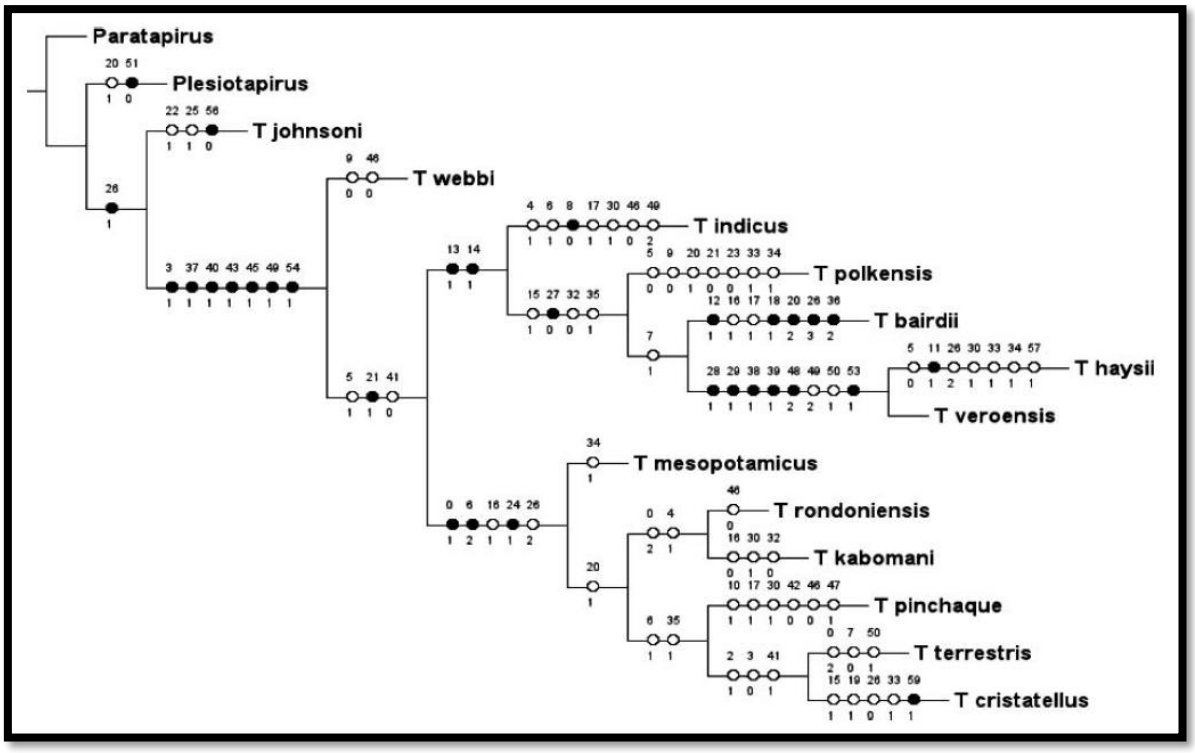

Figure 22. Cozzuol et al. 2013, 2014

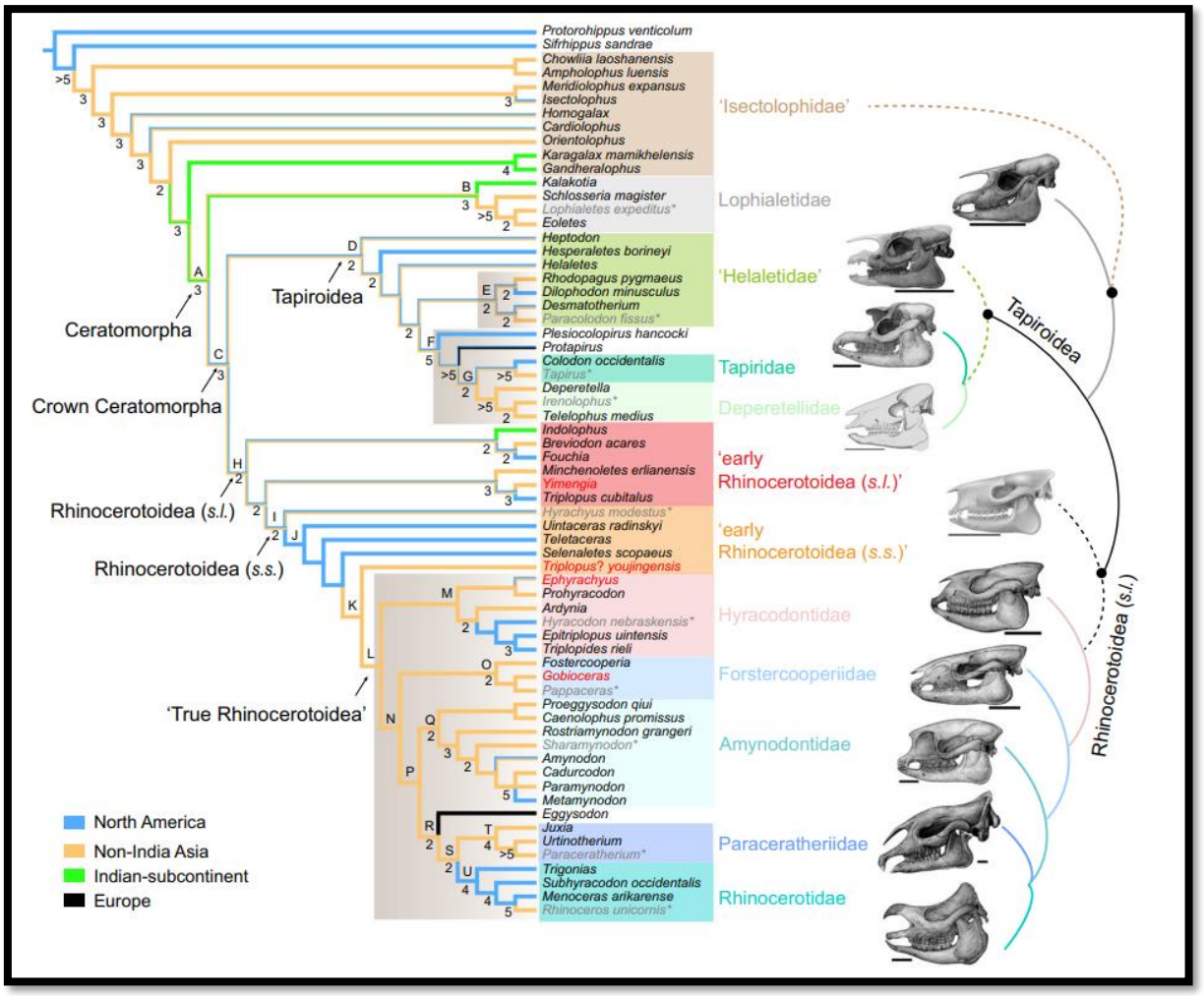

Figure 23. Bai et al. (2020)

Many extinct tapirid species, especially Eurasian but also Asian and South American ones, are known by dental and/or fragmented skull specimens only. Since teeth are shown not to be useful for species identification (Perini et al. 2022, Dumbá et al. 2022), our taxonomic sample was restricted only to species with at least one relatively well-preserved skull. We chose to work with genera as terminal taxa for non-*Tapirus* Tapiridae instead of species in order to minimize missing data (Campbell and Lapointe, 2009).

We followed Catalano et al. (2010) by using landmarks for a low-level phylogenetic investigation (Family level), which in general gives more effective results with this widely used quantitative data in the past years (Parins-Fukuchi 2017). There were no differences between the topologies built based on qualitative data only and discrete plus quantitative geometric morphology data. This can be an indicator of the robustness of the data (Parins-Fukuchi 2017) although previous works have showed that morphometric data have low phylogenetic reliability

(Ascarrunz et al. 2019, Váron-González et al. 2020). Further tests on the behavior of quantitative data, especially morphometric data, need to be assessed to confirm this.

Tapirid phylogenetic relationships on our topologies (Figures 1, 2 and 3) match most of previous works in many ways, as will be discussed in details below. This was expected, as tapiridae have been previously cited as "living fossils", with most of its morphological skull differences being related to the evolution of a mobile proboscis (Dumbá et al. 2019). Even with general resemblances, some differences in the node arrangement and clades were observed compared to previous studies. This probably stems from our expanded taxonomic sampling. Some other differences are clearly associated with the use of different inference criteria. Previous works have demonstrated that Bayesian analysis can contribute to the construction of reliable morphological phylogenetic inferences of morphological data (Puttick et al. 2019, Casali et al. 2022), therefore we also considered this methodological approach in the current work, alongside with traditional Maximum Parsimony approaches.

Regarding the main previous literature that will be hereby compared to, Emry (1989), Hooker (1989), Schoch (1989), Albright (1998), Colbert and Schoch (1998), Hoolbrook (1998) and Holbrook (2001) focused mainly on Tapiromorpha non-Tapiridae. Colbert (2005) presented topologies focused on both Tapiromorpha and Tapiridae, but not focused *Tapirus*. Colbert 2005, Hulbert and Wallace 2005, Ferrero and Noriega (2007), Hulbert (2010), Holanda and Ferrero (2012) and Cozzuol et al. (2013, 2014) focused mainly on *Tapirus* phylogenetic reconstructions. Bai et al. (2020) provided Maximum Parsimony and Bayesian topologies for Ceratomorpha, with very few Tapiroidea sampled. The current study was the first to infer a Bayesian topology while including a broad sample of tapirids.

The Tapiridae non-*Tapirus*, excepting for *Nexuotapirus*, form a clade in both fixed topologies (Figures 1 and 2), but the clock-BI topology (Figure 3) shows a ladder-like sequence for them. In clock-BI analyses, age information can overrule the morphological signal, and this may be the case here (Figure 3) (King 2021, Mongiardino Koch et al. 2021). Nevertheless, Hulbert and Wallace (2005) showed a similar ladder-like pattern for a phylogenetic hypothesis of Tapiridae non-*Tapirus* with a traditional, non-clock analysis, suggesting that there is also some morphological information for such arrangement.

Our clock-BI topology (Figure 3) recovers *Protapirus* as the most basal clade of Tapiridae. This scenario is supported by Scott (1941), Radinsky (1963), Hooker (1984), Schoch (1989) and Colbert (2005), that defined Tapiridae as the clade formed by the most recent common ancestor of *Protapirus* and *T. terrestris.* On the other hand, both non-clock BI and MP topologies recovers *Nexuotapirus* as sister group of remaining Tapiridae. Our MP (Figure 1) and non-clock

BI (Figure 2) scenarios differ from Colbert's (2005) topologies which recovered *Nexuotapirus marslandensis* as sister group of *Tapirus indicus*, the only species of the genus included in his analysis. Holanda and Ferrero (2012) recovered *Nexuotapirus* as the sister taxa of all *Tapirus*, different from our result. Although Holanda and Ferrero (2012) used a discrete matrix most resembling to ours, we did further adaptations to Hulbert and Walace's (2005) matrix. Furthermore, we included *Protapirus*, exclude *Miotapirus* and used *Heptodon* as outgroup instead of *Colodon*. These factors, besides the methodological steps that led into our topologies, might have led to different hypothesis regarding *Nexuotapirus*'s position.

MP (Figure 1) and non-clock BI (Figure 2) topologies are much alike regarding the Tapiridae non-*Tapirus* groups in general. In both, *Colodon*, *Paratapirus*, *Protapirus* and *Plesiotapirus* form a clade. Regarding *Colodon*, there are no previous works resembling this genus as sister clade to *Paratapirus*, *Protapirus* and *Plesiotapirus*. Instead, Tapiridae was discussed as being a family derived from *Colodon* in Radinsky (1963, 1965) and Janis (1984), although, in both cases, without a formal phylogenetic analysis assessed to those discussions. *Colodon* was recovered as sister clade of Tapiridae in the following Tapiromorpha phylogenetic works: Emry (1989), Hooker (1989), Schoch (1989), Colbert and Schoch (1998) and Hoolbrook (1998), which will be commented in detail below. All previous five works recovered topologies that were more focused on sampling more stem Tapiromorpha instead of Tapiridae species. Hooker (1989) performed parsimony analysis based mostly on dental characters. Besides the use of problematic characters for *Tapirus* (dental characters), Hooker stated at the time that the topology published was not the shortest possible tree found (Holbrook 1998). Emry (1989), Schoch (1989) and Colbert and Schoch (1998) phylogenetic hypothesis were built based only in North American taxa, which differs from our wide sampled topologies of tapirids. As in Hooker (1989), Schoch's and Holbrook (1998) phylogenies also include numerous dental characters. Holbrook (2001), for instance, built four phylogenetic hypotheses in consensus cladograms mainly based on cranial and postcranial data-in comparison to its 1999 work, but *Colodon* appears among a polytomy in all hypotheses and, therefore, its position is unclear. Colbert (2005) recovered similar phylogenetic relationships for *Colodon* compared to the present work, placing *Colodon occidentalis* inside Tapiridae. Its position was unclear inside the majority-rule consensus tree, placed in a polytomy with *Plesiotapirus yaggi*, *Teleolophus medius* and *Heteraletes leotanus* (Colbert 2005). At the Adam's consensus though, *Colodon occidentalis* is sister to a clade formed by *Plesiotapirus yaggi* and *Teleolophus medius.* Hulbert and Wallace (2005) chose *Colodon occidentalis*, *Plesiotapirus yaggi*, *Paratapirus helvetius* and *Nexuotapirus marslandensis* as outgroups for *Tapirus*, hence its positions were not evaluated. Holanda and Ferrero (2012) placed *Colodon occidentalis* as the

outgroup on their maximum parsimony analysis. Bai et al. (2020), the most recent phylogeny published including Tapiroidea, considered *Colodon* part of Tapiridae, which agrees with our work. Regarding previous cited works, differences in species sampled, matrix data and phylogenetic methods might have influenced different results in the position of *Colodon*. Since we choose *Heptodon* as an outgroup, *Colodon* will be inside Tapiridae, so it still might not be a tapirid, but a tapiroid non-tapirid instead. Further tapiroid phylogenetic analysis is necessary to confirm the position of *Colodon*.

Still considering MP (Figure 1) and non-clock BI (Figure 2) topologies, *Plesiotapirus* and *Paratapirus* switch positions. *Plesiotapirus* is sister taxa to *Protapirus* in the Bayesian fixed topology, and *Paratapirus* is sister taxa to *Protapirus* in the parsimony topology. Albright (1988) only studied *Protapirus* amongst those three genera, therefore its position will not be discussed here. Holbrook (2001) retrieved *Protapirus* and *Tapirus* as sister taxa, but the author did not include other Tapiridae clades, so we cannot argue if these two taxa are closely related inside the family with just two genera sampled. *Paratapirus helvetius* was recovered as sister group of the polytomy formed by *Colodon occidentalis*, *Plesiotapirus yaggi*, *Teleolophus medius* and *Heteraletes leotanus* in Colbert's (2005) majority-rule consensus tree. *Protapirus simplex* is placed at the same topology as sister taxa to *Plesiocolopirus hancocki*, in a basal position inside Tapiridae. In Colbert's (2005) Adam's Consensus tree, *Paratapirus helvetius* is the sister group of the clade formed by *Nexuotapirus marslandensis* and *Tapirus indicus.* Inside the same phylogeny, *Plesiotapirus yaggi* stem position is sister to *Teleolophus medius* (Colbert 2005). Still in Adam's consensus in Colbert (2005), *Paratapirus* do not share any close relation to *Protapirus* inside Tapiridae, as *Protapirus simplex* is placed at a basal position inside Tapiridae, sister to *Plesiocolopirus hancocki.* These patterns of relation between *Paratapirus*, *Protapirus* and *Plesiotapirus* in Colbert (2005) are different from our current work. However, our clock-BI (Figure 3) topology retrieves *Protapirus* as the most basal tapirid, which agrees with Colbert's (2005) stem definition of Tapiridae as the most recent common ancestor of *Protapirus simplex* and *T. terrestris. Protapirus* was not included in Holanda and Ferrero (2012) analysis, and its phylogenetic hypothesis shows *Paratapirus helvetius* and *Plesiotapirus yaggi* as sister taxa. *Paratapirus* and *Plesiotapirus* were chosen as outgroups in Ferrero and Noriega (2007) and in Cozzuol et al. (2023, 2014) morphological phylogenetic inferences, and therefore will not be further discussed. *Protapirus* is considered sister clade to all Tapiridae in Bai et al. (2020), but only *Protapirus*, *Colodon* and *Tapirus* were included.

Regarding *Tapirus* (total group), common synapomorphies between the three topologies are (see Supporting Information S8): 8 (0), large interparietal bone in postnatal individuals; 9 (0), typically polygonal (hexagonal or diamond shaped) interparietal bone; 20 (0), nasal notch dorsal to orbit; 22 (0), sharp dorsomedial border of maxilla, mostly directed medially; 24 (1), premaxillary-maxillary suture located at the middle of the alveolus of canine; 52 (1), M1 metaloph joins the ectoloph at or near metacone. It is important to point out that the unambiguous synapomorphy recovered for *Tapirus* in Holanda et al. (2012), the only work that discussed a synapomorphy for *Tapirus* on its topology, was not retrieved in any of our phylogenetic hypotheses. The character for which state was recovered as a synapomorphy in Holanda et al. (2012) is not present in our matrix (character 46). As previously mentioned, we did further adaptations to Hulbert and Wallace's (2005) matrix and removed dental characters such as character 46 in Holanda and Ferrero (2012).

Our three topologies (Figures 1, 2 and 3) retrieved *T. johnsoni* as the most basal *Tapirus*. This is consistent with most previous works that studied the evolution of *Tapirus* species (Hulbert and Wallace 2005, Hulbert 2010, Holanda and Ferrero (2012), Cozzuol et al. 2013, 2014). The exception is Ferrero and Noriega (2007), which assessed *T. indicus* as sister to all *Tapirus*. *T. johnsoni* presents fossil records from the Middle Miocene of North America and holds many primitive characteristics for genus *Tapirus*, including small body size, elongated nasals and meatal foramen more anteriorly oriented.

T. webbi is sister to all *Tapirus* but *T. johnsoni* in the three topologies (Figures 1, 2 and 3). This is consistent with Hulbert and Wallace (2005) and Hulbert (2010) most parsimonious arrangements that did not include the fossil Asian *T. hezhengensis*. In Ferrero and Noriega (2007), *T. webbi* is sister to all *Tapirus* but *T. johnsoni* and *T. indicus*. Our stem position of *T. webii* is also in agreement with Holanda and Ferrero (2012) and Cozzuol's et al. 2013, 2014 morphological phylogenetic hypothesis, in which *T. webbi* is sister to all *Tapirus* but *T. johnsoni*.

Regarding *T. augustus*, we follow Tong et al. (2002) and Hulbert (2010) in considering it as *Tapirus*, not in a different genus, *Megatapirus* as originally designated by Matthew and Granger (1923) as there was not enough morphological evidence to support a generic or subgeneric diferentiation. *T. polkensis*, *T. bairdii*, *T. augustus* and *T. indicus* belong to a clade, CLADE A, in all topologies (Figures 1, 2 and 3), with the Asian *T. augustus* and *T. indicus* as a clade inside the previous one. *T. polkensis* and *T. bairdii* were assessed in a politomy in Hulbert and Wallace (2005). *T. polkensis* is sister to a clade formed by *T. bairdii*, *T. haysii* and *T. veroensis* in Ferrero and Noriega (2007). Hulbert (2010) retrieve a clade formed

by *T. polkensis* and *T. bairdii* only, *T. polkensis* as the most basal species in a clade including *T. bairdii T. lundeliusi*, *T. haysii* and *T. veroensis* and a polytomy including those two species inside a clade. *T. polkensis* has also been previously retrieved as part of a clade consisting of *T. bairdii* and *T. indicus* in Holanda and Ferrero (2012) and Cozzuol et al. (2013, 2014), although its stem position is not the same compared to those previous works, where *T. indicus* is the most basal tapir in that clade. Therefore, a close relation between *T. polkensis*, *T. bairdii* and *T. indicus* has been previously obtained in the literature. Our topologies support the hypothesis in which living *T. bairdii* and *T. indicus* are more closely related to other Asian and North American species than with living South American tapirs. *T. augustus* was never included in a phylogenetic hypothesis for *Tapirus*, so its stem position cannot be compared.

The polyphyletic North American *Tapirus* found in our three topologies (Figures 1, 2 and 3) is consistent with Ferrero and Noriega (2007), Hulbert (2010), Holanda and Ferrero (2012) and Cozzuol et al. (2013, 2014). Although amongst the mentioned works Hulbert (2010) did not include the living Asian tapir *T. indicus*, they all share a similar scenario to our current work regarding the polyphyletic nature of North American tapirs. In our three topologies, *T. bairdii* is the most closely related tapir to the Asian clade, followed by *T. polkensis* - both *Tapirus* species with North American distribution, besides a Central America distribution for *T. bairdii*. *T. bairdii* shares many morphological similarities with *T. indicus* and *T. augustus*, such as a dorso-ventrally extended skull, a parasagittal crest and a deep and extensive fossa on the dorsal surface of the nasals. *T. bairdii*, *T. indicus* and *T. augustus* are the only tapirs described with a parassagittal crest. A closer phylogenetic relation between *T. bairdii* and *T. indicus* with North American and Asian tapirs rather than with South American tapirs is supported by molecular data topologies (Cozzuol et al. 2013, 2014). Our results do not support separate genera for *Tapirella bairdii* and *Acrocodia indica* as proposed by Groves and Grubb (2011).

European *T. hungaricus* and *T. arvernensis* belong to a clade, an both join another clade (Clade B, see Figures 1, 2 and 3) formed by the North American *T. haysii* and *T. veroensis*. *T. haysii* and *T. veroensis* have been previously retrieved as a clade in Hulbert and Wallace (2005), Ferrero and Noriega (2007), Hulbert (2010), Holanda and Ferrero (2012) and in Cozzuol et al. (2013, 2014). As previously mentioned, European *Tapirus* were never included in a phylogenetic hypothesis of *Tapirus*, being one of the novelties of our work. Therefore, the inclusion of *T. hungaricus* and *T. arvernenensis* most likely affected the phylogenetic results obtained in the present work in comparison to previous *Tapirus* phylogenetic studies (Hulbert

2010, Holanda and Ferrero 2012, Cozzuol et al. 2013, 2014), influencing the arrangements observed for other clades as well.

T. lundeliusi is sister to all South American *Tapirus* in all topologies (see Figures 1, 2 and 3). The position of *T. lundeliusi* in our topologies are in disagreement with Hulbert (2010) who considered *T. lundeliusi*, *T. haysii*, and *T. veroensis* as a clade named *Helicotapirus.* Holanda and Ferrero (2012) also retrieved those three species as a clade.

South American tapirs form a clade (most of the clade C) in the three topologies (Figures 1, 2 and 3), which is in agreement with previous works (Ferrero and Noriega 2007, Cozzuol et al. 2013, 2014). *T. pinchaque* was recovered in different positions in all three topologies, but always among the South American *Tapirus*. In our MP topology (Figure 1), *T. pinchaque* is the sister group to *T. mesopotamicus*, *T. cristatellus* and *T. terrestris*. The latter arrangment is more consistent to paleogeographic data and recent phylogenetic hypotheses (Ferrero and Noriega 2007, Cozzuol et al. 2013, 2014) where *T. pinchaque* is not the most basal South American tapir. In the non-clock BI topology (Figure 2) it is sister group to all South American tapirs, while it is sister group to the *T. kabomani* and *T. rondoniensis* group in the clock BI topology (Figure 3). The latter scenario is similar to *T. pinchaque*'s position in Holanda and Ferrero (2012), although that work did not recover a South American clade, and we believe that a basal position for *T. pinchaque* is, therefore, less likely Another point of discussion of the latter work is the divergence of *T. pinchaque* on the Oligocene, where there is no fossil record for this Pleistocene species nor was the Panama isthmus already formed (for further Biogeographic and Divergence times information, see the next sections of this Discussion). We believe that more dental characters used on Holanda and Ferrero (2012) and less cranial characters in comparison to our matrix could be reasons for such different results. Hulbert and Wallace (2005) and Hulbert (2010) recovered a clade formed by *T. pinchaque* and *T. terrestris* in all topologies which is not confirmed by our hypothesis, but these were the only South American tapirs studied in those works.

T. cristatellus is sister to a clade formed by *T. indicus*, *T. bardii*, *T. polkensis*, *T. lundeliusi*, *T. veroensis* and *T. haysii* in Holanda and Ferrero (2012), which differs from its position in our topologies. *T. cristatellus* is sister to *T. terrestris* in Cozzuol et al. 2013, 2014, which is in agreement with our three topologies.

In Holanda and Ferrero (2012), *T. mesopotamicus* is sister to all South American tapirs but *T. pinchaque*, which is a different scenario from our three phylogenetic hypotheses (see Figures 1, 2 and 3). *T. mesopotamicus* in Cozzuol et al. (2013, 2014) is sister to all South American tapirs, which differs from our topologies. In the current work, *T. cristatellus* switches

position with *T. rondoniensis* of Holanda and Ferrero (2012) inside a clade with *T. terrestris,* of which *T. mesopotamicus* is sister to.

T. rondoniensis and *T. kabomani* form a clade in our three topologies (Figures 1, 2 and 3). This is consistent with Cozzuol et al. 2013, 2014, papers in which the latter species was described. The inclusion of *T. kabomani*, described after Holanda and Ferrero's (2012) work, besides our adaptations of Hulbert and Wallace's (2005) matrix and different phylogenetic methods used could have influenced on different results for South American tapirs.

Divergence times

Tapiridae diverged in a median estimate near 35-34 Ma ago (see Table 1), in the Late Eocene, which is a divergence comparable to Holanda and Ferrero (2012), which estimated an origin of Tapiridae earlier for the Mid-Eocene (41.2 Ma) based on fossil record and previous discussions, and by Bai et al. (2020), which suggested an origin in the Early Eocene (56-48 Ma). The oldest known Tapiridae fossil records are from later, the Early Oligocene (33-27 Ma), *Colodon* from the White River Group in South Dakota, Colbert 2005). It is crucial that more Tapiridae non-*Tapirus* skull fossil specimens in good conditions are found and included in future analysis to avoid long-branch attraction effects in topologies and further differences in phylogenetic and divergence times estimations for this group. Although there are different interval estimations for the origin of Tapiridae, there is an agreement between our work and the previous cited studies, in confining the divergence of the family to the Eocene, or at most, the earliest Oligocene.

Total group of genus *Tapirus* median divergence time (see Table 1), estimated in our topologies for the Middle Miocene was expected, as the oldest fossil records known for the genus are from the Middle Miocene (Cozzuol et al. 2013, 2014). This is not in agreement with Holanda and Ferrero (2012) and Bai et al. (2020), who estimated the divergence of the genus for the Late Eocene (32-33.9 Ma). We believe that such old estimations for the divergence of the genus are harder to justify, as the earliest fossil records for the grouop (e.g *T. johnsoni,* Cozzuol et al. 2013, 2014) are from more than 15 million years later than the intervals suggested by those works. Furthermore, this is the greatest sampling effort for a phylogenetic hypothesis of tapirs with 17 species, so we believe that our results point to a more robust scenario for the divergence time of *Tapirus*. Clades A, B and C divergences are newly established by the current work, as all of them include a specific node arrangement new to the literature. For instance, Clade A, in regard to the inside phylogenetic relations between *T. bairdii, T. augustus* and *T. indicus* in the three topologies + *T. polkensis* in the MP topology;

Clade B, which includes the European *T. arvernensis* and *T. hungaricus*, never studied before in a phylogenetic approach as previously discussed; and Clade C, that for the first time proposes *T. lundeliusi* as sister to all South American tapirs.

Biogeography

The current work developed the first biogeographic analysis for Tapiridae. Our biogeographic models propose that tapirids mostly dispersed through temporary land bridges and/or continents, where, by vicariant events, isolated and generated new species. Major dispersal events will be discussed in the main text.

The available fossil records indicate that Tapiridae has its origin in North America (Holanda and Ferrero 2012) with later dispersion to other continents, and our three reconstruction models are consistent with that (Figures 4-9). DIVA and DEC models for non-clock BI and MP inferences (Figures 4-7) reconstructed a North American as the most likely ancestral area for Tapiridae later in Early Oligocene (33-32 Ma), which agrees with previous discussions (Albright 1998). DIVA and DEC models for the clock BI topology (Figures 8 and 9) reconstructed a wide possibility for a Tapiridae ancestor in the Late Eocene (35 Ma), coming from either Europe, Asia, or North America.

Regarding Tapiridae non-*Tapirus* biogeographic events, in MP and BI topologies for both its DEC and DIVA reconstructions there is no difference between the dispersion of tapirid non-*Tapirus* moving from North America to Asia, which happened in the Early Oligocene—Late Oligocene (30-25 Ma) (see Figures 4 to 9). This interval is consistent with the formation of the Bering Strait that occurred in the Late Oligocene (26 Ma) (Wen et al. 2016). For the clock non-clock BI topology + DEC (Figure 7) there is a different conformation in which successive dispersion events occurred from North America to Asia for Tapiridae non-*Tapirus* during the Oligocene (30-25 Ma) and later in the Late Oligocene-Early Miocene (25-20 Ma). A dispersion event in the Oligocene interval is once again consistent with the presence of the Bering passage in the Late Oligocene (26 Ma), although an Early Miocene dispersion event is unlikely, as the Bering passage would form again much later in the Middle Miocene (10 Ma) (Wen et al. 2016).

In the clock BI topology + DIVA (Figure 8), there are three dispersion events registered for tapirid non-*Tapirus* from North America. The two first occurring in the Late Eocene-Late Oligocene interval (35-25 Ma), being the first to a most likely ancestral area including Europe, Asia and North America and the second dispersion to an ancestral area including Europe and North America. As discussed before, the formation of the Bering passage in the Late Oligocene (26 Ma) happened in that interval, being consistent with mainly the latter dispersion event that occurred earlier.

Both DIVA and DEC models for MP, clock BI and non-clock BI (Figures 4 to 9) retrieve a median for a North American ancestor for *Tapirus* in the Early-Mid Miocene. This pattern was expected as genus *Tapirus* was largely sampled with 17 species, so there was more morphological evidence to support a more certain descendant scenario in this regard, even in different biogeographic models. A North American ancestor for tapirs agrees with previous discussions, although they were not based on formal biogeographic analyses. Holanda and Ferrero (2012) discussed that the most basal species of *Tapirus*, *T. johnsoni*, presents fossil records for the Miocene of North America, which suggests that the genus would have originated in the North American continent. Janis (1984) proposed, on its hand-made "Distribution of the Tapiroidea in space and time" table, that *T. indicus* is derived from a North American lineage of *Tapirus* and later dispersed to Asia, therefore suggesting its closest relation to New World tapirs than to European Miocene ones. This is consistent with our findings in both DEC and DIVA models, that propose a tapir descendant that occupied North America for the clade that includes *T. bairdii*, *T. indicus* and *T. augustus* in all models (Figures 4 to 9). Our findings are not in agreement with McKenna and Bell (1997), who estimated the origin of *Tapirus* for the Oligocene of Europe, with representatives of the genus being registered for the continent until the Lower Pliocene. Guérin and Eisenmann (1994) discussed the origin of the genus for the Middle Miocene of Europe. These authors claimed that during the Middle Miocene and Upper Miocene, genus *Tapirus* dispersed widely through Europe, as observed in the extensive fossil record assigned to the genus for that period in Occidental Europe.

As for dispersion events of *Tapirus* to Eurasia, they happened in similar intervals between all three DEC models (Figures 5, 7 and 9): in the Late Miocene (10-5 Ma) from North America to Europe and in the Late Miocene-Early Pliocene (10-3 Ma) interval from North America to Asia. The dispersion events of *Tapirus* from North America to Asia are more consistent with the most recent formation of the Bering Strait bridge, in the Pliocene (3 Ma) (Wen et al. 2016). DIVA models (Figures 4, 6 and 8) are generally in agreement with DEC reconstructions regarding time intervals of *Tapirus* dispersing to Europe and Asia. In all three DIVA models, *Tapirus* dispersed from North America to Eurasia at least two different times – (Figures 4, 6 and 8).

The most recent dispersion events for tapirs, from North America to South America, occurred during the GABI (Great American Biotic Interchange) (Woodburne 2010; O'Dea et al. 2016). DEC and DIVA models applied to non-clock BI topology (Figures 6 and 7) estimate a 5-4 million-year-old dispersion to South America, in the Miocene-Pliocene transition. DEC and DIVA reconstructions for both MP and clock BI topologies (Figures 4, 5,

8 and 9) estimate a 4-3 million-year-old dispersion to South America, closer to the Pliocene-Pleistocene transition and therefore more consistent with the GABI (Woodburne 2010; O'Dea et al. 2016). The dispersion event of *Tapirus* to South America during the establishment of the Panama bridge is also in agreement with our biogeographic models.

Eberle's (2005) topology and biogeographic analysis were obtained based on dental characters only, including *Heptodon* and *Colodon* as correspondent specimens to our work (Figure 24). The author performed the reconstruction of ancestral states based on parsimony, and coded only the most ancient area for terminals (Eberle 2005). This is a simple methodology that is no longer used. Due to methodological differences and to the high homoplastic characteristic of dental characters, as previously stated (Perini et al. 2011, Scherler et al. 2011, Dumbá et al. 2019, 2022), Eberle (2005) will not be further compared to the present work.

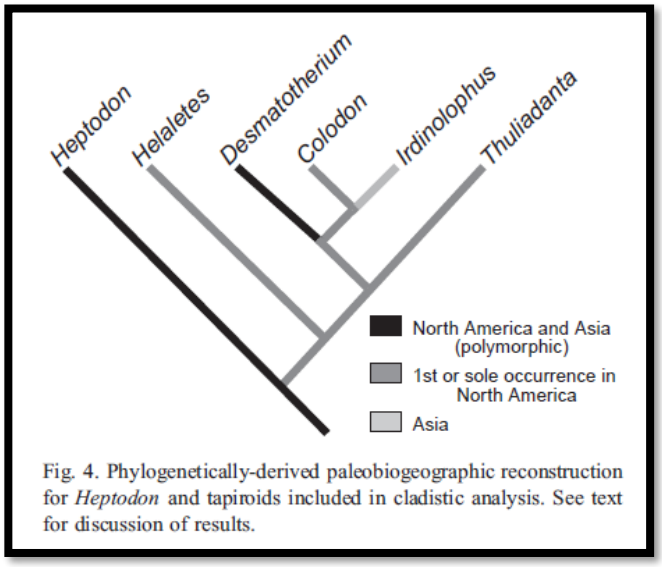

Fig. 4. Phylogenetically-derived paleobiogeographic reconstruction for *Heptodon* and tapiroids included in cladistic analysis. See text for discussion of results.

Figure 24. Eberle's 2005 biogeographic analysis

Our biogeographic reconstructions reinforce our phylogenetic hypothesis of Asian and European clades being derived from North American tapirids, which dispersed to the first mentioned continents.

CONCLUSIONS

Our phylogenetic assessments for Tapiridae, in spite of some clade's stem positions, are mostly in agreement with previous hypotheses. Our data points to the origin of Tapiridae most likely in the Late Eocene of North America, and the origin and early evolution of *Tapirus* in the same continent, later in the Middle Miocene. Non-*Tapirus* Tapiridae (minus *Nexuotapirus*) were recovered as monophyletic in non-clock BI and MP analysis, but as paraphyletic and clock-BI analysis. Genus *Tapirus* was recovered as monophyletic, The

Miocene *T. johnsoni* is sister to all *Tapirus*. North American tapirs are polyphyletic. *T. lundeliusi* is sister to all South American tapirs, and the latter form a clade (Clade C in the current work). The absence of differences between Tapiridae topologies built based on qualitative data only and discrete plus quantitative data points to a necessity to better understand patterns of behavior of quantitative data in different phylogenetic scenarios.

Regarding biogeographic patterns, tapirids dispersed from North America to Eurasia, and tapirs dispersed from North America to Eurasia and South America, where, by vicariant events isolated and formed new species. Most of our dispersion biogeographic inferences are consistent with the presence of transient and/or permanent land bridges.

Morphological phylogenetic analyses are key to better understand mammals' evolutionary history such as Tapiridae, which are mostly represented by extinct species. We strongly encourage the search and recovery of additional Tapiridae specimens from fossil sites, especially from Europe and Asia that still lack fossils in good conditions, to better contribute to further phylogenetic and biogeographic investigations of the family.

The present study contributed with important advances in our understanding of the relationships between tapirids, especially regarding the evolutionary relations amongst European tapirs and its consequences for divergence time estimations and biogeographic patterns. Paleoambiental informations (faunistic associations) in fossils show that extinct tapirids lived in humid environments (Ubilla 2004), which is consistent with current distributions of genus *Tapirus*, that are not described for arid regions. Therefore, the extinction of tapirids in North America in Upper Miocene (Hulbert and 2005) and in Europe in Upper Pliocene (Cozzuol et al. 2023, 2014) is probably associated with climate changes to climate/vegetation that was not tropical or subtropical. This creates an alert for the preservation of living species of tapirs that were much more diverse in the past and are key for the maintenance of tropical forests they inhabit (Olmos 1997, Dumbá et al. 2022).

ACKNOWLEDGEMENTS

We would like to thank Drs Ursula Göhlich (Natural History Museum Vienna), Ursula Menkveld-Gfeller (Natural History Museum Bern), Manuela Aiglstorfer (Natural History Museum Mainz), Ingmar Werbeburg (Paleontological collection of the University of the University of Tubingen), Gertrud Rößner (Bavarian Natural History Collections), Anneke van Heteren (Bavarian Natural History Collections), Loïc Costeur (Natural History Museum Basel), Martina Schenkel (Zoology Museum of the University of Zurich), Olivier Pauwels (Royal Belgian Institute of Natural Sciences) and Joséphine Lesur (National Museum of Natural History, France) for providing access to museums across Europe. We would also like to thank

Dr. Jamie MacLaren (University of Antwerp) for his contributions to tarsal characters' discussions. Thank you to Dr. Richard Hulbert (Florida Museum of Natural History) for granting the Florida Museum of Natural History International Travel Grant 2019 (L.C.C.S.D.) that I hope to use in the brief future and for your contributions on informations regarding North American *Tapirus* morphology and pictures. This project was funded by Coordenação de Aperfeiçoamento de Pessoal de Nível Superior (CAPES) in two categories: doctoral funding (L.C.C.S.D.) and Doutorado Sanduíche Capes PrInt funding (L.C.C.S.D.); Deutscher Akademischer Austauschdienst (DAAD) short-term grant funding (L.C.C.S.D.); Royal Belgian Zoological Society grant 2019 (L.C.C.S.D.); Fundação de Amparo à Pesquisa do Estado de Minas Gerais (M.A.C.); and the grant #2022/00044-7, São Paulo Research Foundation (FAPESP) for the financial support to D.M.C.

DATA AVAILABILITY

Supplemental material is available in the Supporting Information. Original research data underlying this chapter are available under reasonable request to the first author.

REFERENCES

Albright LB (1998). New genus of tapir (Mammalia: Tapiridae) from the Arikareean (earliest Miocene) of the Texas Coastal Plain. J. Vertebr. Paleontol. 18:200-217

Ascarrunz E, Claude J, Joyce WG (2019). Estimating the phylogeny of geoemydid turtles (Cryptodira) from landmark data: an assessment of different methods. PeerJ 7:e7476 DOI 10.7717/peerj.7476

Bai B, Meng J, Zhang C, Gong X, Wang YQ (2020). The origin of Rhinocerotoidea and phylogeny of Ceratomorpha (Mammalia, Perissodactyla). Commun. Biol. 3.

Barido-Sottani J, Aguirre-Fernández G, Hopkins MJ, Stadler T, Warnock R (2019). Ignoring stratigraphic age uncertainty leads to erroneous estimates of species divergence times under the fossilized birth–death process. Proc. R. Soc. B Biol. Sci. 286:20190685.

Boev Z (2017). Fossil record of Tapirs (Tapirus Brünnich, 1772) (Tapiridae Gray, 1821 - Peryssodactyla Owen, 1848) in Bulgaria. ZooNotes 108: 1-3

Bookstein FL (1991). Morphometric tools for landmark data: geometry and biology. Cambridge University Press, Cambridge

Burnham KP, Anderson DR (2002). Model selection and multimodel inference: A practical information-theoretic approach. New York: Springer-Verlag.

Campbell V, Lapointe FJ (2009). The use and validity of composite taxa in phylogenetic analysis. Syst. Biol. 58:560–572

Casali DM, Boscaini A, Gaudin TJ, Perini FA (2022). Reassessing the phylogeny and divergence times of sloths (Mammalia: Pilosa: Folivora), exploring alternative morphological partitioning and dating models. Zool. J. Linn. Soc. 0:0–0.

Catalano SA, Goloboff PA, Gianninia NP (2010). Phylogenetic morphometrics (I): the use of landmark data in a phylogenetic framework. Cladistics 26 (2010):539–549

Cerdeño E, Ginsburg L (1988). Les Tapiridae (Perissodactyla, Mammalia) del' Oligocène et du Miocène inférieur Européens. Annales de Paléontologie 74:71–96

Cione AL, Gasparini GM, Soibelzon E, Soibelzon, LH, Tonni EP (2015). The Great American Biotic Interchange. A South American Perspective. Springer Bries Monographies in Earth System Sciences. Springer, Dordecht

Colbert MW, Schoch RM (1998). Tapiroidea and other moropomorphs. Cambridge University Press 1:569-582

Colbert MW (2005). The facial skeleton of the early Oligocene Colodon (Perissodactyla, Tapiroidea). Palaeontologia Eletronica 8(1):1-27

Cozzuol MA, Clozato CL, Holanda EC, Rodrigues FHG, Nienow S, de Thoisy B, Redondo RAF, Santos FR (2013). A new species of tapir from the Amazon. J. Mammal. 94:1331–1345

Cozzuol MA, de Thoisy B, Fernandes-Ferreira H, Rodrigues FHG, Santos FR (2014). How much evidence is enough evidence for a new species? J. Mammal. 95:899-905

Dasheveg D, Hooker JJ (1997). New ceratomorph perissodactyls (Mammalia) from the Middle and Late Eocene of Mongolia: Their implications for phylogeny and dating. Zool. J. Linn. Soc. 120:105–138

Desmarest AG (1819). Nouveau dictionnaire d'histoire naturelle, appliquee aux art, principalement a l'agriculture et a l'economie rurale et domestique; par une societ´ e de naturalists: Nouvelle edition, presqu' entierement refondue et considerablement augmentee. Deterville, Paris

Dumbá LCCS, Parisi Dutra R, Cozzuol MA (2019). Cranial geometric morphometric analysis of the genus Tapirus (Mammalia, Perissodactyla). Journal of Mammal Evolution 26: 545–555.

Dumbá LCCS, Rodrigues, FHG, MacLaren, JA, Cozzuol, MA (2022). Dental occlusal surface and seed dispersal evolution in (Mammalia: Perissodactyla). Biological Journal of the Linnean Society, 20:1-18.

Eberle JJ (2005). A new "tapir" from Ellesmere Island, Arctic Canada – Implications for northern high latitude palaeobiogeography and tapir palaeobiology. Palaeogeogr. Palaeoclimatol. Palaeoecol. 227:311-322

Emry RJ (1989). A tiny new Eocene ceratomorph and comments on "tapiroid" systematics. J. Mamm. 70(4):794–804.

Ferrero BS, Noriega JI (2007). A new upper Pleistocene tapir from Argentina: remarks on the phylogenetics and diversification of Neotropical Tapiridae. J. Vertebr. Paleontol. 27:504–511

Ferrero BS, Soibelzon E, Holanda C, Gasparini GM, Zurita AE, Miño-Boilini AR (2013). A taxonomic and biogeographic review of the fossil tapirs from Bolivia. Acta Palaeontologica Polonica 59(3):505-516

Gill T (1865). T. bairdii. Proceedings of the National Academy of Sciences of Philadelphia 17:183

Goloboff PA (1993). Estimating character weights during tree search. Cladistics 9:83–91.

Goloboff PA (2003). Improvements to resampling measures of group support. Cladistics 19:324–332.

Goloboff PA, Arias JS (2019). Likelihood approximations of implied weights parsimony can be selected over the Mk model by the Akaike information criterion. Cladistics 35:695–716.

Goloboff PA, Catalano SA (2016). TNT version 1.5, including a full implementation of phylogenetic morphometrics. Cladistics. 32:221–238.

Goloboff PA, Torres A, Arias JS (2018). Weighted parsimony outperforms other methods of phylogenetic inference under models appropriate for morphology. Cladistics. 34:407–437.

Groves C, Grubb P (2011). Ungulate Taxonomy. Johns Hopkins University Press, Baltimore, Maryland 317 pp.

Guérin C, Eisenmann V (1994). Les tapirs (Mammalia, Perissodactyla) du Miocène supérieur d'Europe occidentale. Geobios 27(1):113-127

Hammer Ø, Harper DAT, Ryan PD (2001) PAST: Paleontological Statistics Software Package for Education and Data Analysis. Palaeontologia Electronica 4:1-9

Harmon LJ (2018). Phylogenetic comparative methods: Learning from trees. https://lukejharmon.github.io/pcm/.

Heath TA, Huelsenbeck P, Stadler T (2014). The fossilized birth-death process for coherent calibration of divergence-time estimates. Proc. Natl. Acad. Sci. 111:E2957–E2966.

Hooker JJ (1984). A primitive ceratomorph (Perissodactyla, Mammalia) from the early Tertiary of Europe. Zoological Zool. J. Linn. Soc. 82:229–244

Hooker JJ (1989). Character polarities in early perissodactyls and their significance for Hyracotherium and infraordinal relationships. In "The Evolution of Perissodactyls" (D. R. Prothero and R. M. Schoch, Eds.) 79–101. Oxford Univ. Press, New York.

Holanda EC, Ferigolo J, Ribeiro AM (2011). New Tapirus species (Mammalia: Perissodactyla: Tapiridae) from the upper Pleistocene of Amazonia, Brazil. J. Mamm. 92:111–120

Holanda EC, Ferrero B (2012). Reappraisal of the genus Tapirus (Perissodactyla, Tapiridae): systematics and phylogenetic affinities of the South American tapirs. J. Mamm. Evol. 20:33–44

Holbrook LT (1998). The Phylogeny and Classification of Tapiromorph Perissodactyls (Mammalia). Cladistics 15:331–350

Holbrook LT (2001). Comparative osteology of early Tertiary tapiromorphs (Mammalia, Perissodactyla). Zool. J. Linn. Soc. 132:1–54

Hulbert RCJR (1999). Nine million years of Tapirus (Mammalia, Perissodactyla) from Florida. J. Vertebr. Paleontol. 19(3):1-53

Hulbert RCJR (2005). Late Miocene Tapirus (Mammalia, Perissodactyla) from Florida, with description of a new species, Tapirus webbi. Bulletin of the Florida Museum of Natural History 45:465–494

Hulbert RCJR, Wallace SC (2005). Phylogenetic analysis of late Cenozoic Tapirus (Mammalia, Perissodactyla). J Vertebr Paleontol 25 (supplement to 3): 72A

Hulbert RCJR (2010). A new early pleistocene tapir (Mammalia: Perissodactyla) from Florida, with a review of blancan tapirs from the State. Florida Museum of Natural History Bulletin 49(3):67-126

Janis C (1984). Tapirs as Living Fossils. Division of Biology and Medicine, Brown University, Providence, RI02912

Kass R, Raftery AE (1995). Bayes Factors. J. Am. Stat. Assoc. 90:773–795.

Kerber L, Oliveira EV (2008). Sobre a presença de Tapirus (TAPIRIDAE, PERISSODACTYLA) na formação Touro Passo (Pleistoceno Superior), Oeste do Rio Grande do Sul. Biodiversidade Pampeana PUCRS, Uruguaiana 6(1): 9-14

King B (2021). Bayesian Tip-Dated Phylogenetics in Paleontology: Topological Effects and Stratigraphic Fit. Syst. Biol. 70(2):283–294

Lloyd GT (2016). Estimating morphological diversity and tempo with discrete character-taxon matrices: implementation, challenges, progress, and future directions. Zool. J. Linn. Soc. 118:131-151.

Landis MJ, Matzke NJ, Moore B, Huelsenbeck JP (2013). Bayesian analysis of biogeography when the number of areas is large. Syst. Biol. 62:789–804.

Lewis PO (2001). A likelihood approach to estimating phylogeny from discrete morphological character data. Syst. Biol. 50:913–925.

Matthew WD, Granger W (1923). New fossil mammals from the Pliocene of Szechuan, China. Bulletin of the American Museum of Natural History 48:563-598

Matzke NJ (2013). BioGeoBEARS: BioGeography with Bayesian (and Likelihood) Evolutionary Analysis in R Scripts. http://CRAN.R project.org/package=BioGeoBEARS.

Matzke NJ (2014). Model selection in historical biogeography reveals that founder-event speciation is a crucial process in island clades. Syst. Biol. 63:951–970.

McKenna MC, Bell SK (1997). Classification of Mammals – Above the Species Level. Columbia University Press, New York

Miller MA, Pfeiffer , Schwartz T (2010). Creating the CIPRES Science Gateway for inference of large phylogenetic trees. 2010 Gatew. Comput. Environ. Work. GCE:1–8.

Mongiardino Koch N, Garwood RJ, Parry LA (2021). Fossils improve phylogenetic analyses of morphological characters. Proc. R. Soc. B 288: 20210044.

Padilla M, Dowler RC (1994). Tapirus terrestris. Mammalian Species 481:1-8

O'Dea A, Lessios HA, Coates AG, Eytan RI, Restrepo-Moreno SA, Cione AL, Stallard RF, Collins LS, de Queiroz A, Farris DW, Norris RD, Stallard RF, Woodburne MO, Aguilera O, Aubry MP, Berggren WA, Budd AF, Cozzuol MA, Coppard SE, Duque-Caro H, Finnegan S, Gasparini GM, Grossman EL, Johnson KG, Keigwin LD, Knowlton N, Leigh EG, Leonard-Pingel JS., Marko PB., Pyenson ND., Rachello-Dolmen PG, Soibelzon E, Soibelzon L, Todd JA, Vermeij GJ, Jackson JB (2016). Formation of the Isthmus of Panama. Science Advances 2:e1600883

Olmos F (1997). Tapirs as seed dispersers and predators in: Tapirs—status survey and conservation action plan. IUCN Publications Services Unit, Cambridge

Parins-Fukuchi C (2018). Use of Continuous Traits Can Improve Morphological Phylogenetics. Syst. Biol. 67(2):328–339

Perini FA, Oliveira JA, Salles L, Moraes R, Neto PG, Guedes LFB, Oliveira M (2011). New fossil records of Tapirus (Mammalia, Perissodactyla) from Brazil, with a critical analysis of intra-generic diversity assessments based on lower molar size variability. Geobios 44:609–619

Puttick MK, O'Reilly JE, Pisani D, Donoghue PCJ (2019). Probabilistic methods outperform parsimony in the phylogenetic analysis of data simulated without a probabilistic model. Palaeontology, 62, 1: 1–17

Qiu ZX, Yan DF, Sun B (1991). A new genus of Tapiridae from Shanwang, Shandong. Vertebrata Palasiatica 29:119–135

R Core Team (2022). R: A language and environment for statistical computing. https://www.r-project.org/.

Radinsky LB (1963). The perissodactyl hallux. American Museum Novitates 2145:1-8

Radinsky LB (1965). Evolution of the tapiroid skeleton from Heptodon to Tapirus. Bulletin of the Museum of Comparative Zoology 134(3):69-106

Ree RH, Smith SA (2008). Maximum likelihood inference of geographic range evolution by dispersal, local extinction, and cladogenesis. Syst. Biol. 57:4–14.

Rohlf FJ, Slice D (1990). Extensions of the Procrustes method for the optimal superimposition of landmarks. Syst. Zool. 39(1):40-59

Ronquist F (1997). Dispersal-vicariance analysis: A new approach to the quantification of historical biogeography. Syst. Biol. 46:195–203.

Ronquist F, Klopfstein S, Vilhelmsen L, Schulmeister S, Murray DL, Rasnitsyn AP (2012a). A total-evidence approach to dating with fossils, applied to the early radiation of the Hymenoptera. Syst. Biol. 61:973–999.

Ronquist F, Teslenko M, van der Mark P, Ayres DL, Darling A, Höhna S, Larget B, Liu L, Suchard Ma, Huelsenbeck JP (2012)b. MrBayes 3.2: efficient Bayesian phylogenetic inference and model choice across a large model space. Syst. Biol. 61:539–42.

Rosa BB, Melo GAR, Barbeitos MS (2019). Homoplasy-based partitioning outperforms alternatives in Bayesian analysis of discrete morphological data. Syst. Biol. 68:657–671.

Roulin X (1829). Memoire pour servir a l'histoire du Tapir; et description d'une espece nouvelle appartenant aux hautes regiones de la Cordillere des Andes. Annales des sciences naturelles (1re Serie) 17:26-56

Rustioni M, Mazza P (2001). Taphonomic analysis of Tapirus arvenensis remains from the lower Valdarano (Tuscany, central Itay). Geobios 34(4):469-474

Spassov N, Ginsburg L (1999). Tapirus balkanicus nov. sp., nouveau tapir (Perissodactyla, Mam malia) du Turolien de Bulgarie. Annales de Paleontologie 85:265–276

Scherler L, Becker D, Berger Jean-Pierre (2011). Tapiridae (Mammalia, Perissodactyla) of the Swiss Molasse Basin during the Oligocene-Miocene transition. J. Vertebr. Paleontol. 31(2): 479-496

Schoch, RM (1989). A review of the tapiroids. In “The Evolution of Perissodactyls” (D. R. Prothero and R. M. Schoch, Eds.). Oxford Univ. Press, New York 298–320.

Scott WB (1941). The Mammalian Fauna of the White River Oligocene, Part V: Perissodactyla. Transactions of the American Philosophical Society 28:747–980

Tong HW, Liu J, Han L (2002). On fossil remains of early Pleistocene tapir (Perissodactyla, Mammalia) from Fanchang, Anhui. Chinese Science Bulletin 47:586–590

Varón-González C, Whelan S, Klingenberg CP (2020). Estimating Phylogenies from Shape and Similar Multidimensional Data: Why It Is Not Reliable. Syst. Biol. 69(5):863–883

Wall WP (1980). Cranial evidence for a proboscis in Cadurcodon and a review of snout structure in the family Amynodontidae (Perissodactyla, Rhinocerotoidea). J. Paleontol. 54(5):968–977

Wen J, Nie Ze-Long, Ickert-Bond SM (2016). Intercontinental disjunctions between eastern Asia and western North America in vascular plants highlight the biogeographic importance of the Bering land bridge from late Cretaceous to Neogene. J Syst Evol doi: 10.1111/jse.12222

Woodburne MO (2010). The Great American Biotic Interchange: dispersals, tectonics, climate, sea level and holding pens. J. Mamm. Evol. 17:245–264

Zhang C, Stadler T, Klopfstein S, Heath TA, Ronquist F (2016). Total-evidence dating under the fossilized birth-death process. Syst. Biol. 65:228–249.

SUPPORTING INFORMATION

SUPPORTING INFORMATION S1

Character list for the qualitative phylogenetic morphological analysis. Number between parentheses indicates the characters from Hulbert and Wallace (2005).

1. (1). Adult height of sagittal crest (modified from Hulbert and Wallace 2005): (0) moderate (1) low, less than 2 mm; (2) very high, more than 50 mm.

2. (2). When during ontogeny do temporal crests meet to form a sagittal crest (modified from Hulbert and Wallace 2005): (0) young juvenile (before eruption of M1); (1) older juvenile (after eruption of M1, before eruption of M2); (2) subadult (after eruption of M2, before loss of DP4); (3) young adult (after eruption of P4 and M3); (4) never.

3. (3). Where temporal crests meet to form the sagittal crest (modified from Hulbert and Wallace 2005): (0) very near the frontal-parietal suture; (1) well anterior to the frontal-parietal suture (2) crests do not meet.

4. Sagittal crest morphology in adults (modified from Abernethy 2011). (0) two parasagittal crest ridges close to one another along midline of skull (1) true crest composed of two thin parassagittal ridges which merge and run for a distance before separating (2) flattened table.

5. (4). Dorsal table of frontal. (0) relatively narrow or small; (1) relatively broad.

6. (5). Frontal inflation: (0) weak or absent; (1) frontal very strongly inflated.

7. (6). Nasal-frontal lateral profile: (0) nasals and frontal approximately on same plane; (1) nasals notably stepped down from frontals.

8. (7). Presence and size of interparietal bone in postnatal individuals (modified from Hulbert and Wallace 2005): (0) present, large; (1) present, small; (2) absent.

9. (8). Shape of interparietal bone: (0) typically polygonal (hexagonal or diamond shaped); (1) typically triangular.

10. (9). Interparietal fusion with occipital: (0) occurs early in ontogeny (before loss of DP4); (1) occurs late in ontogeny (after eruption of P4).

11. (10). Nasal length: (0) long (longer than 1.5 times the width of combined nasals); (1) short (shorter than 1.5 times the width of combined nasals).

12. (11). Shape of anterolateral margin of nasal (modified from Hulbert and Wallace 2005): (0) relatively straight; (1) distinctly concave.

13. (12). Shape of posterolateral margin of nasal (modified from Hulbert and Wallace 2005): (0) relatively flat; (1) curved downward.

14. (13). Presence of descending sigmoid process of nasal (modified from Hulbert and Wallace 2005): (0) present; (1) absent.

15. (14). Morphology of fossa for meatal diverticulum on nasal (modified from Hulbert and Wallace 2005): (0) shallow and without distinct margins; (1) deep and with distinct margins.

16. (15). Extent of fossa for meatal diverticulum on posterior dorsal surface of nasal (modified from Hulbert and Wallace 2005): (0) not extensive, does not extend near midline; (1) very extensive, approaches within a few mm of midline.

17. (16). Development of fossa for meatal diverticulum on dorsal table of frontal (modified from Hulbert and Wallace 2005): (0) very limited or absent; (1) broad exposure with distinct posterior margin.

18. (17). Morphology of supraorbital groove for nasal diverticulum (modified from Hulbert and Wallace 2005): (0) broad and shallow; (1) narrow and deep.

19. (18). Exposition of posterodorsal process of maxilla (modified from Hulbert and Wallace 2005) : (0) widely exposed dorsally above the orbit forming the base of trough for meatal diverticulum; (1) not widely exposed dorsally above the orbit, not forming base of trough for meatal diverticulum.

20. (19). Position of nasal notch relative to orbit (modified from Hulbert and Wallace 2005): (0) dorsal to orbit; (1) posterior to orbit; (2) anterior to orbit.

21. (20). Orientation of lambdoidal crests in adults (modified from Hulbert and Wallace 2005): (0) mostly posteriorly, with little or no outward flair; (1) posterolateral orientation, with notable lateral flair.

22. (21). Shape of dorsomedial border of maxilla (modified from Hulbert and Wallace 2005): (0) sharp border that is mostly directed medially; (1) rounded border that is directed ventromedially; (2) border up-turned and expanded as an extension of dorsal flange.

23. (22). Position of infraorbital foramen relative to the cheek teeth (modified from Hulbert and Wallace 2005): (0) dorsal to P4; (1) dorsal to P2 or P3.

24. (23). Position of premaxillary-maxillary suture relative to alveolus of canine (in lateral view) (modified from Hulbert and Wallace 2005): (0) suture located anterior to canine alveolus; (1) suture located in the middle of alveolus of canine.

25. (24). Presence of anteromedial process of maxilla: (modified from Hulbert and Wallace 2005) (0) absent; (1) present

26. (25). Lateral exposure of anteromedial process of maxilla: (0) maxilla well exposed in lateral view dorsal to premaxilla; (1) maxilla covered by premaxilla, not visible in lateral view or barely so.

27. (26). Presence and development of dorsal maxillary flange (modified from Hulbert and Wallace 2005): (0) absent; (1) present, slightly developed; (2) present, extensively developed.

28. (27). Length of posterior process of premaxilla: (0) long, terminates posterior to P1; (1) terminates dorsal to or just in front of P1; (2) ends about midway over C-P1 diastema; (3) very short, terminates well anterior to midway point of diastema.

29. (28). Width of maxillary bar between infra-orbital foramen and lacrimal: (0) narrow, usually less than 5 mm; (1) wide, more than 5 mm.

30. (29). Shape of lacrimal: (0) narrow, much taller than long; (1) broad, about as long as it is high.

31. (30). Contour of facial surface of lacrimal (modified from Hulbert and Wallace 2005): (0) flat or convex; (1) concave.

32. (31). Presence and development of anterior lacrimal process(es) (modified from Hulbert and Wallace 2005): (0) absent or very weak; (1) present, well-developed.

33. (32). Presence of posterior (preorbital) process of lacrimal (modified from Hulbert and Wallace 2005): (0) present; (1) absent.

34. (33). Shape of posterior process of lacrimal (modified from Hulbert and Wallace 2005): (0) broad and flat; (1) slender, pointed or knobby.

35. (34). Typical number of lacrimal foramen: (0) two; (1) one.

36. (35). Exposure of lacrimal foramen visible in lateral view (modified from Hulbert and Wallace 2005): (0) visible, at least one; (1) not visible in lateral view.

37. (36). Incisive foramen position relative to canine (modified from Hulbert and Wallace 2005): (0) terminates posteriorly about midway between canine and P1; (1) terminates posteriorly at P1 or further

38. (37). Relative diastema length (modified from Hulbert and Wallace 2005): (0) short (ldl/p2m3L< 0.40); (1) intermediate (0.40 ≤ ldl/p2m3L < 0.50); (2) long (ldl/p2m3L ≥ 0.50). [ldl = lower diastema length; p2m3L = length from anterior point of p2 to posterior point of m3]

39. (38). Relative location of mental foramen: (0) anterior to the p2; (1) directly ventral to the p2.

40. (39). Orientation of anterior margin of ascending ramus of mandible in lateral view: (0) projects vertically and posteriorly, not anteriorly (does not overlie the m3); (1) projects anteriorly as well as vertically below the coronoid process, often lies dorsal to m3.

41. (41). Relative crown height of cheek teeth: (0) short, relatively brachydont; (1) taller.

42. (43). P1 morphology (modified from Hulbert and Wallace 2005): (0) single, small posterolingual cusp (=hypocone of some) and lingual cingulum, but no cross lophs or other cusps; (1) large posterolingual cusp, sometimes with accessory cusps and often with some development of a transverse loph; (2) large posterolingual cusp with strong, complete transverse loph; (3) no distinct posteriorlingual cusp, only a cingulum.

43. (44). P1 TW/L ratio: (0) on average, less than or equal to 0.80; (1) on average, greater than 0.80.

44. (45). P2 – P4 ATW/PTW ratio (modified from Hulbert and Wallace 2005): (0) on average, less than or equal to 0.85; (1) on average, greater than 0.85.

45. (46). Presence of P2 lingual cingulum (modified from Hulbert and Wallace 2005): (0) present; (1) absent.

46. (47). Separation of transverse lophs on P2-P4 and p2-p4 (modified from Hulbert and Wallace 2005): (0) poorly separated; 1; well separated.

47. (48). P2 protoloph position relative to ectoloph (modified from Hulbert and Wallace 2005): (0) does not reach ectoloph; (1) just reaches to base of ectoloph; (2) merges midway or higher onto ectoloph.

48. (49). P3 protoloph position relative to ectoloph (modified from Hulbert and Wallace 2005): (0) does not reach ectoloph; (1) just reaches to base of ectoloph; (2) merges midway or higher onto ectoloph.

49. (51). P2 metaloph position relative to ectoloph (modified from Hulbert and Wallace 2005): (0) does not reach ectoloph; (1) just reaches to base of ectoloph; (2) merges midway or higher onto ectoloph.

50. (55). Parastyle development on P3-M3 (modified from Hulbert and Wallace 2005): (0) moderate; (1) strong.

51. (56). Presence of labial cingulum on posterior half of upper cheek teeth (modified from Hulbert and Wallace 2005): (0) present on half or more of P3-M3; (1) absent or very rare on P3-M3.

52. (57). Where M1 metaloph joins the ectoloph: (0) near middle of tooth, well in front of metacone; (1) at or near metacone.

53. (67). i1 morphology and size: (0) i1 slightly larger than i2, not procumbent; (1) i1 larger than i2, slightly procumbent; (2) i1 much larger than i2, very procumbent and spatulate.

54. (69). Length of p2 relative to p3: (0) short, (p2 L)/(p3 L) less than 1.1; (1) long, this ratio greater than 1.1.

55. (72). Relative height of unworn protolophid and hypolophid (or hypoconid/entoconid if there is no hypolophid) on premolars: (0) protolophid distinctly taller than hypolophid; (1) the two are approximately equal in height

56. (73). Presence and development of cristid obliqua on p3 (modified from Hulbert and Wallace 2005): (0) strong, blocks interlophid valley labially; (1) very weak or absent.

57. (74). Presence and development of cristid obliqua on p4 (modified from Hulbert and Wallace 2005): (0) strong, blocks interlophid valley labially; (1) very weak or absent.

58. (78). Relatively long limbs (quantified by comparison of the length of the femur and dentary): (0) relatively long limbs (femur greatest length longer than that of dentary); (1) relatively short limbs (femur length less than or equal to that of dentary).

59. (79). Articulation between MT1 and MT4: (0) no articulation between MT1 and MT4; (1) articular facet present on posterior surface of MT4 for articulation with MT1.

60. Height of posttympanic process: (0) it extend near to postglenoid process; (1) extend ventrally to postglenoid process.

SUPPORTING INFORMATION S2

List of species used as novelty in phylogenetic qualitative morphological analysis and corresponding specimens.

T. hungaricus - NHMW 1865-XXIV-1 ; Natural History Museum Wien

T. webbi – 1. UF11007, 2. UF26191 ; Vertebrate Paleontology Collection, Florida Museum of Natural History

T. arvernensis – Unknown specimen from *Camp dels Ninots site*

T. augustus – 1. Unknown specimen from American Museum of Natural History (available in https://www.flickr.com/photos/ggnyc/2530909878), 2. PIMUZAV1781 ; Palaeontological Museum of the University of Zurich

Nexuotapirus – *Nexutapirus marlandensis* SDSM 631 ; South Dakota School of Mines and Technology

Protapirus – 1. *Protapirus simplex* … (available in http://digimorph.org/specimens/Protapirus_simplex/), 2. *Protapirus obliquidens* SDSM 2829; Digimorph South Dakota School of Mines and Technology, Museum of Geology

Paratapirus – *Paratapirus helvetius* NMSG-P1500 ; Naturhistorisches Museum Sankt Gallen

Colodon occidentalis - (available in http://digimorph.org/specimens/Colodon_cf_occidentalis/AMNH/)

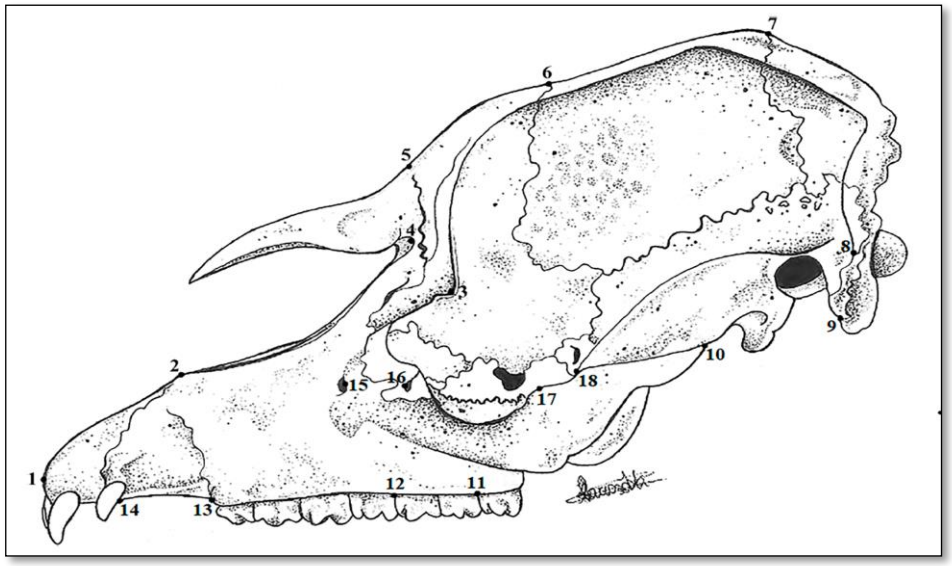

SUPPORTING INFORMATION S3

Figure 1: Eighteen cranial landmarks for the lateral view of the skull used in phylogenetic quantitative morphological analysis, adapted from Dumbá et al. 2019: 1: Rostral tip of premaxilla; 2: Dorsal border of premaxilla-maxilla suture, lateral view; 3: Postorbital process of frontal; 4: Posterior margin of nasal opening; 5: Naso-frontal suture; 6: Fronto-parietal suture; 7: Parieto-occipital suture; 8: Point at squamosal-occipital-mastoid suture 9: Paraoccipital process; 10: Posterior end of jugal-squamosal suture; 11: Posterior end of upper molar 2; 12: Posterior end of upper premolars13: Anterior border of P1 alveolus; 14: Posterior margin of canine alveolus; 15: Posterior end of infraorbital foramen; 16: Posterior process of lacrimal bone; 17: Postorbital process of the jugal; 18: Anterior end of jugal-squamosal suture.

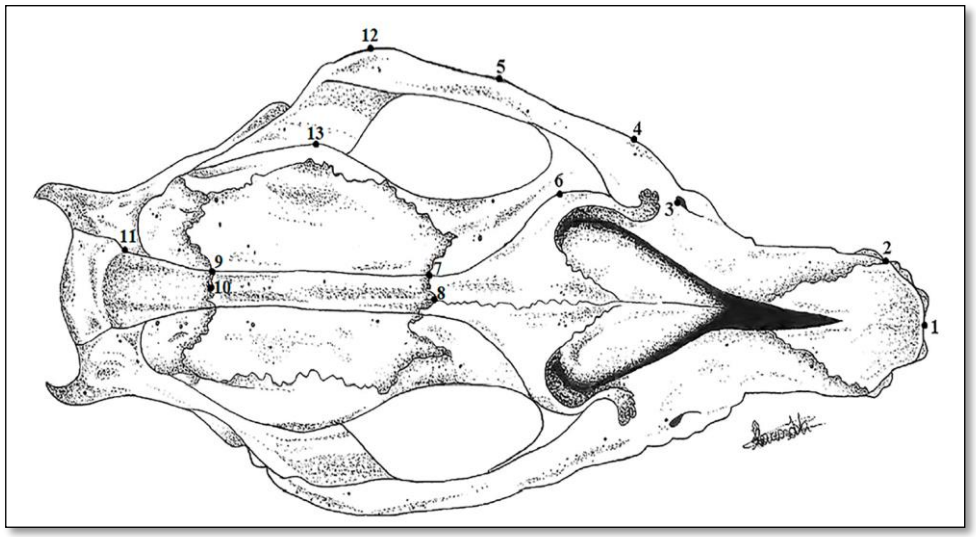

SUPPORTING INFORMATION S4

Figure 2: Thirteen cranial landmarks for the dorsal view of the skull used in phylogenetic quantitative morphological analysis, adapted from Dumbá et al. 2019: 1: Anteriormost rostral point of premaxilla; 2: Anterior border of canine alveolus; 3: Posterior border of infraorbital foramen; 4: Anterior end of jugal; 5: Lateral border of jugal at level of postorbital process of jugal; 6: Fronto-lateral border at level of naso-frontal suture; 7: Lateral border of sagittal crest/table at the fronto-parietal suture; 8: Medial point of sagittal crest/table at the fronto-parietal suture; 9: Lateral border of sagittal crest/table at the parietal-occipital suture 10: Medial point of of sagittal crest/table at the parieto occipital suture;

11: Lambdoidal crest origin; 12: External border of squamosal at level of anterior border of glenoid cavity; 13: Lateralmost point of braincase at squamosal base.

SUPPORTING INFORMATION S5

Geometric morfometry cranial data acquired for PCA analysis – Lateral view (n = 38)

Specimen	Species	Collection	Locality
10899	*Protapirus sp*	Princeton University Museum	-
MCZ17670	*Heptodon posticus*	Museum of Comparative Zoology, Cambridge, Massachusetts	Wind River basin, USA
Filhol	*Protapirus obliquidens*	unknown	North America
SDSM 631	*Nexuotapirus marslandensis*	South Dakota School of Mines and Technology	Monroe Creek Formation, South Dakota, USA
taugustus	*T. augustus*	American Museum of Natural History	No locality data
UF1211036	*T. lundeliusi*	Florida Museum of Natural History	Florida, USA
tpinchaqueecuador	*T. pinchaque*	Florida Museum of Natural History	No locality data
pinchaque2	*T. pinchaque*	Florida Museum of Natural History	No locality data
I 1545141042863166f02	*T. pinchaque*	University of Michigan	No locality data
MN1607	*T. kabomani*	Museu Nacional do Rio de Janeiro	South America
MN1700	*T. kabomani*	Museu Nacional do Rio de Janeiro	GO, Brazil
MN600	*T. kabomani*	Museu Nacional do Rio de Janeiro	South America
UFMG4560	*T. kabomani*	Universidade Federal de Minas Gerais, Coleção de Mastozoologia	Lábrea, AM, Brazil
UFMG3177	*T. kabomani*	Universidade Federal de Minas Gerais, Coleção de Mastozoologia	Porto Velho, RO, Brazil
MN57069	*T. kabomani*	Museu Nacional do Rio de Janeiro	South America
MN57138	*T. terrestris*	Museu Nacional do Rio de Janeiro	South America

UFMG4565	*T. terrestris*	Universidade Federal de Minas Gerais, Coleção de Mastozoologia	Parque Estadual do Rio Doce, Ipatinga, MG, Brazil
UFMG4586	*T. terrestris*	Universidade Federal de Minas Gerais, Coleção de Mastozoologia	Parna Amazônia, Tapajós, PA, Brazil
UFMG4559	*T. terrestris*	Universidade Federal de Minas Gerais, Coleção de Mastozoologia	Lábrea, AM, Brazil
MN57071	*T. terrestris*	Museu Nacional do Rio de Janeiro	South America
UFMG6027	*T. terrestris*	Universidade Federal de Minas Gerais, Coleção de Mastozoologia	Parque Estadual Chandless, AC, Brazil
ZSM 1905 1102	*T. indicus*	Bavarian State Collection of Zoology	Asia
NMB C.3761	*T. indicus*	Natural History Museum Basel	Asia
NMB8125	*T. indicus*	Natural History Museum Basel	Asia
PIMUZ15966	*T. indicus*	Palaeontological Museum of the University of Zurich	Asia
PIMUZ10879	*T. indicus*	Palaeontological Museum of the University of Zurich	Asia
ZSM 1905 1101	*T. indicus*	Bavarian State Collection of Zoology	Asia
1451	*T. bairdii*	Coleção de Mastozoologia do Museo de La Plata	No locality data
FLM534	*T. bairdii*	Bavarian State Collection of Zoology	No locality data
CICYTTP-PV-M-1-23	*T. mesopotamicus*	Centro de Investigaciones Científicas y Transferencia de Tecnología a la Producción, Diamante, Argentina	Província Entre Ríos, Formação Arroyo Feliciano, Argentina
37302	*T. johnsoni*	American Museum of Natural History	North America
Tapirus haysii Germany	*T. haysii*	Natural History Museum Karlsruhe Germany	North America
NHMW 1865-XXIV-1	*T. hungaricus*	Natural History Museum Vienna	Europe
ninots	*T. arvernensis*	unknown	*Camp dels Ninots*
tapir002	*T. polkensis*	unknown	unknown

ChM PV4257	*T. veroensis*	-	South Carolina
ZSM AM 538	*Tapirus sp*	Bavarian State Collection of Zoology	No locality data
NMB VT.630	*Tapirus sp*	Natural History Museum Basel	Europe

SUPPORTING INFORMATION S6

Geometric morfometry cranial data acquired for PCA analysis – Dorsal view (n = 36)

Specimen	Species	Collection	Locality
10899	*Protapirus sp*	Princeton University Museum	-
MCZ17670	*Heptodon posticus*	Museum of Comparative Zoology, Cambridge, Massachusetts	Wind River basin, USA
Filhol	*Protapirus obliquidens*	unknown	North America
SDSM 2829	*Protapirus simplex*	South Dakota School of Mines and Technology	North America
SDSM 631	*Nexuotapirus marslandensis*	South Dakota School of Mines and Technology	Monroe Creek Formation, South Dakota, USA
UF121736	*T. lundeliusi*	Florida Museum of Natural History	Florida, USA
UF160715	*T. lundeliusi*	Florida Museum of Natural History	Florida, USA
1140797	*T. pinchaque*	Museo Nacional da Escola Politécnica de Quito, Ecuador	Ecuador
P1070249 UF/C6110	*T. pinchaque*	Florida Museum of Natural History	No locality data
RBINS1186	*T. pinchaque*	Royal Belgian Institute of Natural Sciences	No locality data
1140814	*T. pinchaque*	Museo Nacional da Escola Politécnica de Quito, Ecuador	Ecuador
MN1607	*T. kabomani*	Museu Nacional do Rio de Janeiro	South America
MN1700	*T. kabomani*	Museu Nacional do Rio de Janeiro	GO, Brazil
MN600	*T. kabomani*	Museu Nacional do Rio de Janeiro	South America
UFMG4560	*T. kabomani*	Universidade Federal de Minas Gerais, Coleção de Mastozoologia	Lábrea, AM, Brazil
UFMG3177	*T. kabomani*	Universidade Federal de Minas Gerais,	Porto Velho, RO, Brazil

		Coleção de Mastozoologia	
MN57069	*T. kabomani*	Museu Nacional do Rio de Janeiro	South America
UFMG4559	*T. terrestris*	Universidade Federal de Minas Gerais, Coleção de Mastozoologia	Lábrea, AM, Brazil
UFMG4588	*T. terrestris*	Universidade Federal de Minas Gerais, Coleção de Mastozoologia	Parna Amazônia, Tapajós, PA, Brazil
UFMG4195	*T. terrestris*	Universidade Federal de Minas Gerais, Coleção de Mastozoologia	Terra indígena Karitiana, Porto Velho, RO, Brazil
UFMG4557	*T. terrestris*	Universidade Federal de Minas Gerais, Coleção de Mastozoologia	Floresta do Jamari, RO, Brazil
UFMG4556	*T. terrestris*	Universidade Federal de Minas Gerais, Coleção de Mastozoologia	Floresta do Jamari, RO, Brazil
UFMG4564	*T. terrestris*	Universidade Federal de Minas Gerais, Coleção de Mastozoologia	Parque Estadual do Rio Doce, Ipatinga, MG, Brazil
NMB C.3761	*T. indicus*	Natural History Museum Basel	Asia
NMB8125	*T. indicus*	Natural History Museum Basel	Asia
ZSM 1905 1101	*T. indicus*	Bavarian State Collection of Zoology	Asia
MN57063	*T. indicus*	Museu Nacional do Rio de Janeiro	Asia
NMBE1024418	*T. indicus*	Natural History Museum Bern	Asia
AMNH 35661	*T. indicus*	American Museum of Natural History	Asia
AMNH 80076	*T. indicus*	American Museum of Natural History	Asia
1451	*T. bairdii*	Coleção de Mastozoologia do Museo de La Plata	No locality data
FLM534	*T. bairdii*	Bavarian State Collection of Zoology	No locality data
CICYTTP-PV-M-1-23	*T. mesopotamicus*	Centro de Investigaciones Científicas y Transferencia de Tecnología a la Producción, Diamante, Argentina	Província Entre Ríos, Formação Arroyo Feliciano, Argentina

ChM PV4257	*T. veroensis*	-	South Carolina
AMNH 130108	*T. veroensis*	American Museum of Natural History	No locality data
ZSM AM 538	*Tapirus sp*	Bavarian State Collection of Zoology	No locality data

SUPPORTING INFORMATION S7

Age and geographic distribution for Tapiridae used in estimation of Divergence Times and Biogeographic analysis

TAXA	LAD	FAD	E	A	N	S	REFERENCE
Heptodon	48.6	50.3	-	-	-	-	Palmer 1999
Colodon	23.03	40.0	0	1	1	0	Marsh 1980, Holbrook 1998, Holanda et al. 2007 2005
Protapirus	20.0	33.9	1	1	1	0	Albright 1998, Hulbert 2005, Bayshashov and Billa 2011
Paratapirus	15.97	23.03	1	0	0	0	Cerdeño and Ginsburg 1988, Hulbert 2005, Hulbert 2010
Plesiotapirus	6.0	17.25	0	1	0	0	Qiu, Yan and Sun, 1991
Nexuotapirus	15.97	24.8	0	0	1	0	Albright 1998, Hulbert 2005
Tapirus_webbi	8	9.5	0	0	1	0	Hulbert 2005
Tapirus_johnsoni	4.9	13.6	0	0	1	0	Holanda and Ferrero 2012, Hulbert 2005, Schultz, Martin and Corner 1975
Tapirus_polkensis	4.5	7	0	0	1	0	Gibson 2011, Hulbert 2005
Tapirus_hungaricus	2.58	11.63	1	0	0	0	Spassov and Ginsburg, 1999, Hulbert 2005
Tapirus_arvernensis	2.6	3.11	1	0	0	0	Rustioni 1992, Rustioni and Mazza 2001, Hulbert 2005
Tapirus_haysii	1	2.5	0	0	1	0	Hulbert 2009
Tapirus_cristatellus	0.012	2.58	0	0	0	1	Holanda et al. 2007
Tapirus_lundeliusi	0.011	2.2	0	0	1	0	Hulbert 2010
Tapirus_veroensis	0.011	2	0	0	1	0	Hulbert 2010
Tapirus_mesopotamicus	0.011	0.800	0	0	0	1	Ferrero and Noriega 2007

Tapirus_augustus	0.011	0.126	0	1	0	0	Tong et al. 2002
Tapirus_rondoniensis	0.011	0.045	0	0	0	1	Holanda et al. 2011
Tapirus_terrestris	0	0.012	0	0	0	1	Cozzuol et al. 2013, 2014
Tapirus_kabomani	0	0	0	0	0	1	Cozzuol et al. 2013, 2014
Tapirus_pinchaque	0	0	0	0	0	1	Cozzuol et al. 2013, 2014
Tapirus_bairdii	0	0.012	0	0	1	1	Cozzuol et al. 2013, 2014
Tapirus_indicus	0	0.045	0	1	0	0	Cozzuol et al. 2013, 2014, Canbrook and Piper 2009

SUPPORTING INFORMATION S8

Synapomorphies of selected clades in the three phylogenetic hypotheses - maximum parsimony (MP), non-clock Bayesian inference (ncBI) and clock Bayesian inference (cBI).

Clade	Synapomorphy	MP	ncBI	cBI
Tapirus (total)	5 (0)	relatively narrow or small dorsal table of frontal		x
Tapirus (total)	8 (0)	large interparietal bone in postnatal individuals	x	x
Tapirus (total)	9 (0)	typically polygonal (hexagonal or diamond shaped) interparietal bone	x	x
Tapirus (total)	14 (0)	presence of a descending sigmoid process		x
Tapirus (total)	20 (0)	nasal notch dorsal to orbit	x	x
Tapirus (total)	22 (0)	sharp dorsomedial border of maxilla, mostly directed medially	x	x
Tapirus (total)	24 (1)	premaxillary-maxillary suture located at the middle of the alveolus of canine	x	x
Tapirus (total)	27 (1)	presence of a slightly developed dorsal maxillary flange		x
Tapirus (total)	28 (1)	posterior process of premaxilla terminates dorsal to or just in front of P1		
Tapirus (total)	38 (1)	intermediate diastema length (0.40 >= ldl/p2m3L < 0.50)		x
Tapirus (total)	43 (1)	P1 TW/L ratio greater than 0.8		x
Tapirus (total)	52 (1)	M1 metaloph joins the ectoloph at or near metacone	x	x
Tapirus (crown group)*	5 (1)	relatively broad dorsal table of frontal		

Tapirus (crown group)*	10 (1)	interparietal fusion with occipital occurs late in ontogeny, or do not occur		
Tapirus (crown group)*	16 (1)	fossa for meatal diverticulum on posterior dorsal surface of nasal is very extensive, approaches within a few mm of midline		x
Tapirus (crown group)*	17 (1)	fossa for meatal diverticulum on dorsal table of frontal with a broad exposure with distinct posterior margin		x
Tapirus (crown group)*	23 (1)	infraorbital foramen dorsal to P2 or P3	x	
Tapirus (crown group)*	24 (0)	premaxillary-maxillary suture located anterior to canine alveolus	x	
Tapirus (crown group)*	38 (0)	short relative diastema length (ldl/p2m3L< 0.40)		x
Tapirus (crown group)*	39 (1)	mental foramen located directly ventral to the p2		x
Tapirus (crown group)*	48 (2)	P3 protoloph merges midway or higher onto ectoloph		x
Tapirus (crown group)*	55 (1)	very weak or absent cristid obliqua on p3	x	
Clade A	3 (2)	sagittal crests do not meet	x	
Clade A	4 (2)	sagittal crest morphology as a flattened table	x	
Clade A	7 (1)	nasal stepped down from frontals		x
Clade A	12 (1)	anterolateral margin of nasal distinctly concave		x
Clade A	19 (1)	posterodorsal process of maxilla not widely exposed dorsally above the orbit, not forming the base of trough for meatal diverticulum	x	x
Clade A	22 (0)	sharp dorsomedial border of maxilla that is mostly directed medially		x
Clade A	23 (1)	infraorbital foramen located dorsal to P2 or P3		x
Clade A	25 (1)	presence of the anteromedial process of maxilla		x
Clade A	36 (0)	lacrimal foramen visible in lateral view		x
Clade A	38 (2)	long diastema length (ldl/p2m3L <= 0.50)	x	x
Clade A	56 (1)	very weak or absent cristid obliqua on p3		x
Clade B + C	9 (1)	typically triangular interparietal bone	x	
Clade B + C	24 (0)	premaxillary-maxillary suture located anterior to canine alveolus		

Clade B + C	27 (0)	dorsal maxillary flange absent	x	x
Clade B + C	28 (2)	posterior process of premaxilla ends about midway over C-P1 diastema	x	x
Clade B	40 (1)	anterior margin of ascending ramus of mandible projects anteriorly as well as vertically below the coronoid process	x	x
Clade B	49 (2)	P2 metaloph merges midway or higher onto ectoloph	x	x
Clade B	54 (1)	ratio of p2 relative to p3 greater than 1.1	x	x
Clade C	1 (1)	low sagittal crest low, less than 2 mm	x	x
Clade C	7 (1)	nasals notably stepped down from frontals		x
Clade C	15 (0)	fossa for meatal diverticulum on nasal shallow and without distinct margins	x	
Clade C	22 (1)	rounded dorsomedial border of maxilla that is directed ventromedially	x	x
Clade C	26 (1)	anteromedial process of maxilla covered by premaxilla, not visible in lateral view (or barely so)	x	x
Clade C	47 (0)	P2 protoloph does not reach ectoloph	x	
Clade C	56 (1)	very weak or absent cristid obliqua on p3		

CONCLUSION

This thesis provides evidences for the problematic usage of teeth characters alone in the description of new species of *Tapirus*, using traditional morphometrics and statistic approaches. The preliminary results of 2D morphometrics that will be finalized and submitted confirm the traditional morphometrics results of Chapter 1. Furthermore, we confirm previous results of the relatively small teeth comparing to the body size for *T. bairdii*, related to its small upper and lower teeth OSAs. The present work confirms the importance of the endangered *T. indicus* on the dispersion of small seeds, the only seed types that seem to be able to escape its high OSA. This thesis also provides trends in seed dispersal predictions related to OSA calculations for extinct species of *Tapirus*, therefore presenting interesting palaeoecological trends for the genus.

Our phylogenetic hypothesis for Tapiridae points to the origin of the family in the Late Eocene of North America, and the origin and early evolution of *Tapirus* in the same continent in the Middle Miocene. Genus *Tapirus* was recovered as monophyletic and the Miocene *T. johnsoni* is sister to all *Tapirus*, confirming previous works. North American tapirs are polyphyletic, agreeing with the literature. *T. lundeliusi* is sister to all South American tapirs all of which form a clade. We provide the first phylogenetic hypothesis for Tapiridae including European *Tapirus.* The absence of differences between Tapiridae topologies built based on qualitative data only and qualitative plus quantitative data yields to a necessity to better understand patterns of behavior of quantitative data in different phylogenetic scenarios. We intend in the future to test 2D morphometric data behavior under various phylogenetic methods.

Tapirids dispersed from North America to Eurasia. *Tapirus* dispersed from North America to Eurasia and South America, where, by vicariant events isolated and gave origin to new species. Most of our biogeographic inferences are consistent with the presence of transient and/or permanent land bridges. This is the first work to provide a formal biogeographic analysis for Tapiridae.

This thesis provides ecomorphological, phylogenetic and biogeographic analysis for tapirids. We hope that those data can supply solid evidences for the *Tapirus* conservation. Most of the genus diversity is now extinct, probably due to climate changes. Tapirs are key species to maintain the tropical and subtropical forests they inhabit, and this thesis creates an alert for the conservation of a group that was much more diverse in the past.

REFERENCES

Albright LB (1998) New genus of tapir (Mammalia: Tapiridae) from the Arikareean (earliest Miocene) of the Texas Coastal Plain. J. Vertebr. Paleontol. 18:200-217

Bai B, Meng J, Zhang C, Gong YX, Wang YQ (2020). The origin of Rhinocerotoidea and phylogeny of Ceratomorpha (Mammalia, Perissodactyla). Commun. Biol. 3.

Bayshashov BU, Billia EME (2011). Records of Tapiroidea Gray, 1825 (Mammalia, Perissodactyla) from Kazakhstan – An overview. Acta Palaeontologica Romaniae 74:1-7

Casali DM, Boscaini A, Gaudin TJ, Perini FA (2022). Reassessing the phylogeny and divergence times of sloths (Mammalia: Pilosa: Folivora), exploring alternative morphological partitioning and dating models. Zool. J. Linn. Soc. 0:0–0.

Cerdeño E, Ginsburg L (1988). Les Tapiridae (Perissodactyla, Mammalia) del' Oligocène et du Miocène inférieur Européens. Annales de Paléontologie 74:71–96

Colbert MW, Schoch RM (1998). Tapiroidea and other moropomorphs. Cambridge University Press 1:569-582

Colbert MW (2005) The facial skeleton of the early Oligocene Colodon (Perissodactyla, Tapiroidea). Palaeontologia Eletronica 8(1):1-27

Dumbá LCCS, Parisi Dutra R, Cozzuol MA. (2019) Cranial geometric morphometric analysis of the genus Tapirus (Mammalia, Perissodactyla). J Mammal Evol 26: 545–555.

Dumbá LCCS, Rodrigues FHG, Maclaren JÁ, Cozzuol MA (2022) Dental occlusal surface and seed dispersal evolution in Tapirus (Mammalia: Perissodactyla). Biol. J. Linn. Soc. 20:1-18

Ferrero BS, Noriega JI (2007). A new upper Pleistocene tapir from Argentina: remarks on the phylogenetics and diversification of Neotropical Tapiridae. J. Vertebr. Paleontol. 27:504–511

Holbrook LT (1998) The Phylogeny and Classification of Tapiromorph Perissodactyls (Mammalia). Cladistics 15:331–350

Holbrook LT (2001) Comparative osteology of early Tertiary tapiromorphs (Mammalia, Perissodactyla). Zool. J. Linn. Soc. 132:1–54

Holanda EC, Ferrero B (2012) Reappraisal of the genus Tapirus (Perissodactyla, Tapiridae): systematics and phylogenetic affinities of the South American tapirs. J Mammal Evol 20:33–44

Hulbert RC Jr (2010) A new early Pleistocene tapir (Mammalia: Perissodactyla) from Florida, with a review of Blancan tapirs from the state. Bull Florida Mus Nat Hist 49(3):67–126

Janis C (1984) Tapirs as Living Fossils. In: Eldredge N, Stanley SM (eds) Living Fossils. Casebooks in Earth Sciences. Springer, New York, NY

Lewis PO (2001). A likelihood approach to estimating phylogeny from discrete morphological character data. Syst. Biol. 50:913–925.

Matthew WD, Granger W (1923). New fossil mammals from the Pliocene of Szechuan, China. Bulletin of the American Museum of Natural History 48:563-598

McKenna MC, Bell SK (1997) Classification of Mammals – Above the Species Level. Columbia University Press, New York

Osborn HF (1918) Equidae of the Oligocene, Miocene, and Pliocene of North America, iconographic type revision, Memoirs of the American Museum of Natural History 2 1, 1-217

Perini FA, Oliveira JA, Salles LO, Moraes CR, Neto PG, Guedes LFB, Oliveira M (2011) New fossil records of *Tapirus* (Mammalia, Perissodactyla) from Brazil, with a critical analysis of intra-generic diversity assessments based on lower molar size variability. Geobios 44:609–619

Qiu ZX, Yan DF, Sun B (1991). A new genus of Tapiridae from Shanwang, Shandong. Vertebrata Palasiatica 29:119–135

Radinsky LB (1965) Evolution of the tapiroid skeleton from *Heptodon* to *Tapirus*. Bulletin of the Museum of Comparative Zoology 134: 69–106.

Schoch, R. M. 1989. A review of the tapiroids. In “The Evolution of Perissodactyls” (D. R. Prothero and R. M. Schoch, Eds.). Oxford Univ. Press, New York 298–320.

Tong HW, Liu J, Han L (2002) On fossil remains of early Pleistocene tapir (Perissodactyla, Mammalia) from Fanchang, Anhui. Chinese Science Bulletin 47:586–590

JA Wilson, JA Schiebout (1984). Early Tertiary Vertebrate Faunas, Trans-Pecos Texas: Ceratomorpha less Amynodontidae. Pearce-Sellards Series 39:1-47